Norwegian University
of Life Sciences

Master's Thesis 2018 60 ECTS

Department of Medical Genetics, Oslo University Hospital Ullevål
Main Supervisor Ph.D Nina Iversen

The functional role of coagulation factor V in liver cancer

Cathrine McCoig

Biotechnology
Faculty of Chemistry, Biotechnology and Food Sciences

THE FUNCTIONAL ROLE OF COAGULATION FACTOR V IN LIVER CANCER

Oslo University Hospital,
Department of Medical Genetics

and

The Norwegian University of Life Sciences (NMBU),
Faculty of Chemistry, Biotechnology and Food Sciences

© Cathrine McCoig, 2018

Acknowledgements

The work described in this thesis was performed at the Department of Medical Genetics, Oslo University Hospital as a part of the master program in Biotechnology at the Norwegian University of Life Science (NMBU) at the Faculty of Chemistry, Biotechnology and Food Science (KBM) from August 2017 to May 2018.

First and foremost, I would like to thank my supervisors with the Department for Medical Genetics at Oslo University Hospital, Dr. Philos Nina Iversen and Ph.D Mari Tinholt for allowing me to join the research group and letting me work with this exciting project. Your knowledge, patience and supervision have been excellent during this work, and I could not have done it without you. I would also like to thank Department Engineer Marit Sletten for her excellent help and guidance in the laboratory. Your experience and expertise in the lab have been an invaluable help for my thesis. Finally, I would like to thank my internal supervisor at NMBU, Prof. Harald Carlsen at the Faculty of Chemistry, Biotechnology and Food sciences.

Moreover, I would like to thank Marianne Staff Fredhjem, my fellow master student for a nice time together at Ullevål, sharing joys and frustrations. This year would not have been the same without you. I would also like to thank my family and friends for all encouragement and support.

Oslo, May 2018

Cathrine McCoig

Sammendrag

Sammenhengen mellom koagulasjon og kreft er velkjent. Kreftpasienter har en dokumentert økt risiko for trombose, og kreftceller kan også frigi kreft-prokoagulanter og mikropartikler som direkte aktiverer koagulasjonssystemet. Koagulasjonsfaktor V (FV) har vist seg å være uttrykt i flere ulike kreftvev, og samtidig ha potensielle effekter på kreftprogresjonen. Ved å forstå dette forholdet og de underliggende mekanismene bak effektene bedre, kan man oppnå bedre individuell behandling for pasienter som lider av kreft eller kreft-relaterte koagulasjonskomplikasjoner.

I denne oppgaven har vi derfor som mål å få en bedre forståelse for de funksjonelle rollene til FV i kreftprogresjon. En cellemodell for nedregulering av FV ble laget for leverkreft cellelinjene Huh7 og HepG2. Den ble deretter optimalisert for å kunne studere de funksjonelle effektene av FV og potensielle celle- signaleringseffekter. Cellene ble også behandlet med doxorubicin for å observere sensitiviteten samt effekten av denne behandlingen på FV uttrykk.

Undersøkelsene gjort i denne oppgaven resulterte i en effektiv nedregulering av FV i begge cellelinjene ved bruk av 27mer siRNA. De funksjonelle effektene av FV ble også studert, og viste ingen signifikante effekter av cellevekst i leverkreft, derimot ble det observert økt apoptose og redusert migrasjon ved nedregulering av FV. Videre analyser på kreft-assosierte signalveier viste at Wnt og JNK signalveiene ble mest påvirket under FV nedregulering. Men ved å se på effekten av JNK signalveien på apoptose, ble ingen signifikante forskjeller observert. Basert på dette, og på studier som dokumenterte at koagulasjonssystemet har en sentral rolle (spesielt TF) i progresjon og overlevelse, antydes FV å ha onkogene egenskaper i leverkreft. Men, det kan være andre mulige mekanismer enn de vi har studert, som påvirker effekten av FV, og denne effekten kan komme av andre medlemmer av koagulasjonssystemet som er verdt å undersøke videre.

Med hensyn til doxorubicin-behandling av leverkreftcellene, viste de sensitivitet overfor behandlingen. Samtidig ble det observert at doxorubicin induserte *F5* mRNA-uttrykket betraktelig i HepG2 celler. Men det var ingen antydning til noen interaksjon mellom p53-indusert apoptose, og FV hadde ingen effekt på celleveksten under doxorubicin-behandlingen. Gjennom våre resultater av FV som et mulig onkogen, og med ingen observert interaksjon med doxorubicin, har oppgaven gitt et bedre innblikk og bidratt med kunnskap og forståelse om rollen til FV i leverkreft.

Abstract

The relationship between cancer and coagulation is well known, and cancer patients have been documented to have an increased risk of thrombosis. Tumor cells themselves have in fact been shown to release cancer procoagulants and microparticles that directly activate the coagulation cascade. Coagulation factor V (FV) has been shown to be expressed in different cancer tissues, and to have possible effects on the progression. By understanding the relationship and the underlying mechanisms better, one can obtain more individualized treatment for patients suffering from cancer or cancer-related thrombosis.

Throughout this thesis, we therefore aim to gain a better understanding of these underlying mechanisms by relating FV and cancer progression. A FV knockdown model was created and optimized to study the functional effect of FV, and possible effects of cell signaling in liver cancer cells. The cells were also tested for doxorubicin treatment, and the effect of this treatment on FV expression.

The study performed for this thesis revealed an effective knockdown model in both cell lines by the use of 27mer FV siRNAs. Our experiments investigated the functional effects of FV showed no significant effects in liver cancer cell growth, and an increased apoptosis and reduced migration under FV knockdown was observed. In further cancer pathway cell signalling experiments the Wnt and JNK pathways were seen to be the most down-regulated in Huh7 cells under FV knockdown. Yet, an assay of the effect of the JNK pathway on apoptosis did not reveal any significant differences. Based on these results, and based on studies establishing a central role of the coagulation system, especially TF, in liver cancer progression and survival, FV seems to have oncogenic characteristics in liver cancer. However, there may be other possible mechanisms than ones studied in this thesis that influence the effect of FV, and this effect may originate from other members of the coagulation system which are worth investigating further.

Results regarding doxorubicin treatment of the liver cancer cell lines revealed sensitivity to treatment. In addition, doxorubicin seemed to induce *F5* mRNA expression significantly in the HepG2 cell line. However no interaction was seen in p53-induced apoptosis, and FV had no effect on cell proliferation under doxorubicin. Thus our results of FV as a possible oncogene, and no particular interaction of FV with doxorubicin, give a better knowledge and understanding of the role of FV in liver cancer.

Abbreviations

APC	Activated Protein C
Arg	Arginine
AT	Antithrombin
Bp	Base pair
BSA	Bovine serum albumin
bFGF	Basic fibroblast growth factor
cDNA	Complementary DNA
CT	Threshold cycle
ddNTP	Dideoxyribonucleotide
DMEM	Dulbecco's modified eagle medium
DNA	Deoxyribonucleic acid
dNTP	Deoxyribonucleotide
dsRNA	Double stranded RNA
E.coli	*Escherichia coli*
EC	Endothelial cells
ELISA	Enzyme Linked immunosorbent assay
EMT	Epithelial mesenchymal transition
F	Factor
F5	Factor V gene
FBS	Fetal bovine serum
FV	Factor V protein
FVa	Activated factor V
FVac	Activated anticoagulant factor V
FVII	Factor VII
FVIII	Factor VIII
FIX	Factor IX
FX	Factor X
GAPDH	Glyceraldehyde 3-phosphate dehydrogenase
HBV	Hepatitis B virus
HCC	Hepatocellular carcinoma
HCV	Hepatitis C virus
HRP	Horseradish peroxidase
LAR II	Luciferase Assay Reagent II
mRNA	Messenger ribonucleic acid
miRNA	Micro RNA
NTC	Non template control
p53	Tumor protein 53
PAR	Protease activated receptor
PBS	Phosphate buffered saline
PCR	Polymerase chain reactin
PFT- α	Pifithrin α
PLB	Passive lysis buffer
PMM1	Phosphomannomutase 1
RIPA	Radioimmunoprecipitation assay buffer
RISC	RNA-Inducing Silencing Complex
RNA	Ribonucleic acid
RNAi	RNA Interference
qRT-PCR	Real time quantitative PCR

SD	Standard deviation
SE	Standard error
siRNA	Short interfering RNA
TBS	Tris-buffered saline
TBST	Tris-buffered saline with Tween 20
TF	Tissue factor
TFPI	Tissue factor pathway inhibitor
Top2	Topoisomerase II
VEGF	Vascular endothelial growth factor
VEGFR	Vascular endothelial growth factor receptor
VTE	Venous thromboembolism
Wt	Wild type

Table of Contents:

1. INTRODUCTION

1.1 Hepatocellular carcinoma (HCC)

1.1.1 The cancer hallmarks

Development of cancer is caused by a fundamental abnormality, involving unregulated proliferation of cells. Cancer cells exhibit loss of growth control, and thus, do not respond to the normal cell cycle signals of regulation. Instead, they grow and divide uncontrollably, which may lead to invasion of normal tissues and eventually spreading throughout the body (Cooper, 2000; Reece *et al*. 2011).

The framework called "the hallmarks of cancer" was developed by Weinberg and Hanahan, and defined as: "*distinctive and complementary capabilities that enable tumor growth and metastatic dissemination"*. The hallmarks present the biological traits that underlie the transformations of normal cells to cancer cells (Figure 1, left). There are six hallmarks, and for cancer to be fully developed, the cells need to exhibit all of these six hallmarks (Hanahan & Weinberg, 2011):

1) Sustaining proliferative signaling
2) Evading growth suppressors
3) Activating invasion and metastasis
4) Enabling replicative immortality
5) Inducing angiogenesis
6) Resisting cell death

Research also suggests that there are two additional emerging hallmarks and two enabling characteristics (Figure 1, right). The emerging hallmarks involve the ability to modify cellular metabolism to most effectively support neoplastic proliferation, and allowing the cancer cells to evade immunological destruction. The enabling characteristics consist of genome instability, where genetic mutations in cancer cells evolve during growth leading to chromosomal abnormalities. In addition, a tumor-promoting inflammation characteristic is involved, where the cancer cells are induced by inflammation, leading to angiogenesis and induced blood flow (Hanahan & Weinberg, 2011).

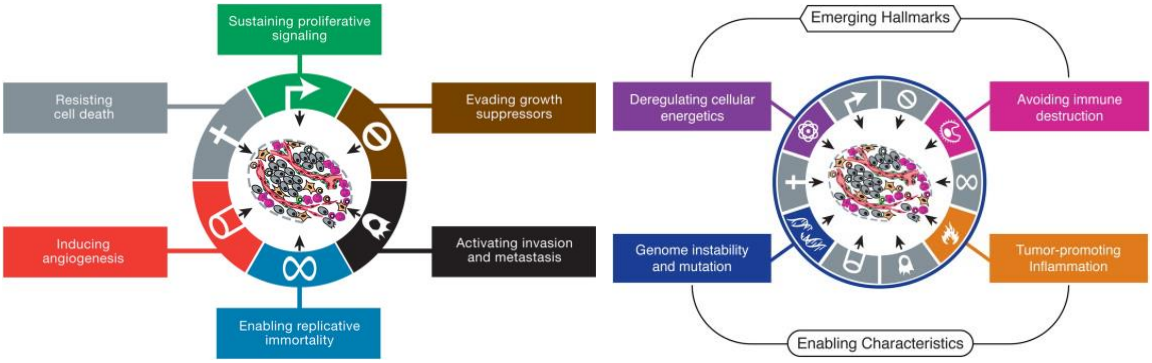

Figure 1: **Schematic diagram showing the hallmarks of cancer.** Illustration of the six biological hallmarks of cancer (left), in addition to emerging hallmarks and two enabling characteristics (right) (Hanahan & Weinberg, 2011).

1.1.2 Epidemiology and etiology of HCC

Primary liver cancer is defined as a primary malignancy in the liver, and the most prevalent form of primary liver cancer is called **hepatocellular carcinoma (HCC)**. It is the sixth most common cancer in the world, and is one of the leading causes of death from cancer worldwide (©CancerResearchUK 2014). HCC can be divided into three categories based on the Barcelona Clinic Liver Cancer staging system: early, intermediate-advanced and end-stage HCC (Llovet *et al.* 1999). The early stage has best prognosis, but is also the hardest to diagnose, intermediate stages show varied prognosis and symptoms, reflecting the heterogeneity of the disease and of the population itself. End-stage HCC (terminal stage) is associated with poor functional status among patients, and poor prognosis with an average survival rate of only 3 months (Llovet *et al.* 1999).

1.1.2.1 Risk factors:

Apart from the rising incidences of cirrhosis (chronic scarring of the liver) growing with the problem with obesity, hepatitis B virus (HBV) and hepatitis C virus (HCV) infections are identified as the two main risk factors for HCC, accounting for 75-80% of the cases of primary liver cancer worldwide (IARC, 2012). There are also great geographic variations of incidences, with most cases reported in the developing world (Globocan, 2012). However, there are positive trends to be seen for the global incidences in these parts of the world. The recent decline is partly due to increased vaccinations against hepatitis B and C. In contrast, the developing world is actually experiencing an acceleration of HCC because of the rising epidemic of obesity, diabetes and non-alcoholic steatohepatitis (NASH) (El-Serag *et al*. 2000).

HBV and HCV infections:

Both HBV and HCV are direct inflammation-mediators of HCC by means of proliferative signaling, and indirectly promoting replication of the virus through short periods of high-activity hepatitis, resulting in liver damage without virus clearance (Zemel *et al*. 2011). The pathogenesis of HCC in chronic HBV and HCV infection is a result of multiple steps of cell proliferation and apoptosis of the host cells, inflammation, fibrosis, cirrhosis and eventually dysplasia (Feitelson, 1999). It also involves a mechanism resulting from oxidative damage that promotes the development of mutations (Bréchot, 2004). In both HBV and HCV infections, activation of oncogenic pathways by viral oncogenes leads to development of cancer hallmarks by the infected cell (Figure 1):

- Resisting cell death by blocking apoptosis
- Influence replicative immortality
- Induce angiogenesis by fibrogenesis
- Driven by genome instability and mutations. HBV and HCV driven tumor initiation and progression is a result of genome instability (HBV DNA fragments are found in clusters near or within the fragile sites in cancer-associated regions that are prone to genetic instability) (Feitelson & Lee, 2007).

For HBV infections, HBx (HBV-encoded antigen) is required for the transcription of the viral genome. It stimulates the cell-cycle entry by activating cyclins and cyclin-dependent pathways like Wnt, ras, JAK-STAT, NF-kB and Hedgehog that promote survival and growth (Figure 2) (Martin-Vilchez *et al*. 2011). Nuclear HBx also regulates the transcription that affects host cell gene expression (Kumar *et al*. 2011).

In HCV infections, HCV-encoded core non-structural protein 3 and 5A (NS3 and NS5A) promote liver cell proliferation via the β-catenin pathway (Figure 2). In addition, they alter immune-mediated inflammation that contributes to tumorigenesis (indirectly) by binding to cellular signaling molecules and suppressing immune responses, tumor suppressors and apoptosis (Kumar *et al*. 2011).

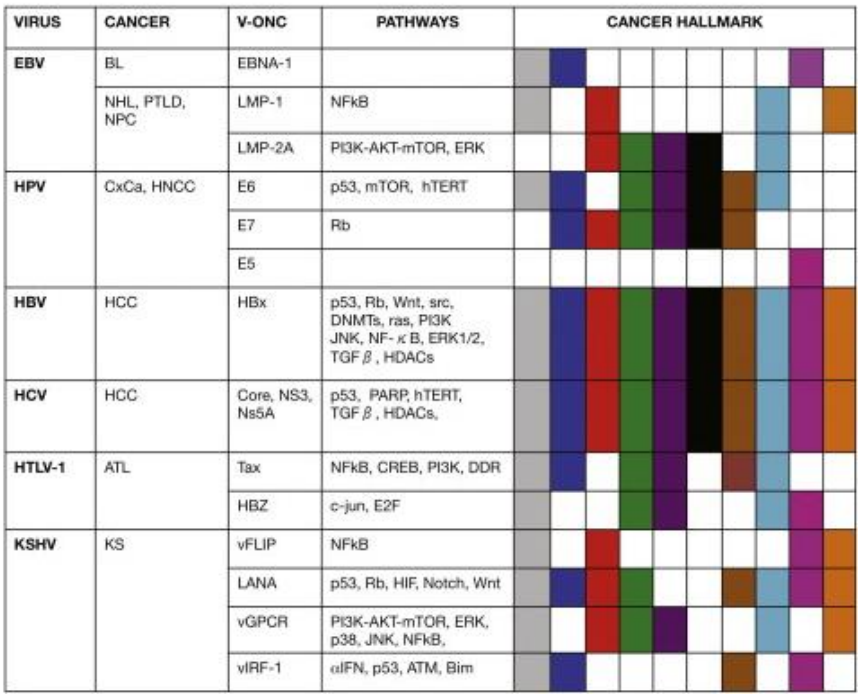

Figure 2: **Diagram showing the cancer hallmarks activation by human oncoviruses.** The figure presents the activation of oncogenic pathways by viral oncogenes that lead to acquisition of cancer hallmarks by the infected cell (Mesri *et al.* 2014).

Molecular classification and staging of HCC:

HCC tumors can be classified or subdivided defined by a set of genes associated with biological phenotypes that reflect the clinical outcomes. The tumors are primarily classified into two major subgroups based on specific traits; tumors with aggressive biological/clinical traits and tumors with less aggressive traits. The aggressiveness and prognosis of the cancer is based on the activation of different pathways and genes (Hoshida *et al.* 2009). More aggressive tumors generally have more abundant mutations, biological markers and more activated pathways. These aggressive features of HCC tumors include cellular proliferation, ubiquitination and poorer prognosis. Whilst the less aggressive group includes traits like preserved hepatocyte function, smaller and less differentiated tumors and a better overall prognosis. (Reviewed by Goossens *et al.* 2015).

Treatment:

Treatment of HCC is a challenge because liver cancer resists most chemotherapeutic drugs, however there are multiple options depending on the stage of the cancer (Dhanasekaran *et al.* 2012). Doxorubicin, 5-fluorouracil and cisplatin have shown to be effective to some extent. Sorafenib is a molecular target drug for HCC that has shown to be beneficial for patients with advanced tumors. Nevertheless, transplantation remains the most viable treatment option

because resection is not possible with marginal liver function as a consequence of the cancer. (Llovet *et al.* 2008).

1.1.3 Genetic alterations in HCC

Among the modified pathways and genetic changes in HCC progression, the most affected signaling pathways include the Wnt-β-catenin pathway and the Hedgehog pathway, both leading to uncontrolled cell division in HCC (Vilchez *et al*. 2016). The Wnt- pathway is a fundamental mechanism directing cell proliferation, cell polarity, and cell fate determination during embryonic development and tissue homeostasis (Logan & Nusse, 2004). And as a result, mutations in this pathway are often linked to cancer and other diseases.

The most common Wnt pathway is canonical Wnt signaling, which regulates the amount of the transcriptional co-activator β-catenin to control key developmental gene expressions (Clevers, 2006). The Wnt/ β-catenin pathway is also known to be frequently downregulated in HCC, and is involved in tumor progression and metastasis. With decreased Wnt signaling, β -catenin complexes with tumor suppressors and the nuclear accumulations of β-catenin are associated with β -catenin mutations which lead to phosphorylation and destruction of the β -catenin gene (Kumar *et al*. 2011; MacDonald *et al*. 2009).

An important genetic change is the mutated p53. This gene is mutated in 61% of HCC cases (cBIOPortal, McCoig unpublished, 2018). Studies suggest that p53 mutations are not the cause of liver cancer (HCC), but rather the consequence of the disease development by contributing to tumor progression and metastasis (Ueda *et al*. 1995).

1.2 Coagulation (Hemostasis)

Coagulation (hemostasis) is defined as the stopping of bleeding, and is a highly regulated, dynamic process under strict control of several inhibitors in the body that limit clot formation and avoid generation of thrombus (stops bleeding at the site of injury) (Palta *et al*. 2014).

The coagulation cascade may be triggered by either the intrinsic or the extrinsic pathway. The intrinsic pathway is initiated when factor XII (FXII) is activated by the presence of collagen in an injured vessel, and goes on to activate factor X (FX) through the FVIII/FXI complex (Figure 3). The extrinsic pathway concerns the activation of FX through tissue factor (TF) and factor

VII (FVII), and the pathway eventually unites with the intrinsic one to form thrombin through the common coagulation pathway (Figure 3) (Fujikawa *et al*. 1974).

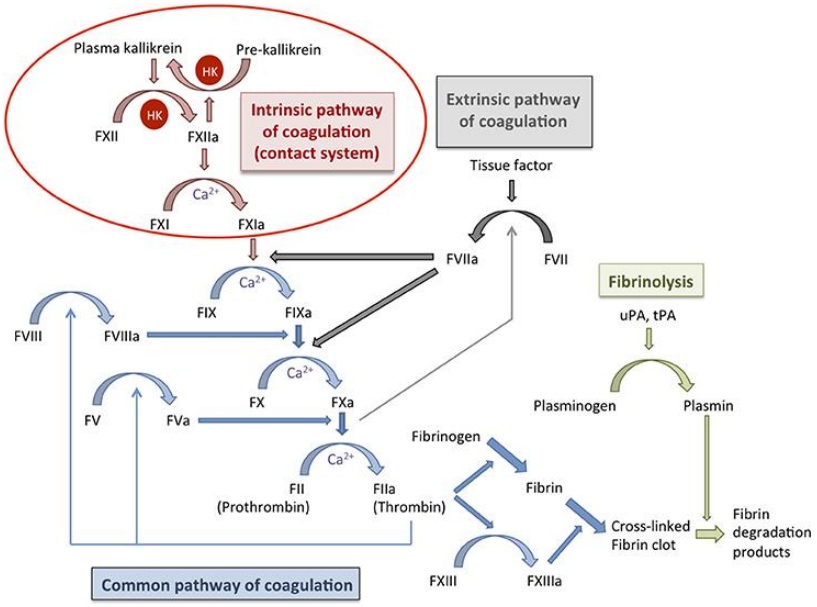

Figure 3: **A schematic representation of the coagulation cascade.** The coagulation cascade (blue arrows) is activated during hemostasis via the intrinsic pathway (red arrows) or extrinsic pathway (grey arrows) that eventually converge into the common pathway of coagulation. Both pathways activate FXa and thrombin subsequently, which is required for the further conversion of fibrinogen to fibrin and for activating FXIII (From Loof *et al.* 2014).

1.2.1 Primary hemostasis

Primary hemostasis mainly involves platelet aggregation and platelet plug formation, which means that platelets are activated and exposed to the subendothelial matrix. The exposure causes adherence of the platelets to the injury site, and to each other, making a hemostatic plug to stop the bleeding. Thus, this will only happen by the site of an injury, and does not take place under normal conditions, in healthy blood vessels with normal blood flow (Gale, 2011).

1.2.2 Secondary hemostasis (The cell based model)

The degradation of insoluble fibrin generated by the coagulation cascade is a process called secondary hemostasis, and links the coagulation and the fibrinolytic processes (Gale, 2011). The process involves a cascade of coagulation serine proteases that end up in the cleavage of soluble fibrinogen by thrombin. However, as in primary hemostasis, healthy and intact vessels will not have an activated cascade because of the presence of multiple anticoagulant mechanisms preventing this activation from happening. The understanding of the coagulation mechanism is established from a cell-based model involving three overlapping phases in coagulation: initiation, priming (or amplification) and propagation (Hoffman & Monroe, 2001).

TF is defined as the primary coagulation trigger in the cell based model and is a transmembrane glycoprotein found on the surface of various cells (Bach, 1988). TF is also the main initiator of the extrinsic coagulation cascade (Figure 3). When injury occurs in the vascular system and the vessel wall is disrupted, TF-expressing cells in the underlying cell layers will be exposed to the bloodstream (Drake *et al*. 1989).

The **initiation** of coagulation begins the process by TF binding to activated factor VII (FVIIa), and activates factor IX (Figure 3). This triggers the extrinsic coagulation pathway. The TF/FVIIa complex proteolytically cleaves FX to FXa, which activates factor V to factor Va (FVa) and complexing with it to form the prothrombinase complex (Hoffman & Monroe, 2001; Monroe *et al*. 2002). The prothrombinase complex then converts prothrombin to thrombin, and eventually, thrombin will induce the formation of fibrin from fibrinogen, initiating the production of a blood clot (Drake *et al*. 1989).

During the **priming/amplification** phase, the produced thrombin acts on protease-activated receptors (PAR) to activate platelets, releasing the contents of α-granules, including factor V (FV). Thrombin then cleaves factor VIII (FVIII) which dissociates from VWF, and activates it along with FV and factor XI (Figure 3). In addition, the tissue factor pathway inhibitor (TFPI) will inactivate the FVIIa/TF/FXa complex (Hoffman & Monroe, 2001; Monroe *et al*. 2002).

Propagation involves binding of TF/FVIIa to activated platelets and generating FIXa on the platelet surface. The tenase complex of FVIIIa/FIXa activates FX, which complexes with FVa and generates a thrombin burst (Cosemans *et al.* 2011; Monroe *et al*. 2002). The generated thrombin binds and cleaves fibrinogen, releasing fibrinopeptides A and B, which then polymerize by forming protofibrils with adjacent fibrin molecules. In addition, thrombin will activate factor XIII (FXIII) which stabilizes the fibrin clot by forming cross-links (Scott *et al*. 2004; Schroeder & Kohler, 2013) (Figure 3).

Fibrinolytic components are on the surface of a fibrin clot to mediate the degradation of fibrin. Tissue-type plasminogen facilitates this process because it is enhanced in the presence of fibrin. The plasminogen activator cleaves plasminogen to plasmin, an active enzyme, which produces fibrin degradation products. This system is tightly controlled by inhibitors

where thrombin acts as an activator of a further inhibitor of fibrinolysis and linking the coagulation system with this process (Rijken & Lijnen, 2009).

1.2.3 Regulation of coagulation

The coagulation pathway is highly regulated at each phase, either by various enzymatic inhibition or modulation of cofactor activity. The tissue pathway inhibitor (TFPI) is the mediator of one of the three main inhibitory mechanisms, by binding and inhibiting the TF/FVIIa/FXa complex generated during the initiation phase, and this activity is enhanced by protein S (Iakhiaev A *et al.* 1999).

The second inhibition mechanism is performed by antithrombin (AT). AT is a serine protease inhibitor contributing to down-regulation of coagulation and is referred to as the most important inhibitor of coagulation (Jeffery & Weitz, 2010). AT inhibits the procoagulant enzymes thrombin and FXa among other clotting enzymes in a reaction accelerated by heparin (Pike *et al.* 2005) (Figure 3).

Protein C is responsible for the last main inhibitory mechanism in the coagulation cascade. Protein C is a plasma protein activated by the thrombin-thrombomodulin complex, and the endothelial protein C receptor (EPCR). Once activated to activated protein C (APC), the protein (with the help of protein S) cleaves FVIIIa and FVa to inactivate them (Esmon, 1989). As a result of this inactivation, FVa loses its high affinity for FXa and prothrombin binding interactions (Guinto & Esmon, 1984). The complexes between proteases and cofactors (procoagulant and anticoagulant) are formed on negatively charged membrane surfaces that are provided by activated platelets. This localization of the coagulation cascade reactions is critical to restrict coagulation to the site of injury (Cramer *et al*. 2010; Schen & Dahlbäck, 1994; Walker, 1980).

Lastly, thrombin is also involved in down-regulation of the coagulation cascade by binding to thrombomodulin on endothelial cells before activating protein C. Thrombomodulin is expressed on the surface of endothelial cells and serves as a receptor for thrombin. When bound to thrombomodulin, thrombin can no longer serve as a procoagulant and cannot activate platelets, convert fibrinogen to fibrin or amplify its generation (Esmon, 2006).

1.3 Cancer and coagulation

It is a well-known fact that cancer patients have an increased risk of thrombosis. Thromboembolic events are in fact the second leading cause of death in cancer patients after cancer itself. On the other hand, thrombosis can also be the first sign of a malignant disease, preceding the diagnosis of cancer by months, or even years (Falanga *et al.* 2013). The risk factors of these coagulation events are either related to the patient, the cancer or to the treatment. It has been documented that treatment of cancer enhances the risk of venous thromboembolism (VTE). Chemotherapy for instance, is associated with a 2- to 6-fold increased risk of VTE compared with the general population. Similarly, the drug sorafenib, a non-chemotherapeutic drug targeting the angiogenesis pathway, used in treatment of liver cancer, has shown to elevate the risk of arterial events (Khorana, 2012).

Patients with thrombosis-associated malignancies are also reported to have a higher mortality rate than those without. However, this survival rate may not be due to the thrombotic event, but is instead related to tumors with more aggressive behavior. This provides evidence that cellular and circulating hemostatic factors have a central role in tumor progression including angiogenesis and metastasis (Lima *et al*. 2013).

1.3.1 The role of coagulation in cancer progression

Coagulation activation and tumor progression are closely linked. Tumor cells may actually activate the hemostatic system in multiple ways; by releasing procoagulant TF, cancer procoagulants and microparticles that directly activate the coagulation cascade. Tumor cells can also activate the host's hemostatic cells by either the release of soluble factors or by direct adhesive contact (Figure 4) (Falanga *et al.* 2009).

Tumor growth and aggressiveness rely on the capacity of cancer cells to promote neoangiogenesis and metastasis, and components of the hemostatic system like TF, thrombin, FVIIa and fibrinogen have been documented to be involved in both clotting dependent and clotting-independent cancer promoting mechanisms (Falanga *et al.* 2009; Falanga *et al*. 2013).

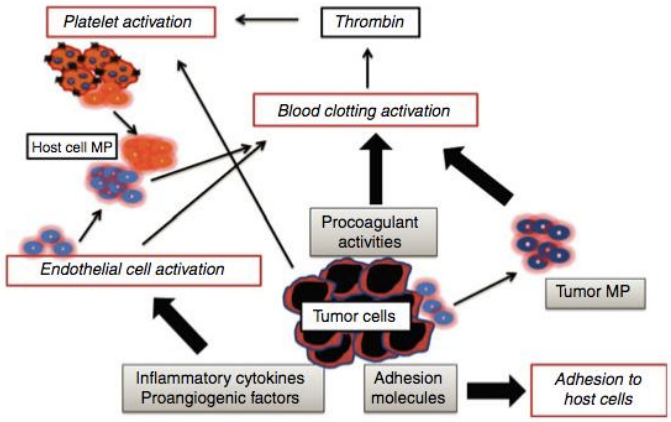

Figure 4: **Tumor-hemostatic system interactions.** Tumor cells can activate the hemostatic system in multiple ways by releasing procoagulant tissue factor, cancer procoagulant and microparticles (MP). Tumors cells can also activate the hemostatic cells by release of soluble factors or by direct adhesive contact, and thereby enhancing the clotting activation further (Falanga *et al.* 2013)

1.3.1.1 Clotting dependent mechanisms and cancer progression

Fibrin is deposited in the tumor vasculature and facilitates angiogenesis by providing a scaffold for new vessel formation. The fibrin deposition is thought to favour the metastatic process by stabilising tumor cell adhesion (Falanga *et al.* 2009). Platelets can be directly or independently activated from thrombin, by tumor cells through release of pro-aggregating substances or through adhesion mechanisms (Lowe *et al.* 2012). The formation of tumor cell-platelet thrombin can support metastasis formation by preventing interactions between tumor and innate immune cells (Palumbo *et al*. 2005).

1.3.1.2 Clotting independent mechanisms and cancer progression

Malignant cells also produce various procoagulant factors themselves. Among these are tissue factor (TF), and thrombin, which both contribute to tumor progression by interaction with specific receptors belonging to the family of protease-activated receptors (PAR) expressed by platelets and tumor cells (Falanga *et al.* 2009).

TF binds to FVIIa and initiates downstream signalling cascades that promote increased endothelial cell adhesion and migration. In addition, TF in complex with FVIIa and FXa, activates one or more PARs to support angiogenesis *in vivo* (Uusitalo-Jarvinen *et al.* 2007). Other procoagulants have been demonstrated in human tumors, including a factor XIII-like activity capable of fibrin covalent cross-linking. In addition, FVa bound to the tumor cell surface on the plasma membrane has been seen to serve as an FXa receptor site, facilitating the assembly of the prothrombinase complex (VanDerWater *et al.*1985).

Thrombin is known to upregulate several angiogenesis-related genes in endothelial cells, including VEGF and VEGFR (Ruf, 2007). Thrombin-activated platelets also become proangiogenic by releasing proangiogenic factors from their granule contents, including VEGF and platelet-derived growth factor (PDGF) (Mohle *et al*. 1997).

In addition to these mechanisms, the Tissue Factor Pathway Inhibitor (TFPI) has been documented by our research group to decrease adhesion and migration and thereby indicated an anti-tumor characteristic in breast cancer. (Pollen, 2014). Stavik *et al.* (2011) also reported an association between TFPI and a decrease in breast cancer cell growth, migration and invasion.

1.3.2 The role of coagulation in liver cancer

Studies have established that coagulation has a role in liver diseases, and also in liver cancer. Increased plasma TF levels are closely related to occurrence of chronic liver diseases and it has been shown that tissue levels of TF have a significant association with venous invasion, tumor staging and survival in HCC (Zhou *et al.* 2011).

Hepatocytes occupy more than half of the total liver volume and carry out critical functions in coagulation factor synthesis (TF, FVII, etc.) in the liver. Overexpression of TF has been found in both plasma and liver tissue of HCC patients, and the expression was upregulated in poorly differentiated HCC, which suggests that the expression of TF is related to higher grade tumors and to poorer prognosis (Lin *et al*. 2016). Nevertheless, the basis of the high frequency of coagulation events in cirrhotic patients of chronic liver disease is not yet fully understood (Lin *et al.* 2016). Various studies support the statement of a close relationship between TF/FVIIa initiated coagulation and liver disease in association with reduced autophagy (Lin *et al*. 2016). Lin *et al.* (2016) also suggested a crucial impact of the TF/FVII/PAR2 coagulation pathway on tumor malignancy under certain circumstances, and thus an association between FVII and the clinical staging of HCC.

1.4 Coagulation factor V

1.4.1 Structure and activation of coagulation factor V

Coagulation factor V (FV) is a single-chain glycoprotein of 330-kDa circulating the blood. It is a multidomain (A1-A2-B-A3-C1-C2) procofactor and plays a crucial role in hemostasis as both a procoagulant and anticoagulant cofactor (Figure 5) (Jenny, 1987*;* Kane & Davie, 1987). Removal of the middle B-domain by thrombin or a partly removal of the B-domain by FXa generates the activation of FV to FVa. A cleavage in the A2-domain by APC will induce the activation of FV to anticoagulant activated factor V (FVac) (Asselta *et al.* 2006).

The gene encoding FV is located on chromosome 1, and about 20-25% of total human FV is found on the alfa-granules of platelets where it is stored in a partially proteolyzed form in association with multimerin (Figure 5) (Jenny, 1987). Single chained FV is mainly synthesized in the liver, partially in megakaryocytes where it is absorbed from plasma through endocytosis (Asselta *et al*. 2006; Segers *et al.* 2007).

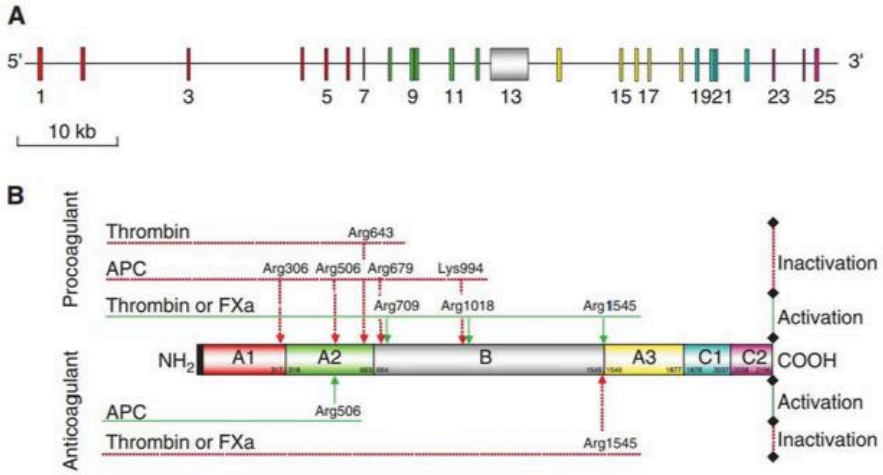

Figure 5: **Schematic structure of the FV gene:** A: Exons and introns of the FV genes, exons are shown with colored structures, while introns are shown as a black line. B: FV domains organized by the correlated colored exons (A). FV cleavage sites for activation or inactivation of anti- and procoagulants, are arrows, red represent inactivation and green represent activation. Amino acid numbers are shown for each cleavage site in the FV protein and signal peptide is represented by NH_2 (Asselta *et al*. 2006).

FV has also been detected in other cell types, in addition to the liver, which suggests that they also contribute to its expression. Dashty *et al.* (2012) showed that FV was expressed by monocytes, suggesting that these cells play a more active role in the coagulation process by activating FX via cell-autonomous FV delivery. FV may be activated by elastase and cathepsin

G, which are both present in monocytes, and this activation can then further stimulate FX activity through FV-dependent mechanisms (Allen & Tracy, 1995).

Because FV has a dual role in the coagulation cascade, genetic or acquired defects and deficiencies may result in thrombotic or hemorrhagic incidents. FV deficiency is a rare bleeding disorder first discovered by Paul Owren in 1943. The disorder is mainly due to development of antibody inhibitors, and results in a blocked clotting reaction because of deficient or non-working FV (WFH®, 2012; Knöbl & Lechner, 1998). In the liver, data reported by Bernuau *et al.* (1986) established FV as the best prognostic indicator in fulminant hepatic failure (FHF). In addition, lower FV levels in patients with FHF were documented from a study done by Izumi *et al.* (1996), to be associated with lower survival rates.

1.4.2 Procoagulant properties of FVa

FV itself has little or no intrinsic procoagulant activity prior to activation, and thus must be activated to FVa to act as a cofactor to achieve this. The activation (or conversion) of FV to FVa happens by a number of proteases including thrombin, FXa and plasmin, in which thrombin is seen as the most significant with respect to biological function (Hockin *et al.* 2002). Thrombin cleaves sequentially at Arg709, Arg1018, and Arg1545, removing the B domain to generate non-covalently associated FVa light and heavy chains (Krishnaswamy *et al.* 1989).

Procoagulant FVa serves as a cofactor for FXa in the prothrombinase complex in activation of prothrombin to thrombin. This activation of FV to FVa is essential for the biological function of FXa because single-chain FV does not bind FXa (Mann K.G. & Kalafatis, 2002). Thus, the amount of thrombin-activated FVa is also crucial for the generation of the prothrombinase complex (Keller *et al.* 1995; Segers *et al*. 2007; Toso & Camire, 2004). Generated activation of thrombin will thus further increase the thrombin-activated FVa (Mann & Kalafatis, 2003).

FV may also be activated by FXa through the same cleavages as in thrombin activation, but in a different order: Arg1018, Arg709 and Arg1545. (Monkovic & Tracy 1990). The cleavage leads to a partial loss of the B-domain and the light and heavy chain are held together by calcium ions and hydrophobic interactions. (Mann & Kalafatis, 2003).

Activated Protein C (APC) down-regulates alfa-thrombin generation along with the coagulation process, and thus proteolytically inactivating FVa and FVIIIa (Esmon, 1987). APC will bind to the light chain of FVa as a competitor to FXa. Conversely, FXa impairs APC cleavage and

inactivates the cofactor (Solymoss *et al.* 1988; Nesheim *et al.* 1982). Hence, APC provides inhibition of coagulation by competition with FXa and by cleavage of FVa (in the heavy chain at Arg506, Arg306 and Arg679) and inactivation (Kalafatis & Mann, 1994).

Plasmin has also been shown to inactivate FVa involving cleavages at Lys309, Lys310, Arg313 and Arg348 and most likely results in the dissociation of the A2 domain of the cofactor from the rest of the molecule (Kalafatis & Mann, 2001).

1.4.3 Anticoagulant properties of FV

Factor V was first viewed as only a procoagulant cofactor, however anticoagulant roles of FV were proposed in 1983 and 1994 (LaBonte, 2013). It was then shown that FV could function as a cofactor for activated protein C (APC). APC is a member of the anticoagulant pathway and downregulates the coagulation process through proteolytic inactivation of factors VIII/VIIIa and both FV and FVa. The FV cofactor activity for APC was in APC inactivation of FVIIIa in the presence of Protein S. Interestingly, protein S alone has little cofactor activity, but in the presence of FV it is significantly enhanced (Thorelli, 1999). Membrane-bound FV and FVa (including the B domain) resulted in an increase in the rate of inactivation of FVIIIa by the APC/Protein S complex when compared to FVa without the B-domain (Lu *et al.* 1996), suggesting that the B region of FVa may be responsible for the cofactor effect of FVa during this inactivation.

In addition, results showed that APC-mediated cleavage at Arg506 converts FV to its anticoagulant cofactor, whereas Arg-306 or Arg679 had no effect on APC-cofactor activity. At the same time this eliminated the remaining procoagulant FV present (Thorelli, 1999). FVa is also inactivated by the cleavage of thrombin or FXa in Arg1545, which results in loss of the B- and A3-domain in FVa (Thorelli *et al.* 1999).

1.4.4 The role of FV in disease (FV Leiden)

Factor V Leiden thrombophilia is an inherited blood clotting disorder, and is the name of a specific gene mutation characterized by a poor anticoagulant response to APC. APC normally inactivates FV by a cleavage at three different amino positions: R 306, R 506 and R 679. The "Factor V Leiden" mutation refers to the specific guanine to adenine substitution at nucleotide 1691 in the *F5* gene, which then predicts the substitution of glutamine for arginine at the Arg 506 APC cleavage site. Because of this amino acid substitution, FVa is resistant to APC and is

inactivated slower than normal, which results in increased thrombin generation (Martinelli *et al.* 1996; Zöller *et al.* 1996; Mazoyer *et al.* 2009).

FV Leiden is the most commonly and inherited form of thrombophilia, where 3-8% of people with European ancestry carry one copy of the mutation, while about 1 in 5000 people have two copies (Genetics Home Reference, 2018). People affected with FV Leiden thrombophilia also show a 50% greater risk of developing deep venous thrombosis (DVT) than the general population (Kreidy, 2012). In addition, FV Leiden increases the risk of clots breaking away from original sites and traveling through the bloodstream, however only about 10 percent of individuals with this FV Leiden mutation ever develop abnormal clots (Genetics Home Reference, 2018).

FV Leiden is often suspected in individuals with a history of VTE. The diagnosis for FV Leiden thrombophilia is established in a proband by identification of heterozygous or homozygous c.1691G>A variant in conjunction with coagulation tests such as APC resistance assay. Evidence has also shown that heterozygosity for the Leiden variant has, at most, a modest effect on risk for recurrent thrombosis after initial treatment of a first VTE (Kujovich, 1999).

1.4.5 Other biological roles of FV

FV has been shown to participate in inflammatory responses. When cleaved by APC in Arg506, it functions together with protein S as a cofactor for APC-mediated anti-inflammatory cell signaling in a sepsis model (of endotoxemia and infection) in mouse (Liang *et al.* 2015). This anti-inflammatory cofactor function of FV involved the same structural features that control FV's cofactor function for the anticoagulant effects of APC, however, the anti-inflammatory activities did not involve proteolysis of activated FVa and FVIIIa (Liang *et al.* 2015).

In addition to its involvement in coagulation and inflammation, FV has other biological roles in the body. A study done on Factor V Leiden showed that homozygous carriers of the prothrombotic FVL polymorphism had an increased risk of colorectal cancer compared to noncarriers, presenting a role of FV in cancer (Vossen *et al.* 2011). A study done by VanDerWater et al (1985) also found that FVa is bound to the plasma membrane surface together with calcium to generate the active enzyme prothrombinase in tumor cells.

Wojtukiewicz *et al.* (1989) studied coagulation mechanisms and found from a staining that FV was present in perivascular and intercellular areas of colon cancer tumors. A more recent study

conducted by Tinholt *et al.* (2014) revealed a connection of *F5* SNPs with breast cancer. A breast cancer cohort and three breast cancer data sets were used to determine the association between the *F5* gene expression (tumor-specific), circulating FV, *F5* SNPs, clinical characteristics and breast cancer survival. It was found that FV was a possible marker of aggressive breast cancer, and also a predictor of favorable outcome for patients. This evaluation may be useful for clinical prognosis and treatment of decisions in aggressive breast cancer (Tinholt *et al. 2018)*.

1.4.5.1 Studies of FV in liver cancer

FV is, as mentioned, synthesized in the liver, and is thus highly expressed in the liver. We studied this expression in comparison to other cancers for illustration. From TCGA data, we found that FV was overexpressed in liver cancer tissue when compared to other cancer types (Figure 6).

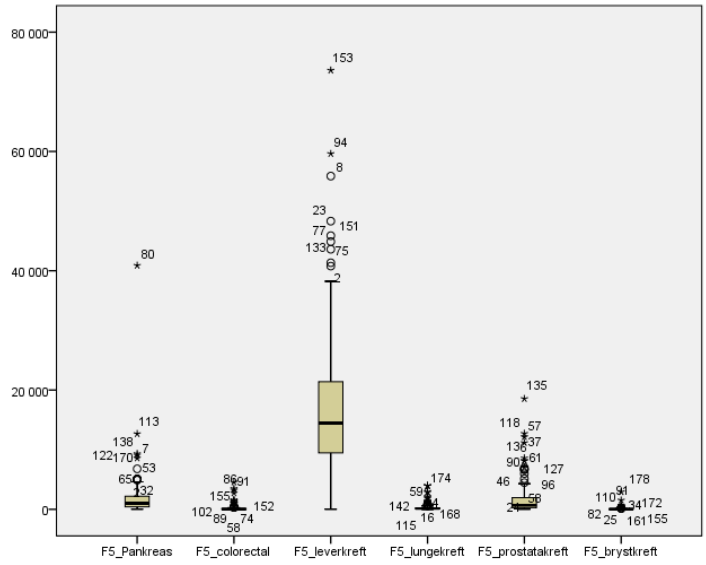

Figure 6: **A comparison of *F5* expression between different cancer types from TCGA data** (McCoig unpublished, 2018).

Figure 7 presents the expression of FV in normal tissue versus tumor tissue in different cancer types, and FV expression is again clearly higher in HCC (red square, Figure 7) compared to the others. Not much difference was observed between the expression in tumor and normal tissue.

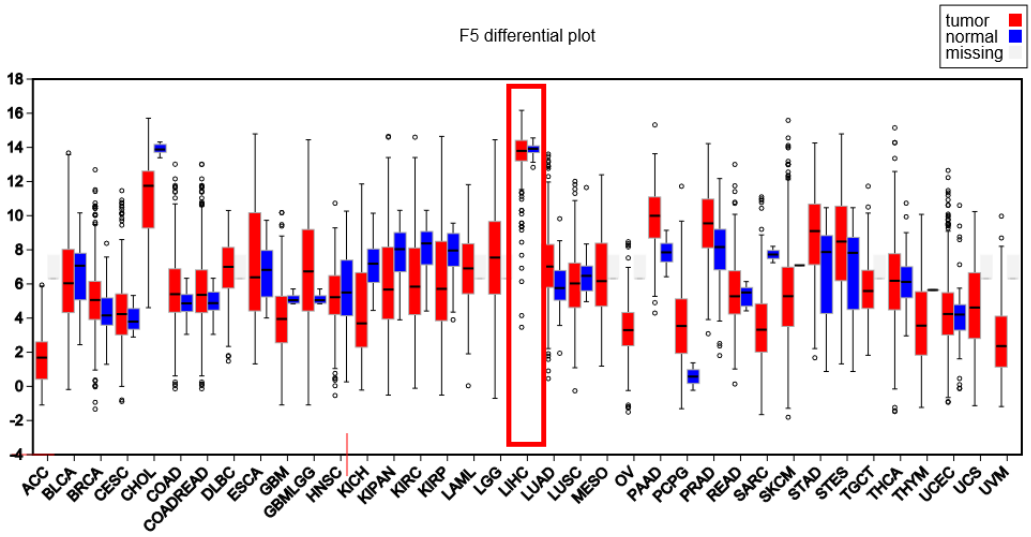

***Figure 7: F5* expression in cancer tissue vs. normal tissue in different cancer types.** Derived from TCGA data (McCoig unpublished, 2018).

The liver consists of different cell types: hepatocytes (or liver epithelial cells), which take up about 60-80% of all cells in the liver, in addition there are hepatic stellate cells (also called fat-storing cells), Kupffer cells (liver macrophages) and liver-derived endothelial cells. Most HCC cells are derived from hepatocytes, including Huh7 and HepG2, however, it is not fully known exactly where all HCC cells originate from (Sia *et al.* 2017).

Multiple cell types may differentiate to hepatocellular carcinoma, and primary liver cancer tumors can be classifies by the tissue of origin, either from mesenchymal cells or from epithelial cells. Thus, FV could be expressed in different cell types in the liver and thereby not exhibiting a big difference in expression between tumors and normal tissue.

The cellular events during hepatocarcinogenesis illustrate that HCC may arise from cells at various stages of differentiation in the hepatocyte lineage. There are four levels of cells in the hepatic stem lineage: bone marrow cell, hepato-pancreas stem cells, oval cell and hepatocyte. All these four levels of cells in the hepatic stem cell lineage may be targets of hepatocarcinogenesis (Wu & Chen, 2006).

1.5 Cytostatic treatment of cancer

1.5.1 Chemotherapy

Chemotherapy is an aggressive chemical drug therapy meant to destroy rapidly growing cells (tumors) in the body. It is considered a systemic treatment, circulating the body, which means it also affects nearly all cells, and is why it can treat cancer cells in almost any tissues. Chemotherapy interferes with the cancer cell's ability to divide and reproduce by damaging the genes inside of the cell nucleus. Thus, it will also cause side effects by affecting healthy tissues where cells are constantly growing and dividing. This involves hair, bone marrow, skin and the lining of the digestive system (©Cancer Research, 2017). However, because cancer cells divide more rapidly and more uncontrollably than normal cells, chemotherapy is more likely to kill the cancer cells than normal dividing and healthy cells in the body (HealthLine®, 2016).

1.5.2 Chemotherapy and coagulation

The fact that cancer patients have a highly increased risk of venous thrombosis, is well documented. In fact, the overall risk of thrombosis was increased 7-fold in patients with a malignancy when compared to persons without (Blom *et al*. 2005). In addition, cancer chemotherapy is a major contributor to the increased thrombosis incidents in cancer patients. Studies have shown that higher incidences of thrombosis occurred during chemotherapy in about 17% in breast cancer patients, but the effect was also seen for multiple myeloma patients, confirming the association between chemotherapy and thrombosis (Goodnough *et al.* 1984; Libourel *et al.* 2010).

Chemotherapy can affect the body and increase the risk of thromboembolic diseases in patients through alterations in blood flow and damage of endothelial cells. (Kim *et al*. 2011; Letal & Kuter. 1999). The treatment can cause a reduction in the levels of anticoagulant protein C and S.

In order to prevent this chemotherapy-related thrombosis, the mechanism behind it needs to be understood, and many studies have been conducted in order to uncover this. Cytotoxic chemotherapy contributes to the risk of thrombosis in several ways. It induces vascular injury through apoptosis. Platelets are considered to play a critical role in increased thrombotic risks in the patients under chemotherapy, however the exact mechanisms are not yet fully understood (Bernat & Herbert, 1994; Togna *et al.* 2000). Following exposure to prothrombotic stimuli,

platelets undergo aggregation under exposure to prothrombotic stimuli and express procoagulant activity through phosphatidylserine (PS) exposure and thrombin generation (Gawaz, 2004; Ruggeri, 2002; Lentz, 2003). In addition, platelets release vasoactive mediators like serotonin and thromboxane (Lee *et al.* 1998).

1.5.3 Doxorubicin

Doxorubicin has been shown to be associated with a 7-fold increase in the risk of deep vein thrombosis in patients with multiple myeloma (Zangari *et al.* 2001). Doxorubicin is an anthracycline anticancer cytostatic drug used for treatment of a range of different types of cancers, including liver cancer.

Doxorubicin's mode of action involves two proposed mechanisms. One is the intercalation between adjacent basepairs of the DNA double helix, and binding DNA-associated enzymes like topoisomerase, and effect on membranes (Bodley *et al.* 1989). The other mechanisms comprise the generation of free radicals and their damage to cellular membranes, DNA and proteins (Thorn *et al.* 2011). In short, doxorubicin is oxidized to semiquinone, an unstable metabolite, which is then converted back to doxorubicin in a process that releases reactive oxygen species. This can lead to lipid peroxidation, and membrane damage, DNA damage, oxidative stress, and triggers apoptotic pathways of cell death (Doroshow, 1986). Alternatively, doxorubicin may also enter the nucleus and poison topoisomerase-II, resulting in DNA damage and cell death as well (Tewey *et al.* 1984).

Studies have shown that doxorubicin induces apoptotic signaling mechanisms, and the transcription factor p53 has an important role in apoptosis. Mutational inactivation of p53 is also frequently observed in multiple human cancers (included liver cancer), and the activation of p53 promoting apoptosis in tumor cells is a key mechanisms in antitumor drugs like doxorubicin (Lowe *et al.* 1994; Lotem *et al*. 1996).

1.6 In-vitro knockdown cell models in liver cancer

Technological advances in molecular biology of human or mammalian cells *in vitro* have increased the ability to introduce functional genes into a variety of cell types. Cancer cell lines are valuable models for studying cancer as they are easily manipulated and molecularly

characterized (van Staveren *et al*. 2009). In addition, research into characterization of cancer cell lines gives important insights into biological mechanisms involved in disease and is essential for development of new anticancer drugs and understanding the pattern of sensitivity/resistance of chemotherapeutics already in use (Louzada *et al.* 2012; Engel *et al.* 1978). Most commonly, studies on specific gene function in cell models are done by creating either overexpression models or knockdown models of specific genes.
Overexpression of a certain gene is a complicated process where specific genes are expressed more excessively than normal, and may result in mutant phenotypes. However, it provides an alternative and powerful tool to identify pathway components that might remain undetected using traditional loss-of-functional (knockdown) analysis (Prelich, 2012). A study in 1983 established two major advances in use of overexpression models: that so called library screens were used to identify the targets, and showing that overexpression libraries could be used as both functional probes to clone genes by complementation, and used to identify phenotypes on wild-type cells (Rine *et al.* 1983).

Knockdown *in vitro* can be achieved through RNA interference (RNAi). RNAi is a highly conserved process of posttranscriptional gene silencing, allowing loss of gene function analysis in mammalian cells and animal models (Fire *et al*. 1998; Zamore *et al*. 2000). The RNAi technology uses short interfering RNA (siRNA) molecules to knock down expression of a gene of interest. There are several ways to induce RNAi: either by synthetic molecules, RNAi vectors, and *in vitro* dicing (Dominiska & Dyxhoorn, 2010).

In mammalian cells, siRNAs initiate the specific degradation of a targeted cellular mRNA. In the process of gene knockdown, dsRNAs derived from convergent transcription or from hairpin-structured RNAs, are cleaved by the RNase III family member called Dicer into duplexed siRNAs (Okamura *et al.* 2008). The antisense strand of the siRNA duplex becomes a part of a multi-protein complex, also called an RNA-induced silencing complex (RISC) (Tomari *et al.* 2004). The passenger strand of the siRNA duplex is cleaved and released, leaving the guide strand to direct the activated RISC to the complementary sequence in the target mRNA (Figure 8) (Elbashir *et al*. 2001). The cleaved message is then targeted for degradation which will result in loss of protein expression (Dominiska & Dyxhoorn, 2010). In this thesis factor V was knocked down in the hepatocellular carcinoma cell lines Huh7 and HepG2 by using RNA interference by siRNA transfection.

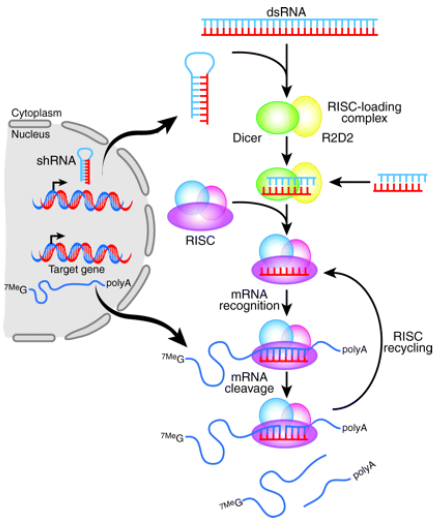

Figure 8: **RNAi-mediated gene silencing**. Large dsRNA or shRNA molecules are transcribed from plasmids in the nucleus and are cleaved by Dicer into smaller siRNA molecules. The siRNAs will associate with proteins and form the RISC complex where the passenger strand of the siRNAs is removed, and the guide strand directs the RISC to complementary mRNA transcripts. Argounate in the RISC will then cleave the mRNA (from Dominiska & Dykxhoorn, 2010).

2. AIMS

It is well known that there is a link between cancer and cancer progression and increased risk of thrombosis. Thus, by studying the molecular connection between cancer and thrombosis, one can achieve a better understanding of these associations and thereby contribute to finding more individualized treatment for cancer patients and for cancer-related thrombosis.
Single nucleotide polymorphisms (SNPs) in the *F5* gene have been identified to be associated with breast cancer. Moreover, *F5* is expressed in breast tumors, and higher expression is a marker for aggressive tumors, yet also better overall survival in breast cancer patients. This suggests FV as a possible tumor suppressor candidate in breast cancer, however the functional relevance of FV in tumor progression is yet to be investigated. Because FV is mainly synthesized in the liver, it was interesting to study the role of FV in progression of liver cancer, in relation to what is already established in breast cancer.

In this thesis, the functional effects of FV downregulation (knockdown) in liver cancer cell lines were studied. In addition, the cell lines were used to study the effect of cytostatic treatment on FV *in vitro*.

The specific aims of this study were as follows:

1) Study the effects of FV knockdown in liver cancer cells
    a. Create a knockdown model of coagulation Factor V (FV) in the liver cancer cell lines; Huh7 and HepG2
    b. Study the functional effects of FV knockdown on cell growth, cell death and cell migration
    c. Studying the molecular mechanisms behind the effects of FV knockdown in cancer progression by cell signalling
    d. Creating a stable knockdown model of coagulation Factor V knockdown in Huh7 and HepG2

2) Study the effects (and sensitivity) of cytostatic treatment in the liver cancer cell lines
    a. Effect on cell proliferation under treatment of doxorubicin
    b. Effect of doxorubicin on FV expression

3. MATERIALS & METHODS

A complete list of solutions, reagents, software, instruments, kits, primers and disposables used during this thesis are listed in the Appendix A, C and D.

3.1 Cell techniques

3.1.1 Liver cancer cell lines

In this thesis, two types of human liver cancer cell lines were used to study the functional role of FV. The HepG2 and Huh7 cell lines (Table 1 and Figure 9) are human hepatocellular carcinoma derived cells and were both used in studies of Coagulation Factor V (FV) knockdown gene expression in association to cell-growth, apoptosis and necrosis, cell migration as well as cell signalling. In addition, the cell lines were used in studies concerning sensitivity to cytostatic treatment.

Table 1: Huh7 and HepG2 cell line characteristics, including ATCC catalogue no., derivation, morphology, growth properties and p53 status.

	HUH-7	HEPG2
ATCC Catalogue No.:	PTA-4583	HB-8065
Organism:	Homo Sapiens	Homo Sapiens
Derivation:	Derived from liver hepatocellular carcinoma of a 57-year-old Japanese male	Derived from liver hepatocellular carcinoma of a 15-year-old Caucasian male
Morphology:	Epithelial (hepatocyte)	Epithelial (hepatocyte)
Growth Properties:	Adherent	Adherent
Growth Media and Serum:	Dulbecco's Modified Eagle Medium (DMEM) supplemented with 10% Fetal Bovine Serum (FBS	Dulbecco's Modified Eagle Medium (DMEM) supplemented with 10% Fetal Bovine Serum (FBS
p53 Status:	Mutated (MUT)	Wild type (WT)

3.1.1.1 Cell Cultivation:

The Huh7 and HepG2 cell lines used were cultured in Nunc™ Cell Culture Treated EasYFlasks™ (T25, T75 and T125). Fetal Bovine Serum was added to the medium because of its growth factors which are necessary for cell growth. Serum also neutralizes Trypsin, which was used to dissociate cell-cell and cell-flask adhesion during splitting of the cells.

The cell lines were incubated in a Steri-cycle CO_2 humidified incubator at 37 °C with 5% CO_2. The cells' morphology and confluence was determined using a Nikon Eclipse TE 300

microscope, and when they reached 80-90% confluence they were split to avoid overgrowth. This was done by discarding the cell culture, washing with DPBS, detaching the cells with Trypsin and adding fresh medium. They were then transferred to a new bottle and incubated.

Both cell lines used were tested for mycoplasma contamination by using the MycoAlert™ Mycoplasma Detection Kit (Lonza) and following the manufacturer's protocol. All cells used in this study were free for mycoplasma.

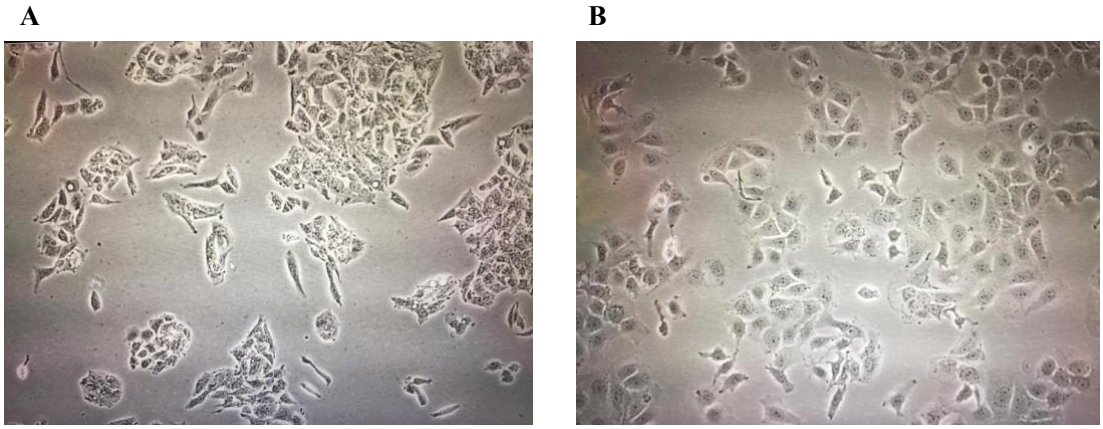

Figure 9: (A) HepG2 and (B) Huh7 Human Hepatocellular carcinoma derived cells during culturing.

3.1.1.2 Cell Quantification:

The NucleoCounter® NC-100™ was used following the manufacturer's manual, to count the cells. In short, 100 µl cell suspension was mixed with 100 µl Reagent A100 (lysis buffer) and 100 µl Reagent B (neutralizer). The suspension was loaded into a NucleoCasette, which contains propodium iodide (PI), a fluorescent dye that stains cell nuclei, by binding DNA, and then counts the cell number per mL.

3.1.2 Transient transfection with *F5* siRNAs

3.1.2.1 Screening of *F5* siRNAs by transient transfection in Huh7

Transfection concerns the process of introducing foreign genetic material (DNA or RNA) into eukaryotic cells, thereby making them genetically modified. In transient transfection, the introduced materials only exist in the cells for a limited time period, and do not integrate into the cells' genome. This enables studies of gene function and expression in live cells (Recillas-Targa, 2006).

F5 specific commercial siRNAs of two different lengths (21mer and 27mer, respectively) were transiently transfected into the Huh7 cell lines by forward transfection, which refers to seeding out cells the day before transfection.

The transfection reagent used was a siRNA-optimized, specially designed cationic lipid Lipofectamine®RNAiMAX reagent (Thermo Fisher). siRNAs are delivered to the cells by the help of the positively charged surface of the liposomal structure formed by the cationic lipids. The positively charged surface mediates interaction with the cell membrane, allowing fusion of the liposome/nucleic acid transfection complex with the cell membrane. When the complex is inside the cell, it diffuses through the cytoplasm and enters the nucleus for gene expression (Figure 10).

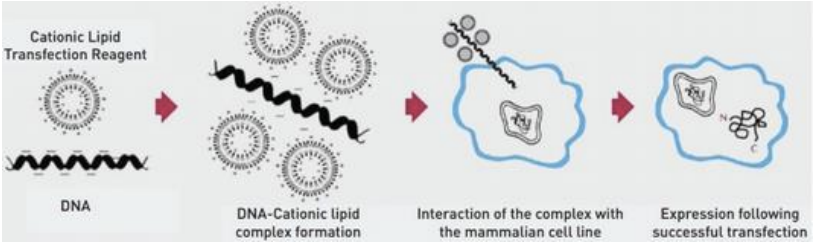

Figure 10: A schematic diagram of the mechanism of cationic lipid-mediated transfection.

The transfection was done to determine which siRNAs would produce the highest knockdown effect of *F5* and which conditions of reagents to use in order to make a knockdown model to study further functional assays of the different cell lines. The various siRNAs used are shown in Table 2.

Table 2: An overview of different FV-siRNAs used in this study, including two negative controls. Lengths, product name, sequence and stock concentrations are showed. The sequences for the negative controls are not shown because these are chosen at random and do not include any of the sequences found in humans.

siRNA:	Product	Length	Sequence	Stock concentration
#SR301500A OriGene	*F5* siRNA duplex	27mer	AAAAUCACAUGAGAUAGACAGUCAT	20 µM
#SR301500B OriGene	*F5* siRNA duplex	27mer	CUUCCAUGAAUUCUAGUCCAAGAAG	20 µM
#SR301500C OriGene	*F5* siRNA duplex	27mer	GGCUGUGAUAUUUACUAGAAUUGAA	20 µM
#SR30004 OriGene	Universal Scrambled Negative Control	27mer	No significant sequence similarity to human gene sequences	20 µM
#s4936 Ambion	*F5* siRNA duplex	21mer	CUGAUGAGGUGAAACGUGA	20 µM
#AM4642 Ambion	Silencer Negative control No.5	21mer	No significant sequence similarity to human gene sequences	50 µM

During the transfection of the different commercial *F5* siRNAs, the ratios and amounts from previous experiments done by the N. Iversen research group were based on the manufacturer's protocol and was also followed for this study, and scaled for 6, 12 and 96-well plate transfection experiments accordingly (Table 3).

Table 3: Details of transfection reagents, cell number, amounts and ratios shown with scaling for 96-, 12- and 6-well experiments. The volumes and numbers are shown for one well on the different well-plates.

	96-well plate	**12-well plate**	**6-well plate**
Total cell number (Huh7/HepG2)	1.5 x 10^4	1.5 x 10^5	3 x 10^5/3.5 x 10^5
DMEM 10% FBS	190 µl	960 µl	1750 µl
Opti-MEM® medium	10 µl	50 µl	250 µl
siRNA	(1pmol)	(4pmol)	(25pmol)
Lipofectamine®RNAiMAX	0,3 µl	3 µl	7,5 µl
Total volume:	200 µl	1000 µl	2000 µl

3.1.2.2 6-Well plate experiment: Forward transfection in the Huh7 cell line

From the knockdown model produced by trial experiments, three different 27mer *F5* siRNAs (Table 2) were transiently transfected into the Huh7 cell line to achieve a knock down of *F5*. The siRNAs included a combination of the two *F5* specific 27mer siRNA duplexes numbered #SR301500B and #SR301500C (called siRNA B and siRNA C) in addition to a Universal Scrambled Negative Control siRNA duplex, (#SR30004) and siRNA #SR301500A (called siRNA Ctrl. A) as a second control.

The *F5* siRNAs B and C in combination and the negative controls were transfected in parallels using forward transfection. In addition, parallels of non-transfected cells were included for observation. 3 x 10^5 Huh7 cells per well were seeded out in the 6-well plates and incubation overnight. The next day, the different *F5* siRNA- and Lipofectamine® mixtures were prepared according to Table 3. Lipofectamine® and siRNAs were diluted separately in OptiMem prior to a 10-minute room temperature incubation. The mixtures were added to the cells, and the cells were harvested 24, 48 and 72 hours after transfection.

3.1.2.3 12-Well plate experiment: Reverse transfection in the HepG2 cell line

Reverse transient transfection was performed to investigate knockdown in the HepG2 cell line. This type of transfection refers to adding the cells freshly to pre-plated transfection complexes. This technique was preferable for the HepG2 cells, because it showed a higher knockdown efficiency than regular (forward) transfection. HepG2 cells were transfected with the *F5* siRNA B and C, the siRNA negative control, and the siRNA A following conditions and volumes of reagents shown in Table 3 for a six well plate experiment. siRNA mixture was prepared as described in section 3.1.2.2, prior to adding 3.5 x 10^5 cells to each well on the plate. The plates were incubated for 48 and 72 hours before harvesting.

3.1.3 Harvesting of cell-medium and lysate

Cell media and cell lysates (RNA and protein lysates), were harvested from the cells transfected with the *F5* siRNAs and controls. The cell medium from each well was carefully removed and transferred to tubes for analysis of protein expression and necrosis analysis. The cells were first washed (once for RNA lysate harvest and three times for protein lysate harvest) using cold DPBS, making sure to not detach the cells in the process. The cells were then lysed and scraped using 600 µl cold RNAqeous lysis buffer for the RNA lysates, and 300 µl RIPA solution with 1X Halt™ Protease and Phosphatase inhibitor cocktail (1:100 RIPA buffer) for protein lysates. All lysates were collected in tubes and immediately placed on ice. Samples were stored at -20°C for short time storage, and -80 °C for long time storage.

3.1.4 Creation of stable cell lines with FV knockdown

To create stable cell lines, Huh7 and HepG2 cells were transfected using the three cloned shRNAs #301500B and C, and shRNA scrambled negative control (See Section 3.7 and Appendix C, Table C3). Huh7 and HepG2 cells were transfected as described in Sections 3.1.2.2 and 3.1.2.3, and following Table 4.

Because the pSiRPG vector (described in Section 3.3) contains a puromycin resistant gene, cells with incorporated plasmids were selected by culturing cells in the presence of 0.5 µg/µl puromycin for 3 weeks. After selection, the selected cells will be frozen for later use.

Table 4: Details of transfection reagents, cell number, amounts and ratios shown with scaling for 12-well experiment, and the volumes and numbers are shown for one well.

Reagents/cell number	Volumes/amounts
Total cell number (Huh7/HepG2)	3 x 105 / 3.5 x 10^5
DMEM 10% FBS	1745 µl
Opti-MEM® medium	250 µl
shRNA plasmid	2.5 µg
P3000 Reagent	5 µl
Lipofectamine®3000	3.75 µl
Total Volume:	2000 µl

3.2 Nucleic acid methods

3.2.1 Total RNA isolation

Total RNA was isolated from cell lysates using the RNAqeous™ Phenol-free total RNA isolation Kit (Thermo Fisher Scientific), following the manufacturer's protocol. In short, the cell lysate was diluted in 64% ethanol buffer and drawn through a spin column with a RNA binding filter, followed by three washing steps to remove contaminants, before the RNA was eluted. The isolated RNA samples were placed directly on ice before it was stored at -20 °C (-80°C for longer time periods).

3.2.1.1 Measurement of RNA purity and concentration

NanoDrop®ND-1000 was used to measure the concentration (in ng/µl) of the isolated total RNA and cloned shRNA plasmids following Maxi- or Miniprep. Quantity of the samples were measured at 260 nm for nucleic acids and a 260/280 purity ratio (protein) of 2.1 ± 0.2 was adequate.

3.2.2 cDNA synthesis

Complementary DNA (cDNA) was synthesized from the total RNA by reverse transcription using the High Capacity cDNA Reverse Transcription Kit® according to the protocol provided by the manufacturer. The RNA was diluted in nuclease-free water in a 96-well plate to ensure an equal input of RNA for each experiment (500 – 5000ng). The cDNA reaction was prepared as described in Table 5. The plate was sealed and centrifuged before it was run on the 2720 Thermal Cycler using the program listed in Table 6.

Table 5: Multiscribe™ Reverse Transcriptase cDNA reaction mixture for one reaction.

Reagent	Volume	Concentration
10X RT Buffer	5.0 µl	
25X dNTP Mix	2.0 µl	100mM (25 mM of each)
10XRT Random primers	5.0 µl	
Multiscribe™ Reverse transcriptase	2.5 µl	
Nuclease-free water	10.5 µl	
RNA	25 µl	
Total	50 µl	

Table 6: The thermal cycler program optimized for the High Capacity cDNA Reverse Transcription Kit

	Step 1	Step 2	Step 3	Step 4
Temperature (°C)	25	37	85	4
Time (minutes)	10	120	5	∞

3.2.3 mRNA quantification using Real Time qRT-PCR

In this thesis, real time quantitative reverse transcription PCR (RT-qPCR) was used to determine and compare the *F5* mRNA expression in cells transfected with *F5* siRNAs. qRT-PCR detects the PCR amplification as it occurs, allowing determination of the starting concentration of nucleic acid. A qRT-PCR contains a Taqman® probe or, for example, SYBR® Green dye to monitor the accumulation of PCR product. Here, Taqman® based assays were used.

The principle of the Taqman® detection system is based on a fluorescent nucleotide probe designed to anneal to the target cDNA between two synthetic primers. The probe contains a fluorescent reporter dye linked to the 5' end of the probe and a non- fluorescent quencher (NFQ) at the 3' end (Figure 11A). While the probe is still intact, the quencher absorbs the fluorescence emitted from the reporter, because of the close proximity. If the target sequence is present, the probe is cleaved by the 5' nuclease activity of the taq DNA polymerase during primer extension. This will separate the reporter dye from the quencher, and thereby increase the fluorescent signal from the reporter dye. Additional reporter dye molecules are then cleaved from their respective probes with each cycle which leads to an increase in the fluorescence intensity, which is proportional to the amount of target gene expression.

The exponential phase measurement used in real-Time PCR provides the most accurate quantification (Figure 11B). In the exponential phase, the real-time PCR instrument calculates: The **threshold** (which is the level of detection at which a reaction reaches a fluorescent intensity above background), and the **C_T value** (the PCR cycle where the amplification curve reaches the threshold) (Figure 11B).

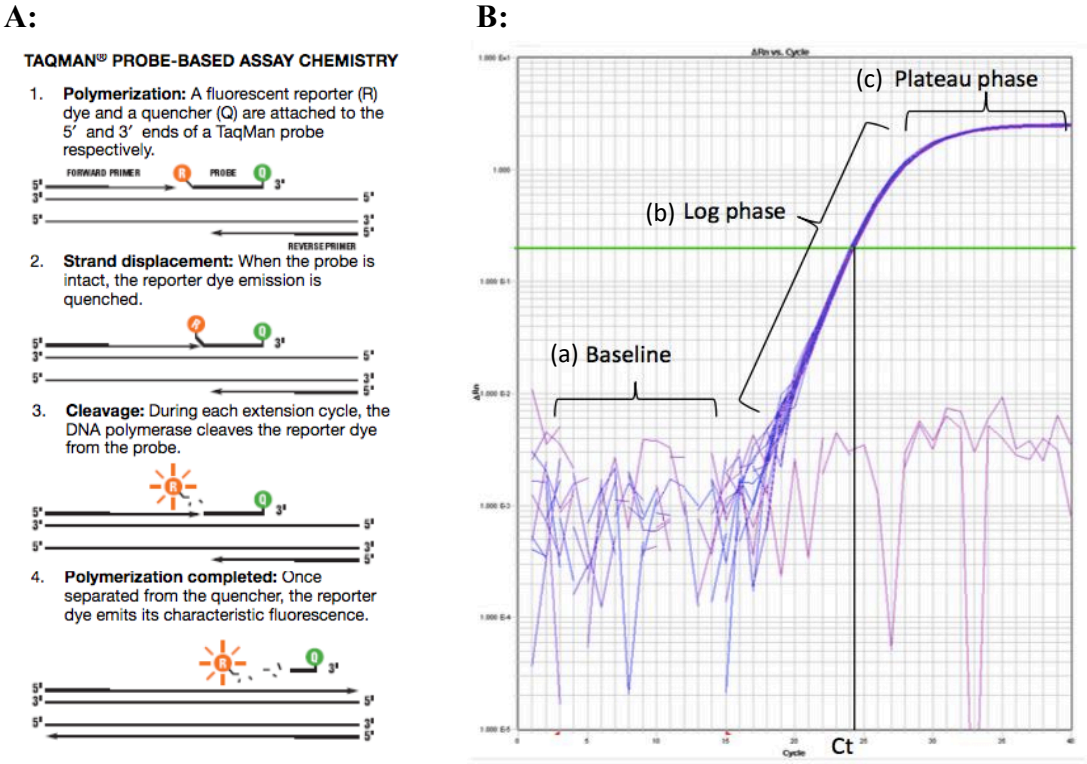

Figure 11: (A) The principle of Taqman® Probe-based assay chemistry in real time qRT-PCR. (B) A qRT-PCR amplification plot showing the baseline phase (a), exponential (log) phase (b) and the plateau phase (c). The green horizontal line indicates the threshold, and the black line indicating the Ct-value is indicated.

The relative changes in gene expression was calculated using the comparative delta C_T method for relative quantitation, which analyses changes in gene expression in a given sample relative to a reference sample. To use this method, the efficiencies of the target and the endogenous control must be <0.1 in slope (this has been previously tested). The C_T values were used to calculate the relative quantity (RQ) to determine the mRNA expression levels of the transfected *F5* siRNAs:

1. $\Delta C_T = C_{T\,(target)} - C_{T(endogenous\ control)}$
2. $\Delta\Delta C_T = \Delta C_{T(Test)} - \Delta C_{T(Control)}$

3. $RQ = 2^{-\Delta\Delta CT}$

In this study, the target sequence was coagulation factor V (FV), while Phosphomannomutase 1 (PMM1) was used as an endogenous control because it was unaffected by up- or downregulation of FV (this was previously tested). GAPDH (Glyceraldehyde 3-phosphate dehydrogenase) was tested against PMM1, and found to be best for use in doxorubicin experiments. The endogenous controls were used as references to correct for variations in cDNA template input or reverse transcriptase efficiency. The real time qRT-PCR reaction mixture was prepared (Table 7) with an equal amount of cDNA (in ng) within the same run. A non-template control (NTC) sample was added for each assay, containing water instead of cDNA. Samples were run in triplicates in a 384 well plate, with 10µl reaction volume in each well (Table 7) and analyzed using the QuantaStudio 12k Flex Instrument with the parameters listed in Table 8.

Table 7: Taqman reaction mix used for one real-time qRT-PCR reaction (one well on the 384-well plate).

Reagents	**Volume**
Taqman® Gene expression master mix (2X)	5 µl
Assay (20X)	0.5 µl
cDNA	4.5 µl
Total volume:	10 µl

Table 8: Cycling Parameters in RT-qPCR

	Step 1	**Step 2**	**Step 3 (x 40)**	
Cycle			1	2
Temperature (°C)	50	95	95	60
Time (minutes)	2’	10’	15’’	1’

3.3 Cloning of F5 shRNA in the pSiRPG vector

In order to study the FV knockdown effect in the liver cancer cell lines over a longer range of time than what is possible for transient transfection, a cloning of *F5* shRNAs in the pSiRPG vector was done prior to transfection and selection for stable cell lines (Figure 12).

Three plasmids were made containing inserted shRNA for siRNA #301500B (called shRNA B from now on) and #SR301500C (called shRNA C), and a Negative Control (scrambled version

of siRNA B) (see Table C3, Appendix C). The shRNAs were constructed towards the SQLE gene (from Dharmacon) because they are complementary to different parts of the SQLE-transcript. The shRNAs include *BstXI* and *BglII* overhangs in the 5' and 3' end which are complementary to the restriction sites in the pSiRPG vector (Figure 12). This allows them to be cloned in the vector. In addition, they consist of the target mRNA sequence, a hairpin loop and the sequence binding to the transcript.

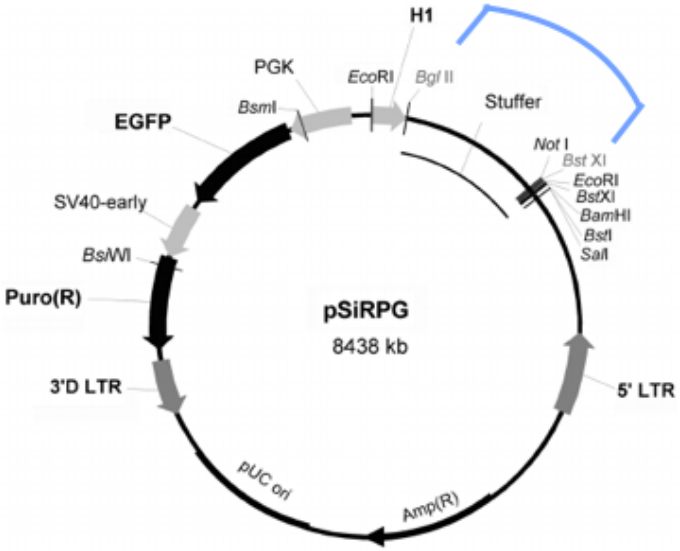

Figure 12: **Schematic map of the pSiRPG vector.** The FV shRNAs are cloned downstream of the H1 promoter, using the *BglII/BstXI* restriction sites (marked by blue lines), removing the stuffer sequence in the cloning process. All promoter sequences are shown in light gray. The purmycin resistance gene (PuroR) and the EGFP marker is shown in black. The size of the vector is 8438kb (Modified from Størvold *et al.* 2007).

3.3.1 Restriction enzyme digestion and ligation of plasmid

The three FV shRNAs were cloned into the pSiRPG vector using the restriction sites *Bgl*II and *Bst*XI. The vector was digested with restriction enzymes *BglII* and *BstXI* and the siRNA oligonucleotides were annealed and ligated into the vector fragment. The digestion was done using the two enzymes in addition to the 10X Fast Digest Buffer and the reaction was incubated at 37°C for 30 minutes for complete digestion (Table 9). This was followed by an inactivation by heating the reaction to 80°C for 5 minutes, before an agarose gel was run. Annealing was done following Table 10, adding sense, and anti-sense from the *F5* siRNA oligos to the mixture before a 10-minute incubation at 96°C.

Table 9: Reagents and volumes used in the restriction enzyme digestion

Reagent:	**Volume :**
Nuclease-free water	x µl
10X Fast Digest Buffer (Green)	4 µl
*Bgl*II enzyme	2 µl
*Bst*XI enzyme	2 µl
pSiRPG vector	x µl (1µg)

Table 10: Reagents and volumes used in one annealing of *F5* siRNA oligos

Reagent:	**Volume :**
siRNA Oligo: sense	1 µl
siRNA Oligo: antisense	1 µl
5XT4 Buffer	4 µl
Nuclease-free water	14 µl

3.3.2 Agarose gel electrophoresis

An agarose gel electrophoresis separates negatively charged macromolecules by size using an electric field. Separation occurs since smaller molecules move faster through the gel pores than larger molecules. The fragments can be visualized because the gel contains GelRed, which when bound to DNA and exposed to ultraviolet light, emits light. The agarose gel electrophoresis was performed to verify the cutting (digestion) of the pSiRPG vector.

Samples were loaded directly to the gel and electrophoresed for 1 hour with 80 Volts in a 1% agarose gel. The gel was photographed using the Omega Lum G imaging system, and the fragments were compared with a Generuler DNA Ladder Mix to estimate sizes. The samples were then purified with Wizard® SV Gel and PCR Clean-Up prior to ligation with shRNAs following table 11.

Table 11: Reagents and amounts used in the ligation reaction

Reagent:	**Volume :**
Oligo-mix (annealed shRNAs)	1 µl
Cut and cleaned pSiRPG vector	x µl (100 ng)
5XT4 Buffer	2 µl
T4 Enzyme	2 µl

3.3.3 Transformation of competent *Escherichia coli (E.coli) cells*

OneShot® TOP10 Chemically competent *E.coli* cells were transformed with FV shRNA B, C and the shRNA negative control in order to produce enough plasmid for making stable cell lines with FV knockdown.

The chemically competent *E.coli* cells were transformed according to Invitrogen OneShot® TOP10 Chemical Transformation Protocol. In brief, 1µg of each plasmid was added to competent *E.coli* cells, and the cells were heat-shocked at 42°C for uptake of plasmids into the cells. The cell solution was incubated for 1 hour in SOC-medium before it was spread on LB agar plates (Appendix D) containing 100µg/mL ampicillin, to select for transformed colonies.

3.3.4 Isolation and purification of plasmid DNA from *E.coli* cultures

Amplification of the plasmids was achieved by picking single colonies of transformed cells for each plasmid and culturing in Lurian Broth (LB) - medium containing 100µg/mL ampicillin, before incubation overnight at 37°C and 200rpm.

Isolation and purification of plasmid DNA from the bacterial culture was performed using the Zuppy™ Plasmid Miniprep Kit for rapid purification of small samples, while ZymoPURE™ Plasmid Maxiprep kit from Zymo research was used for larger samples following the manufacturer's protocol. The principles for the two kits are somewhat the same. However, incubation times for culturing transformed cells using the Miniprep plasmid Kit is 16-24 hours in approximately 4mL selective LB medium containing 100µg/mL ampicillin. For the Maxiprep Kit, a pre-incubation of 8 hours in 4mL selective LB medium containing 100µg/mL ampicillin is required before the culture was added in 150mL of the same medium and then incubated for another 16-24 hours.

3.3.5 DNA Sequencing

Sanger sequencing of the shRNA B, C and the negative control plasmids was performed to confirm the correct sequences. In Sanger sequencing, DNA polymerase will incorporate nucleotides but the nucleotide mix also contains nucleotides lacking the 3' hydroxyl group (ddNTP), and adding one of these ddNTPs will terminate the extension randomly. This results in many fragments with different lengths which are separated by size in capillary columns. The nucleotide analogues are labelled with different fluorescent dyes which make it possible to determine the sequence.

Table 12 presents the reagents used in one sequencing reaction. For each sample one reaction with shRNA forward primer, and one reaction with shRNA reverse primer were run. The products from the reactions were sequenced in the ABI3730 sequencing Analyser. For alignment with the siRNA B, siRNA C and the scrambled siRNA negative control sequences in Sequence Scanner Software 2.0 and BLASTn was used.

Table 12: Reagents and volumes used in one sequencing reaction

Reagent:	**Volume :**
Nucleae-free water	x µl
Plasmid	150 ng
5X Sequencing buffer	2 µl
Primer (forward or reverse)	1 µl
Big Dye® Terminator v3.1 Ready Reaction Mix	0.25 µl

3.4 Protein techniques

3.4.1 Total protein assay

Total protein quantification was performed on the cell lysates from the transfected cell lines to determine total protein concentration in the lysates. The quantification was done using the PIERCE® BCA Protein Assay Kit. The assay depends on a biuret reaction involving production of a light blue to violet coloured chelate complex with cupric ions in an alkaline environment of peptides containing three or more amino acids (proteins, tripeptides and larger polypeptides). The assay also includes colour development reaction where bicinchoninic acid (BCA) reacts with the reduced (cuprous) cation formed in step one and forms an intense purple-coloured reaction product.

In short, a standard dilution series containing five concentrations of Albumin was prepared. The protein lysates were centrifuged at 3500 rpm for 10 minutes to eliminate cell debris. 5 µl of all standards, and samples including one blank were added to a 96-well plate in triplicates before adding 200 µl BCA working reagent (reagent A+B in 1:50 ratio) to the plate as well. The plate was incubated at 37 °C for 30 minutes before absorbance was measured at 570nm using the VersaMax microplate reader. The protein concentrations in the samples were calculated using the SoftMax Pro 6.4 software with a quadratic fit standard curve (See appendix B).

3.4.2. Factor V Enzyme-Linked Immunosorbent Assay (FV ELISA)

Enzyme-Linked Immunosorbent Assay (ELISA) is a common immunoassay used to quantify and detect specific proteins in a sample. The sandwich-ELISA method is a type of capture assay that binds the antigen to be measured between two layers of antibodies, the capture antibody and the detection antibody (Figure 13). In this thesis, the ELISA ZYMUTEST FV was used and the detection antibody is coupled to horse-radish-peroxidase (HRP) and colour develops when the peroxidase substrate tetramethylbenzidine (TMB) is introduced.

The ELISA ZYMUTEST FV to detect the FV protein levels in the culture media of FV knocked down cells. The ELISA test was performed following the manufacturer's protocol closely. The microplates used, had wells pre-coated with monoclonal antibody for FV in which samples were added directly. In addition, standard solutions with concentrations ranging from 0 to 200 ng/mL and a high and low FV control, was included. Added samples, standards and controls were incubated for two hours at 37°C before the polyclonal secondary antibody (HRP) was added. Then followed a second incubation prior to the colour development step by adding the TMB and hydrogen peroxide. The colour gradually appeared, and the amount of colour developed, correlates to the amount of protein present in each sample. The development is stopped by adding sulfuric acid after 10 minutes. Absorbance was measured at 450nm with a 690nm reference wavelength using the VersaMax™ microplate reader. The standards with known concentrations created a standard curve in the SoftMax Pro6.4 software from which concentrations of our samples were determined from (see appendix B).

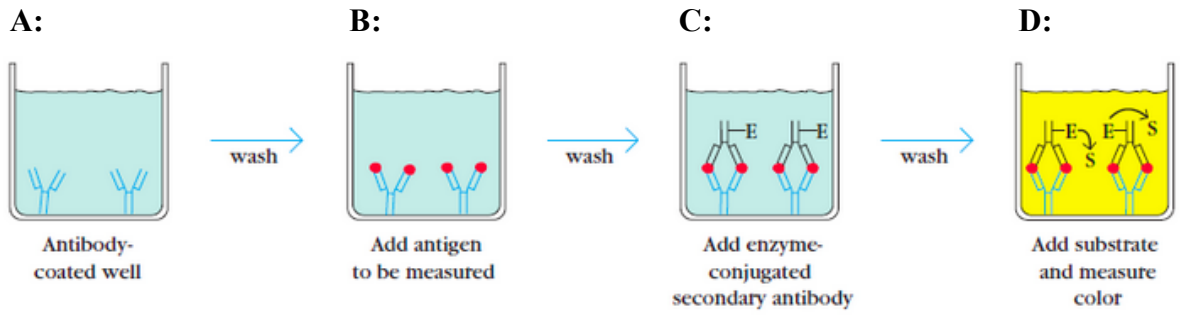

Figure 13: **Diagram of sandwich ELISA assay illustrating the main steps of the methods**. A) The antibody is attached to the well. B) Analyte (or antigen) to be measured is added and binds to the antibody. C) The detection antibody is added and binds to the specific protein investigated. D) Substrate is added, and the colour changes in accordance to protein concentration.

3.4.3. Western blot analysis

Western Blot is a semi quantitative immunoassay method for identifying proteins where an antibody is used to specifically detect its antigen. The specificity of the antibody-antigen interaction identifies the target protein in a complex protein mixture.

The western blot was performed by loading 10µg protein lysates with Precision Protein™ Dual Color Standard onto 10% precast Mini-PROTEAN® TGX™ gels (BioRad Laboratories, Inc.). The samples and standards were blotted onto 0.2µM Nitrocellulose Membranes (Bio-Rad Laboratories, Inc.) and blocked with 5% BSA for one hour to prevent non-specific binding of proteins to unbound membrane sites. After washing the membranes with Tris-buffered saline with Tween 20 (TBST) (see appendix D), they were incubated overnight at 4°C with a target specific primary antibody that will bind to the specific protein of interest. The membranes were then washed a second time, and incubated with a species-specific secondary antibody at room temperature for one hour, which binds to the primary antibody.

In this thesis, western blots were performed to detect the presence of activated JNK by Anisomycin under FV knockdown in Huh7 cells. A rabbit polyclonal Phospho-JNK primary antibody was applied in a 1:1000 dilution, before adding the secondary rabbit antibody labelled with horseradish peroxidase (HRP). In addition, western was performed to detect FV protein in Huh7 and HepG2, the Mouse Anti-Human FV (added in a 5ug/ml concentration) was added as the primary antibody, before adding the secondary rabbit antibody.

The blots were developed using the Amersham™ ECL™ Prime Western Blotting Detection Reagent kit (GE Healthcare UK). Exposure of the blots was performed on the ImageQuant™ LAS 4000, with ImageQuant™ TL 1D v8.1.

3.5 Functional assays

3.5.1 Measuring cell proliferation

The effect of FV knockdown on cell proliferation (cell growth) in Huh7 and HepG2 cell lines were studied using the Cell Proliferation reagent Wst-1. Wst-1 is a tetrazolium salt that is cleaved to form formazan dye. The amount of dye produced after adding Wst-1 to the cell will directly correlate to the number of metabolically active cells in the samples/wells.

The assay was performed by adding 20 µl Wst-1 reagent to cell containing wells in a 96-well plate 1, 24, 48 and 72 hours after reverse transfection with the 27mer *F5* siRNAs and negative controls (Table 2) as described in 3.1.2.5. The plates were incubated for 30 minutes at 37°C and 5% CO_2 before absorbance was measured at 450nm with 750nm as reference, using the VersaMax microplate reader and the SoftMax Pro 6.4 software.

3.5.2 Measuring apoptosis

To study the effect of FV knockdown on apoptosis in Huh7 and HepG2 cell lines, the Cell Death Detection ELISA^{PLUS}® Kit was used. This cell death assay is based on a quantitative sandwich-enzyme-immunoassay-principle using two monoclonal antibodies directed against DNA and histone. This allows the specific determination of mono- and oligonucleosomes in the cytoplasmatic fraction of cell lysates. The sample is placed in a streptavidin-coated MP, before Anti-histone-biotin and Anti-DNA-POD are added and the ELISA-plate is incubated. During the incubation, the Anti-histone antibody binds to the histone component of the nucleosomes and simultaneously captures the immunocomplex to the streptavidicin-coated MP via its biotinylation. Unbound components are then removed in a washing step, and finally, quantitative determination of the amount of nucleosomes by the POD retained in the immunecomplex is done. The POD is determined photometrically with ABTS Substrate (Figure 14).

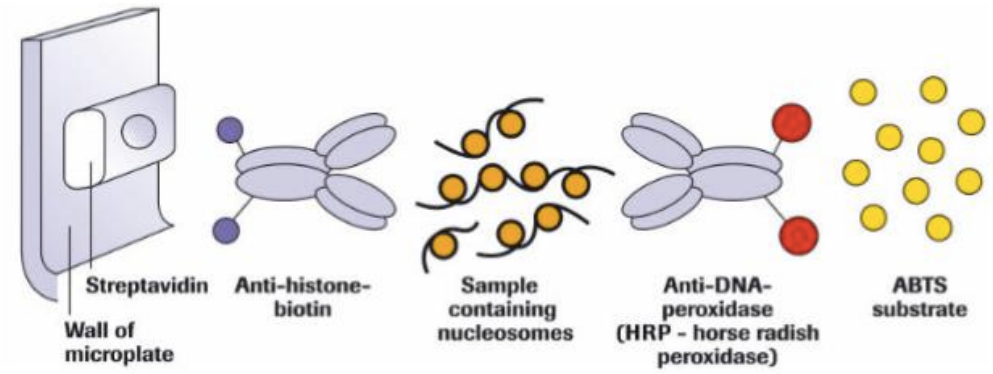

Figure 14: Schematic figure showing the principle of the Cell Death Detection ELISA^{PLUS}.

In this study, the effect on apoptosis and necrosis with FV knockdown was studied in the protein lysates (apoptosis) and medium (necrosis) harvested 48 and 72 hours after transfection (see Sections 3.1.2.4 and 3.1.3). The assay was performed by following the manufacturer's protocol closely. In short, 20 µl sample (diluted 1:10) was added to each well on a 96-well plate, before adding 80µl Immunoreagent. The plate was then incubated on an MP shaker at room

temperature for 2 hours prior to three rinsing steps, and 100 µl of ABTS solution was added to the wells. The plate was then incubated for 10 minutes before the absorbance was measured using the VersaMax™ microplate reader and SoftMax Pro 6.4 software, at 405 nm (with 490nm reference).

3.5.3 Measuring cell migration by scratch wound assay

The migration of *F5* knocked down cells was studied in Huh7 cells by using the Ibidi® Culture-insert 2-Well µ-Dishes (Figure 15). The cells were reverse transfected in 96-well plates as described in section 3.2.1.5, using three parallels of the *F5* siRNA B and C combination, and the siRNA negative control.

1.8 x 10^4 cells were seeded out in 70 µl of cell media in each well of the insert. 24 hours after transfection, the inserts were removed producing a wound between the cells. 1 mL fresh DMEM 10% FBS medium was then added before the Nikon Eclipse Ts2-FL microscope was used to take images of the closing wound at different time points until the wound was completely closed (48 hours after removing insert, i.e. 72 hours after transfection).

Figure 15: Image showing the Ibidi® Culture-Insert Well for studying cell migration.

3.5.4 Measuring cell signalling under FV knockdown by Cignal™ reporter assay

Cignal™ Reporter Assays were used to study the cancer related signaling pathways in order to identify the pathways most affected by FV knockdown. The Cignal™ Reporter assays include a 10 Pathway Reporter Array and Single Reporter Assay Kits that were used in this study.

All Reporter assays are based on dual-luciferase technology, where each reporter consists of a mixture of a pathway-focused transcription factor-responsive firefly luciferase construct and a constitutively expressing Renilla luciferase construct (20:1) (Figure 16). In addition, a positive control (a constitutively expressing GFP construct, a firefly luciferase construct and Renilla luciferase construct) and a negative control (non-inducible firefly luciferase reporter and a Renilla construct) are included.

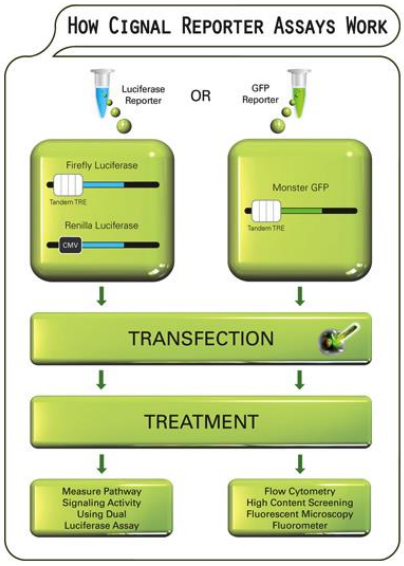

Figure 16: Diagram illustration the function of the Cignal^{TM} Reporter Assay system

The dual-luciferase results are calculated for each transfectant and the change in activity of each signaling pathway is determined by comparing the normalized luciferase activities of the reporter in treated versus untreated transfectants.

3.5.4.1 Cancer 10-pathway reporter array:

The Cignal^{TM} 10-Pathway Reporter Array, Cancer plate contains 10 different pathways related to cancer progression (Table 13). This array was used as a screening to identify signaling pathways activities affected by FV knockdown in liver cancer cell lines.

The Cancer 10-pathway Reporter Luciferase Kit was used according to the manufacturers protocol. In short, reverse transfection of the *F5* siRNA combination B & C in addition to the siRNA negative control was used with 96-well specifications (Table 3). The plate was incubated for 48 hours before the medium was removed and the cells were washed with DPBS and lysed using 20 µl 1xPLB (passive lysis buffer from the Dual-Luciferase® Reporter kit). The plate was then placed on an MP shaker at room temperature for 15 minutes before storage at -80°C until analysis could be done.

Table 13: The 10 pathways and their respective transfection factors included in the Cancer 10-pathway Reporter Luciferase Kit. These are all dried down in each column of the 96-well cell culture plate (there are 8 wells per assay/pathway). Red marked pathways and transcription factors illustrate pathways used for the single reporter assay (described in section 3.4.4.2).

Pathway	Transcription Factor
Wnt	TCF/LEF
Notch	RBP-Jk
p53/DNA Damage	p53
TGF β	SMAD2/3/4
Cell cycle/pRb-E2F	E2F/DP1
NFkB	NFkB
Myc/Max	Myc/Max
Hypoxia	HIF1A
MAPK/ERK	Elk-1/SRF
MAPK/JNK	AP-1
Negative Control	N/A
Positive Control	N/A

3.5.4.2 AP-1 reporter assay (single reporter assay)

The Wnt and JNK pathways were identified as the most affected pathways from the 10-pathway reporter array (Table 13). Thus, the JNK pathway was studied in order to confirm the resulting effects in transcriptional activity under FV knockdown.

The AP-1 Reporter Assay was used according to the manufacturer's protocol. Reverse transfection in 96-well plates were done in the Huh7 cell line (as described in section 3.1.2.3) using the *F5* siRNA B and C in combination, and the negative control siRNA (Table 2) following the conditions stated in Table 3. In addition, signal reporter plasmid for the AP-1 transcription factor was included (Table 13). The plates were then incubated overnight prior to changing medium and addition of the JNK inhibitor. The samples were harvested 48 hours after transfection as described above (Section 3.5.4.1).

3.5.4.3 Analysis by Dual-Luciferase® Reporter (DLR^{MT}) assay system

The plates (lysates) were analysed using the Dual-Luciferase® Reporter (DLR™) Assay System and the Synergy™ H1 microplate reader. The activities of firefly and Renilla luciferases were measured sequentially from a single sample. Firefly luciferase reporter was measured first by adding Luciferace Assay Reagent II (LAR II) to generate a luminescent signal lasting at least

one minute. Then, the reaction was quenched, and the Renilla luciferase reaction is initiated simultaneously by adding Stop & Glo® Reagent to the same sample.

3.5.5 Measuring the effect of AP-1 (JNK) pathway activation on apoptosis under FV knockdown in Huh7 cell lines

3.5.5.1 Verification of JNK activator Anisomcyin in Huh7 cells

To investigate the effect of the JNK activator on apoptosis, a verification showing at what dosages and time-points the activator was most effective was done. Huh7 cells were seeded out in 12-well plates, and treated with Anisomycin for either 24, 2 or 30 minutes prior to harvesting. Concentrations of Anisomycin used were 0, 1, 2.5 and 5 μM for all time-points. For 30 minutes treatment, cells were also treated with serum-deprived or non-serum deprived medium for the mentioned concentrations. Cells were harvested 24, 2 and 30 minutes after treatment and Western Blot Analysis was done to verify the effect (See Section 3.3.3).

3.5.5.2 Measuring the effect of Anisomycin on apoptosis in Huh7 cells under FV knockdown

After verifying the activator, the effect of Anisomycin on apoptosis with FV knockdown in Huh7 cells was investigated. This was done by transfecting the Huh7 cells in 12-well plates with siRNA B and C in combination, in addition to the negative control, according to conditions explained in Section 3.1.2.2 and following Table 3. The cells were treated with 0, 1, 2.5 and 5 μM Anisomycin for 48 and 24 hours prior to harvesting. Cells were harvested for protein lysates, 72 hours after transfection (See Section 3.1.3), and apoptosis was measured as described in Section 3.4.2.

3.6 Cytostatic treatment of liver cancer cell lines

3.6.1 Liver cancer cells exposed to increased concentrations of doxorubicin (dose-response doxorubicin treatment)

To study the FV expression in response to different concentrations of doxorubicin in Huh7 and HepG2 cell lines, a study was done by exposing the cells to increased concentrations of doxorubicin.

Cells were seeded out in 12-well plates with 1.5 x 10^5 cells per well before incubation over night at 37 °C and 5% CO_2. The next day, the medium was extracted, and cells were treated with 0 – 50µM concentrations of doxorubicin for incubation for 24, 48 and 72 hours. The cells were harvested for total RNA isolation (as described in Section 3.1.3). Further, the RNA lysates were used for cDNA synthesis and qRT-PCR for analysis of *F5* mRNA expression.

3.6.2 Cell viability in response to increased concentrations of doxorubicin

The cell viability of the HepG2 and Huh7 cell lines in response to increased concentrations of doxorubicin was also investigated. The cells were seeded out in 96-well plates, with 1 x 10^4 cells in each well. Doxorubicin was added to the wells the next day with increased concentrations of doxorubicin; 0 - 100 µM. After 24, 48 and 72 hours of doxorubicin treatment, 20µl Wst-1 reagent (explained in section 3.4.1) was added to each well, and the absorbance was measured at 450nm and at 750nm as reference, using the VersaMax™ microplate reader and SoftMax Pro 6.4 software. Eight parallels were measured for every transfected siRNA (and for the non-transfected cells) on the plate. In addition, one parallel containing only medium for each doxorubicin concentration was measured to correct for background absorbance.

3.7 Statistical analysis

For statistical analysis in this thesis, the un-paired t-test and ANOVA analysis was used to compare samples in two or multiple groups, respectively. The datasets were assumed normally distributed, independent of each other and with equal variance. A probability value of $P \leq 0.05$ was considered significant, this is indicated by a "*" in figures showing significant differences. Significance between siRNA B and C in combination and the siRNA negative control in cell growth, cell death and cell migration experiments were calculated by t-test Significance in all transfected and non-transfected cells in cell proliferation assays were calculated by ANOVA, and by following Tukey post hoc tests if the ANOVA assays were seen to be significant.

4. RESULTS

4.1 Downregulation of FV in liver cancer cells

4.1.1 Screening of siRNA oligonucleotides for *F5* downregulation in Huh7 cells

To study the functional effects of FV in liver cancer, a knockdown model was created. In order to achieve the most efficient knockdown in the Huh7 cell line for use in further functional studies, a screening of six commercial *F5* siRNAs of two different lengths; two 21mer and four 27mer *F5* siRNAs, including a negative control siRNAs was conducted. The screening was done by transient transfection in the Huh7 cell lines. The FV knockdown effect was analysed at mRNA level by qRT-PCR (Figure 18).

Among the tested siRNAs, the 27mer siRNAs 301500B and 301500C (called siRNA B and C from now on) showed the highest knockdown efficiencies with 71% and 79% knockdown of FV, respectively, compared to the negative control siRNA SR30004 (Figure 17). The 21mer *F5* siRNA s4936 was less efficient with a knockdown efficiency of 61%, when compared to its negative control. The 27mer siRNA 301500A (called siRNA control A) showed no FV knockdown when compared to the negative control. The siRNA sequence was checked using BLAST software and had no similarity to the *F5* gene, which was also later confirmed by the manufacturer. This siRNA was thus further used as an additional negative control.

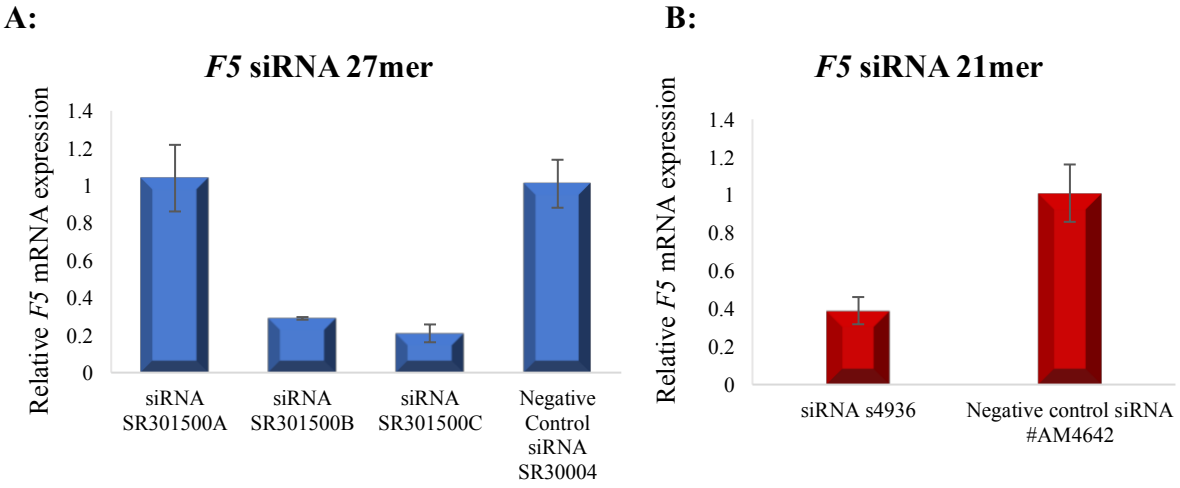

Figure 17: **Relative *F5* mRNA expression levels in Huh7 cells transfected with siRNAs against *F5*.** Huh7 cells were transfected with the indicated *F5* siRNAs and harvested 24 hours after transfection. *F5* mRNA expression was measured using qRT-PCR and normalised against PMM1 as endogenous control. The results are expressed as RQ values compared to the siRNA controls. Mean values (n=3) and +SD of one experiment are presented.

4.1.2 Optimization of *F5* downregulation in Huh7 cells

Based on the screening of *F5* siRNAs in Section 4.1.1, we decided to use only the two most efficient *F5* siRNAs for further studies. The 27mer siRNA B and C were used to further optimize the FV knockdown. siRNAs B and C were also transfected in combination to investigate if this would yield a higher knockdown efficacy than the two siRNAs transfected separately.

The cells transfected with both *F5* siRNAs in combination showed a FV knockdown efficiency of 88% when compared to the negative control. The two siRNAs transfected separately resulted in a 67% and 69% FV knockdown for siRNA B and C, respectively (Figure 18).

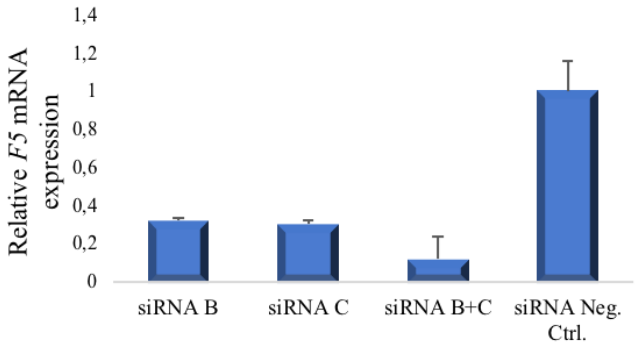

Figure 18: **Relative *F5* mRNA expression levels in Huh7 cells transfected with siRNA B and C.** The cells were harvested 24 hours after transfection and mRNA expression was measured using qRT-PCR, normalised against PMM1 as endogenous control. The results are expressed as relative RQ values compared to the siRNA negative control. Mean values (n=6) and +SD for two experiments are shown.

4.1.3 Time-dependent FV downregulation in Huh7 and HepG2 cells

4.1.3.1 *F5* mRNA expression in Huh7

After having established that the combination of *F5* siRNA B and C yielded the most efficient knockdown of FV in the Huh7 cells, a time-dependent transfection experiment was performed to find the most efficient time points. The *F5* expression was measured 24, 48 and 72 hours after transfection at the mRNA and the protein level (Figure 19 & 20).

The most efficient FV knockdown was obtained 48 hours after transfection with an effect of 87% at the mRNA level when compared to the negative control for this time-point (Figure 19). The effect was still effective 72 hours after transfection with an 80% knockdown when compared to the negative control siRNA.

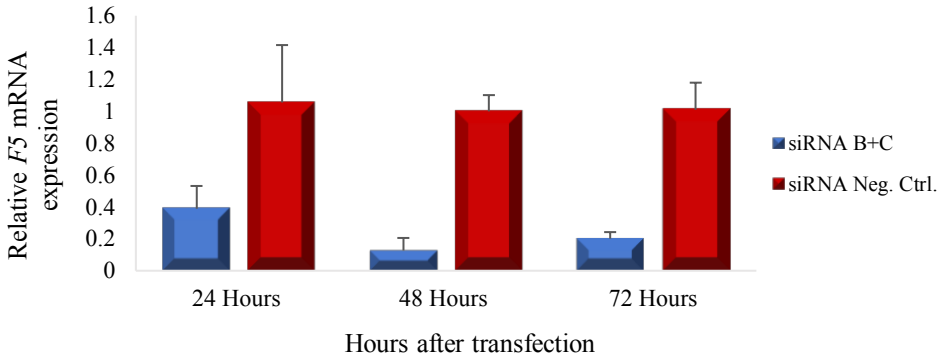

Figure 19: **Time-dependent *F5* mRNA expression levels in Huh7 cells transfected with siRNA B and C**. The cells were harvested 24, 48 and 72 hours after transfection and mRNA were measured using qRT-PCR. They were normalised against PMM1 as endogenous control. Results are expressed as RQ values compared to the negative controls for each time-point. Mean values (n=9) and +SD for three independent experiments are shown.

4.1.3.2 *F5* protein expression levels in Huh7

FV ELISA was used to confirm the knockdown of FV at the protein level in cell media of the FV knockdown cells. No protein could be detected at any time point for cells transfected with *F5* siRNA B and C, confirming the knockdown at the protein level. In contrast, FV protein levels in cells transfected with the negative control siRNA and siRNA control A increased 4-fold from 48 to 72 hours after transfection (Figure 20), and showed similar increase in FV protein level as non-transfected cells (results not shown). FV antigen in cell lysates showed no difference between cells with FV knockdown and control cells for 48 or 72 hours after transfection (results not shown).

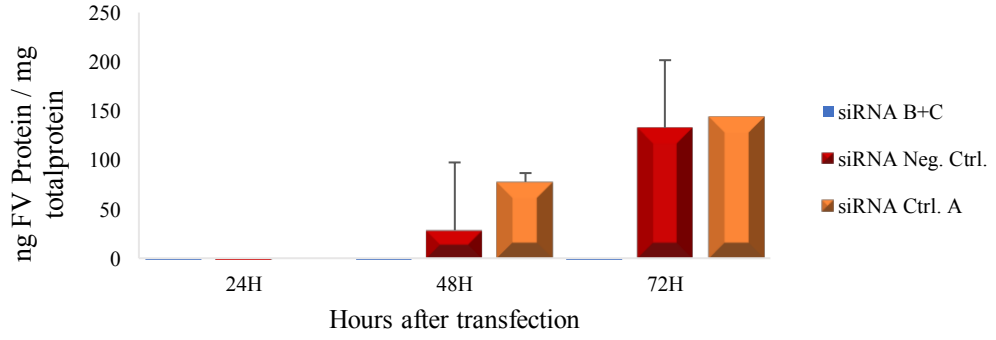

Figure 20: **FV protein levels in medium from Huh7 cells transfected with *F5* siRNA B and C.** siRNA negative control, and siRNA A as a second control was also included in the transfection. Cells were harvested 24, 48 and 72 hours after transfection. FV protein levels were measured by ELISA and corrected for total protein lysate. Mean values (n=9) and + SD from three independent experiments are shown.

4.1.3.3 *F5* mRNA expression levels in HepG2

The knockdown efficiency in the HepG2 cell lines was conducted using the same *F5* siRNAs as established from the Huh7 knockdown model. A time-dependent transfection experiment

was performed in HepG2 at 48 and 72 hours after transfection to measure FV knockdown efficiency at both the mRNA and the protein level (Figure 21 & 22).

The results showed an effective FV knockdown for 48 and 72 hours after transfection; 77% and 76% when compared to the negative control siRNA (red bars) for the respective time point (Figure 21). Cells transfected with siRNA control A showed similar *F5* expression to cells transfected with negative control siRNA.

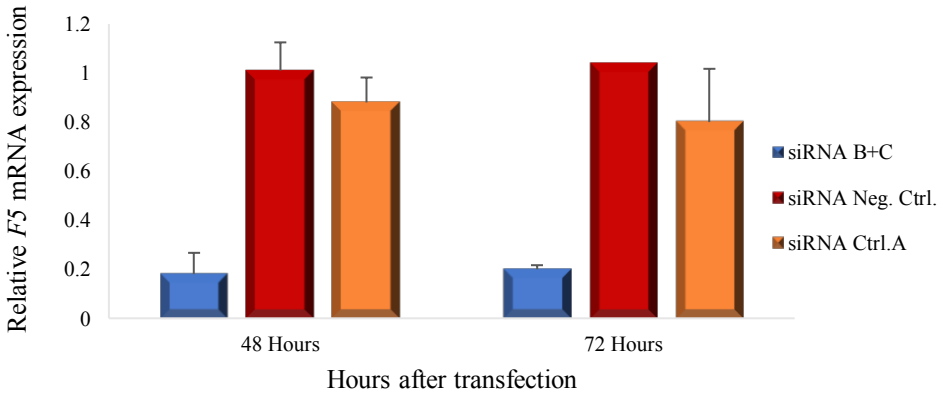

Figure 21: **Time-dependent *F5* mRNA expression levels in HepG2 cells transfected with siRNA B and C**. Cells were harvested 48 and 72 hours after transfection. mRNA was measured using qRT-PCR and normalised against PMM1 as endogenous control. Results are expressed as RQ values compared to the negative controls for each time-point. Mean values (n=9) and +SD for three independent experiments are shown.

4.1.3.4 FV protein expression levels in HepG2

As for Huh7, FV ELISA was used to check FV knockdown at the protein level in HepG2 cells (Figure 22). FV protein was non-detectable in the media of cells transfected with siRNA B and C in combination 48 hours after transfection, and barely detectable after 72 hours when compared to the negative controls. In contrast, FV protein levels in cells transfected with the negative control siRNA and siRNA control A showed an increase of 76% and 48%, from 48 to 72 hours after transfection, respectively. FV antigen in cell lysates showed no difference between cells with FV knockdown and the negative control siRNA for either 48 or 72 hours after transfection (results not shown).

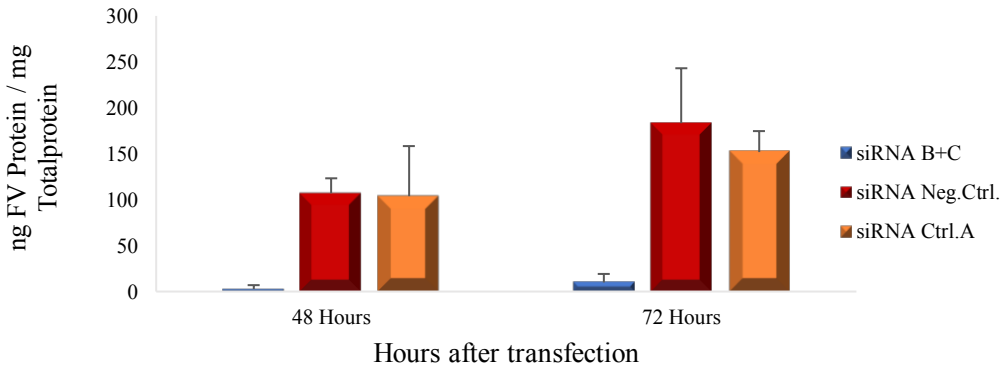

Figure 22: **FV protein levels in medium from HepG2 cells transfected with *F5* siRNA B and C.** In addition, HepG2 cells were transfected with siRNA negative control, and siRNA Ctrl. A as a second control. Cells were harvested 48 and 72 hours after transfection. FV protein levels were measured by ELISA and corrected for total protein lysate. Mean values (n=9) and + SD from three independent experiments are shown.

4.1.4 Stable FV knockdown cell lines

4.1.4.1 Preparation of the pSiRPG/FV shRNA vector

To be able to ligate the pSiRPG vector with the FV shRNAs, linearization of the vector had to be done. The vector was digested with *BglII* and *BstXI* to generate compatible ends for the ligation. Figure 23 confirms the successful digestion of the vector by agarose gel electrophoresis, and it was thereby isolated from the gel and purified for further used (Figure 23, red circle). The shortest fragment observed in the figure is the vector fragment between the restriction sites, indicating both digestion enzymes had worked (Figure 23, red line).

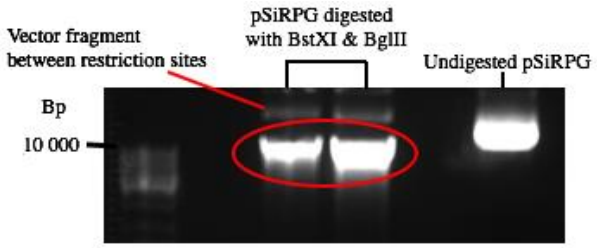

Figure 23: **Agarose gel electrophoresis of pSiRPG/FV shRNA before and after enzyme digestion**. Vector digested with *BglII* and *BstXI* (marked with a red circle) was extracted from the gel and purified. Generuler DNA Ladder Mix was used for comparing sizes of the fragments.

4.1.4.2 Sequencing and transfection of the pSiRPG/FV shRNA plasmids

To confirm the cloning of the FV shRNAs in the pSiRPG vector, the shRNA B, C and the control plasmid from several bacterial colonies were sequenced and aligned against the reference pSiRPG sequence.

As figures 24 and 25 present, the shRNA B and negative control plasmids were successfully introduced into the pSiRPG vector during the cloning procedure, shRNA C was also found to be successfully cloned this way (results not shown). In addition, successful transfection was confirmed by observing green fluorescence protein (GFP) in the transfected Huh7 and HepG2 cells (results not shown).

A

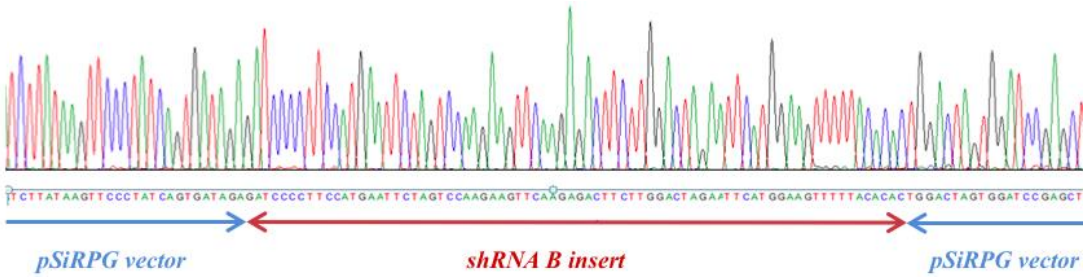

B

Download Graphics

Sequence ID: Query_178903 Length: 75 Number of Matches: 1

Range 1: 1 to 75 Graphics Next Match Previous Match

Score	Expect	Identities	Gaps	Strand
139 bits(75)	4e-38	75/75(100%)	0/75(0%)	Plus/Plus

```
Query  385  GATCCCGAAACTTCCTAACGTCGCTGTATAATTCAAGAGATTATACAGCGACGTTAGGAA  444
            ||||||||||||||||||||||||||||||||||||||||||||||||||||||||||||
Sbjct  1    GATCCCGAAACTTCCTAACGTCGCTGTATAATTCAAGAGATTATACAGCGACGTTAGGAA  60

Query  445  GTTTCTTTTTACACA  459
             |||||||||||||||
Sbjct  61   GTTTCTTTTTACACA  75
```

Figure 24: **Illustrating cloned shRNA B in the pSiRPG vector from sequencing**. (A): illustrating the shRNA B insert in the pSiRPG vector by Sequence Scanner Software 2. (B) Blast sequence alignment of the query sequence obtained from the sequencing and the subject shRNA B sequence, with a 100% identity between them.

A

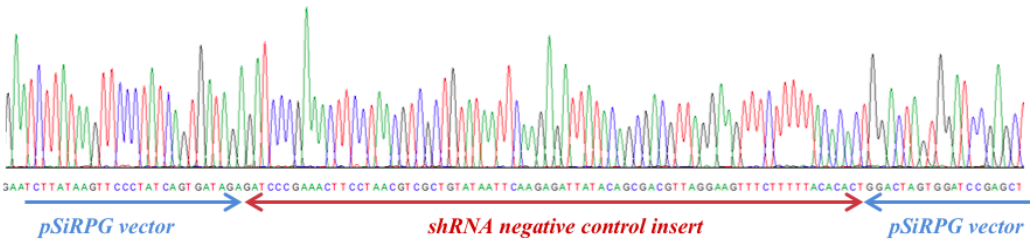

B

Download Graphics

Sequence ID: Query_7119 Length: 75 Number of Matches: 1

Range 1: 1 to 75 Graphics Next Match Previous Match

Score	Expect	Identities	Gaps	Strand
139 bits(75)	5e-38	75/75(100%)	0/75(0%)	Plus/Plus

```
Query  383  GATCCCCTTCCATGAATTCTAGTCCAAGAAGTTCAAGAGACTTCTTGGACTAGAATTCAT  442
            ||||||||||||||||||||||||||||||||||||||||||||||||||||||||||||
Sbjct  1    GATCCCCTTCCATGAATTCTAGTCCAAGAAGTTCAAGAGACTTCTTGGACTAGAATTCAT  60

Query  443  GGAAGTTTTTACACA  457
             |||||||||||||||
Sbjct  61   GGAAGTTTTTACACA  75
```

Figure 25: **Illustrating cloned shRNA negative control in the pSiRPG vector from sequencing**. (A): illustrating the shRNA negative control insert in the pSiRPG vector by Sequence Scanner Software 2. (B) Blast sequence alignment of the query sequence obtained from the sequencing and the subject shRNA negative control sequence, with a 100% identity between them.

4.2 Functional effects of FV knockdown in liver cancer cell lines

4.2.1 Effect on cell proliferation

To investigate possible functional roles and effects of FV knockdown in the liver cancer cell lines, cell proliferation in the Huh7 and HepG2 cell lines were studied using the Wst-1 cell proliferation reagent. The cells were reverse transfected with siRNAs B and C alone and in combination, in addition to siRNA negative control and siRNA control A. Parallels of untreated cells were also included for comparison.

4.2.1.1 Cell proliferation in Huh7

It was observable that all siRNA treatments (included non-transfected cells) in the Huh7 cell line, showed a gradual increase in growth over the measured time points (Figure 26). However, there was no significant differences between the siRNA treatments in the cells established by a one-way ANOVA test, with a following Tukey's multiple comparisons test.

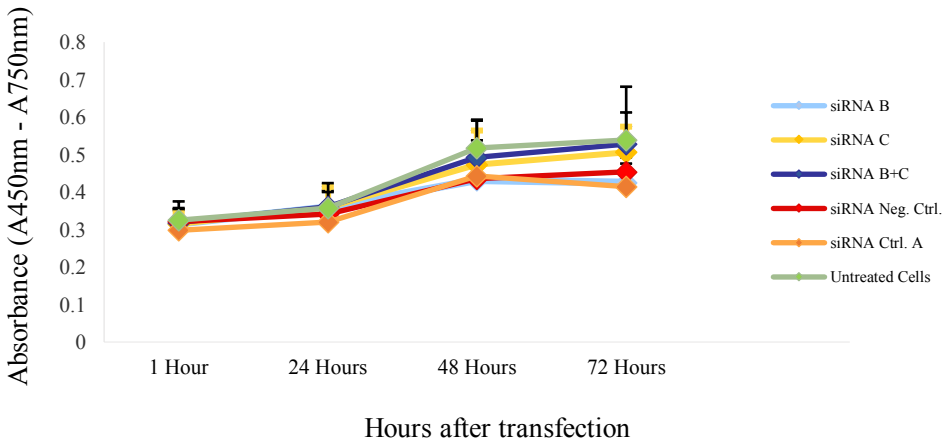

Figure 26: **Cell proliferation in the Huh7 cell line with FV knockdown measured by Wst-1.** The cells were reverse transfected with indicated siRNAs. Cell proliferation was measured by absorbance at 1 to 72 hours after the reverse transfection. Mean values (n=24) and +SD are presented for three independent experiments.

The FV knockdown effect was confirmed by reverse transfection (as described in Section 3.1.2.3), showing a 58-72% effective FV knockdown for each *F5* siRNA when compared to the negative control siRNA (Figure 27).

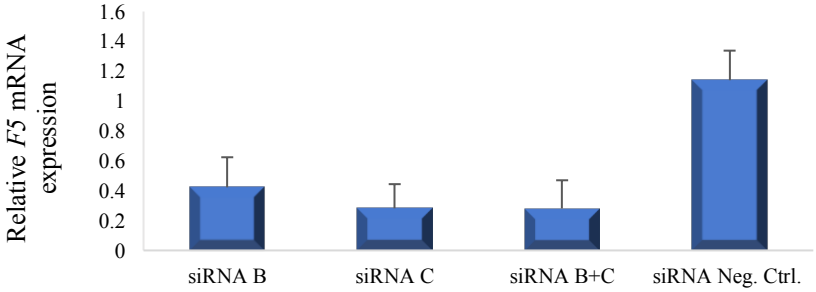

***Figure 27: F5* mRNA expression levels in reverse transfected Huh7 cells.** Cells were transfected with indicated siRNAs and harvested 24 hours after transfection. mRNA expression levels were measured using qRT-PCR and normalised against PMM1 as endogenous control. Results are expressed as RQ values compared to the negative control. Mean values (n=6) and +SD are shown for two independent experiments.

4.2.1.2 Total protein quantification in Huh7 under FV knockdown

Total protein was measured in protein lysates from cells transfected with siRNA B and C in combination, in addition to siRNA negative control and siRNA A (Figure 28). No increase in total protein was observed for cells transfected with the siRNA B and C in combination. Cells transfected with siRNA negative control and control A showed a slight increase of 4.5% and 2.7% in total protein from 48 to 72 hours, respectively.

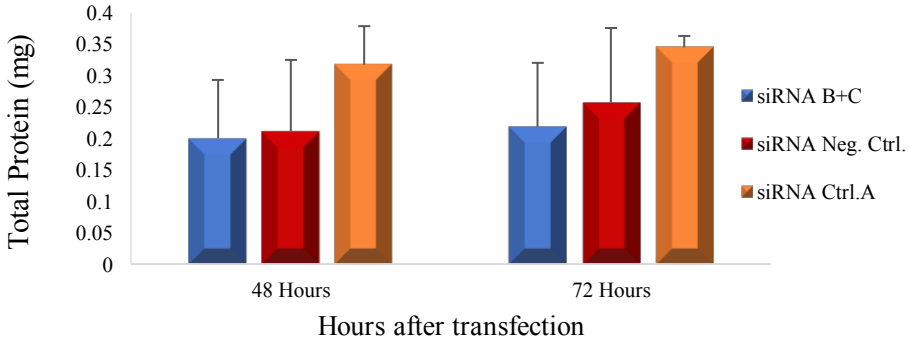

***Figure 28:* Total protein (in mg) in Huh7 cells transfected with indicated *F5* siRNAs.** Cells were harvested 48 and 72 hours after transfection, before total protein quantification was done in protein lysates. Mean values in mg (n=9) and +SD are shown for three independent experiments.

4.2.1.3 Cell proliferation in HepG2

In the HepG2 cell line, all cells (transfected and non-transfected) were seen to have an increase in growth from 1 to 72 hours after transfection (Figure 29 A). Cells transfected with siRNA B and C in combination showed the highest significant cell proliferation (cell viability) after 72 hours when compared to the other transfected and non-transfected cells ($P < 0.00001$) established by a one-way ANOVA test, with a following Tukey's multiple comparisons test (Figure 29 A & B).

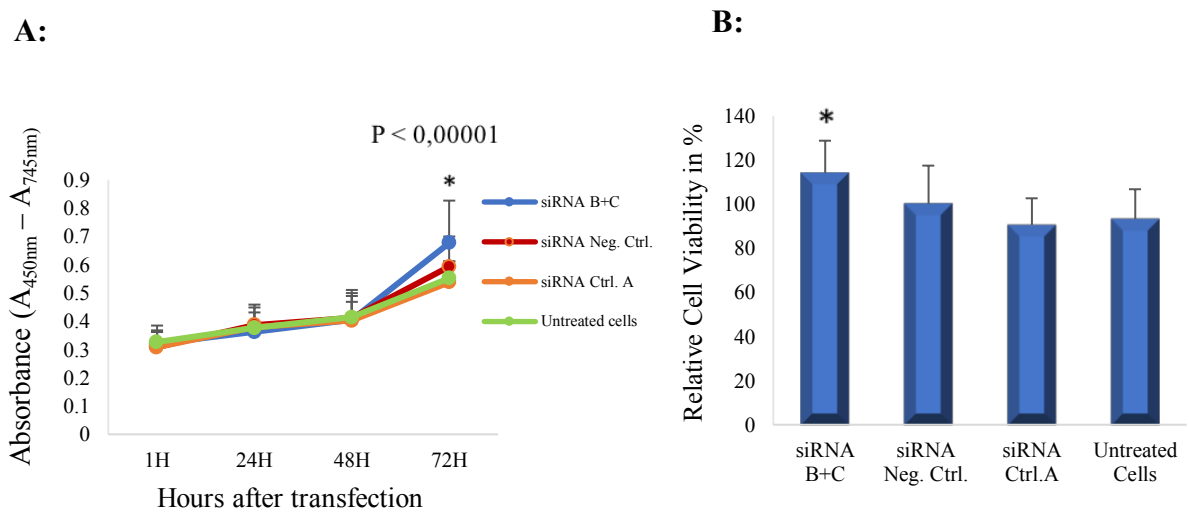

Figure 29: **Cell proliferation in the HepG2 cell line with FV knockdown measured by Wst-1.** The cells were reverse transfected with indicated siRNAs. (A) Cell proliferation was measured by absorbance at 1 to 72 hours after the reverse transfection. Mean values (n=24) and +SD is presented for three independent experiments. The significant ($P \leq 0.05$) difference between siRNA B+C and the negative controls are marked with *. (B) Cell viability 72 hours after reverse transfection in HepG2 cells. Mean values (n=24) are related to the negative control siRNA, and +SD values are shown for three independent experiments.

A verification of the FV knockdown effect in the cell proliferation experiment was done in HepG2 cells, as described for Huh7 cells, and displayed a 80% FV knockdown effect in cells transfected with *F5* siRNA B and C in combination when compared to the negative control siRNA (results not shown).

4.2.1.4 Total protein quantification in HepG2 under FV knockdown

The growth of HepG2 cell lysates under FV knockdown was investigated by measuring total protein (in mg) (Figure 30). Overall, very little growth was observed, and cells transfected with siRNA B and C in combination showed a 2.4% decrease in total protein. However cells transfected with siRNA negative control and control A were observed to have a slight increase in total protein from 48 to 72 hours by 3.7% and 8.3%, respectively.

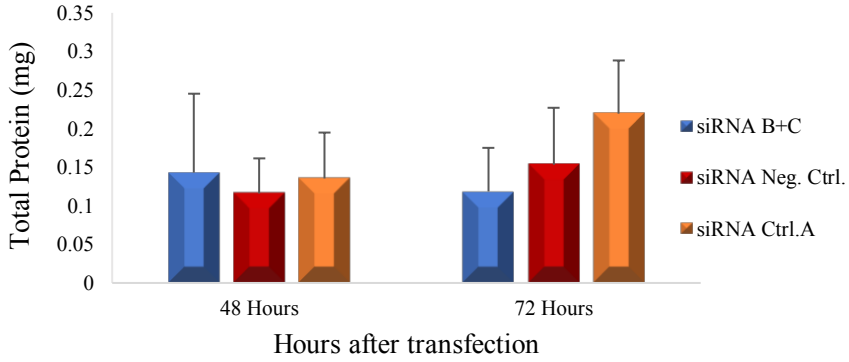

Figure 30: **Total protein (in mg) in HepG2 cells transfected with indicated siRNAs.** Cells were harvested 48 and 72 hours after transfection, before total protein quantification was done on the protein lysates. Mean values in mg (n=12) and +SD are shown for four independent experiments.

4.2.2 The effect of FV knockdown on apoptosis

To study how FV knockdown affected cell death in the liver cancer cell lines HepG2 and Huh7, apoptosis analysis was conducted. The assay involved measuring DNA fragmentation in the lysates from cells transfected with siRNA B and C in combination along with the negative control siRNA and siRNA Control A (Figure 31 A & B). All transfected Huh7 cells were seen with an apoptotic effect increasing by 80% when compared to non-transfected cells (results not shown). No differences were observed 48 hours after transfection (Figure 31 A). However, cells transfected with siRNA B and C showed 45% significantly higher DNA fragmentation (P = 0.0003) when compared to cells transfected with the negative control siRNA at 72 hours of transfection. The same trends were observed when apoptosis was related to total protein, however no significant differences were seen (Figure 31 B).

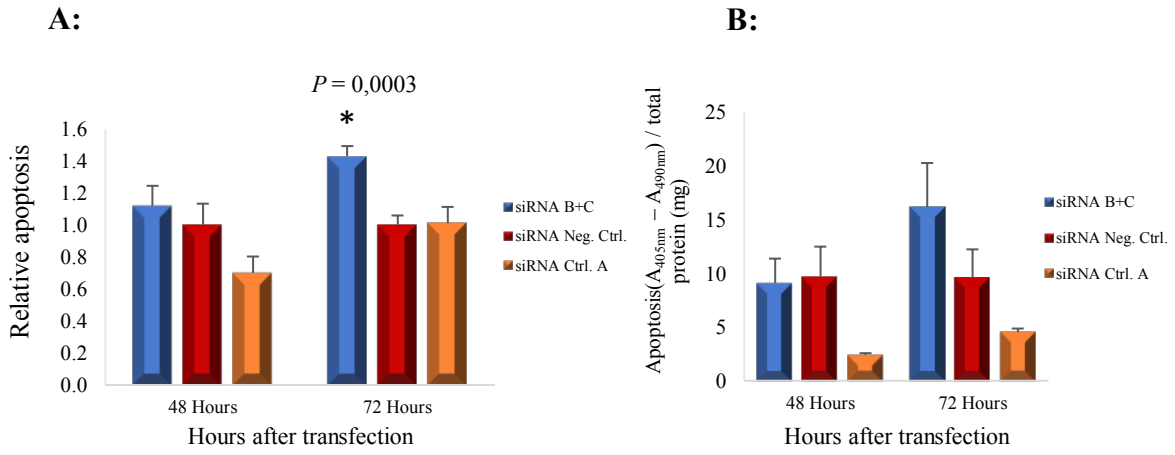

Figure 31: **The effect of FV knockdown on cell death measured by DNA fragmentation in the Huh7 cell line.** Cells were transfected with indicated siRNAs were harvested after 48 and 72 hours. (A) Relative apoptosis from absorbance values ($A_{405nm} - A_{490nm}$) compared to the negative control siRNA. (B) Apoptosis related to mg total protein in each sample. Significant difference ($P \leq 0.05$) to siRNA B & C and negative control (A) is marked with *. Mean values (n=7) and +SE are shown for three independent experiments.

For HepG2, the apoptosis analysis presented a significant difference in DNA fragmentation at both measured time points (P<0.0001) (Figure 32 A). When related to total protein, cells transfected with siRNA B and C in combination had a 272-352% significant increase (P = 0.0045) when compared to the negative control and control A siRNAs after 72 hours (Figure 32 B).

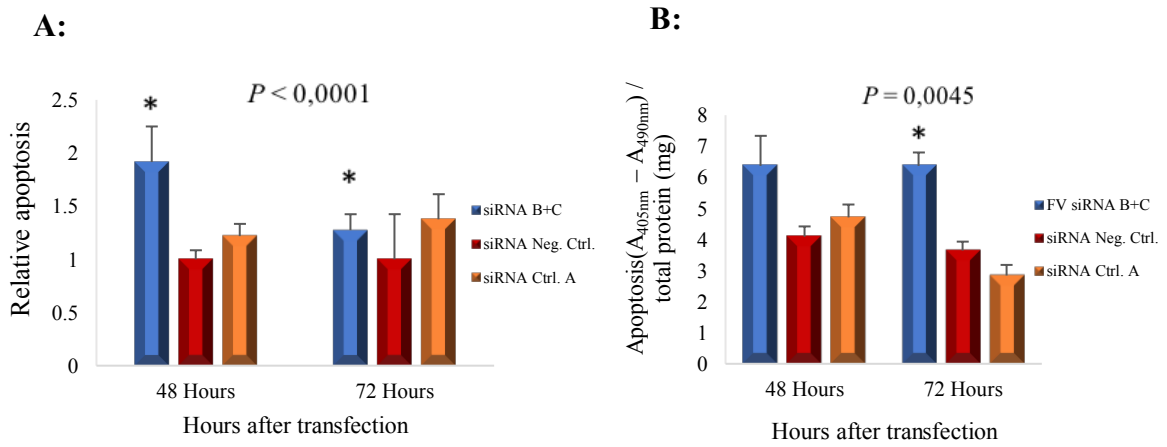

Figure 32: **The effect of FV knockdown on apoptosis measured by DNA fragmentation in the HepG2 cell line.** Cells were transfected with indicated siRNAs were harvested after 48 and 72 hours. (A) Relative apoptosis from absorbance values ($A_{405nm} - A_{490nm}$) compared to the negative control siRNA. (B) Apoptosis related to mg total protein in each sample. Significant differences ($P \leq 0.05$) to siRNA B & C and negative control are marked with *. Mean values (n=12) and +SE are shown for four independent experiments.

4.2.3 The effect of FV knockdown on cell migration in Huh7 cell lines

The effects of FV knockdown on migration in Huh7 cells were investigated using reverse transfection in 2-well migration inserts. After removal of the insert, the resulting wound was measured in µm and plotted against time to study the differences in wound size as a measure of migration for cells transfected with *F5* siRNAs compared to control cells (Figure 33 & 34).

All transfected cells with showed a complete wound healing (closure) after 48 hours of migration (Figure 33 and 34). A significant difference in migration was observed at 24 hours after removing insert (P = 0.03), indicating a trend where FV knockdown resulted in reduced migration with a more open wound when compared to the control cells.

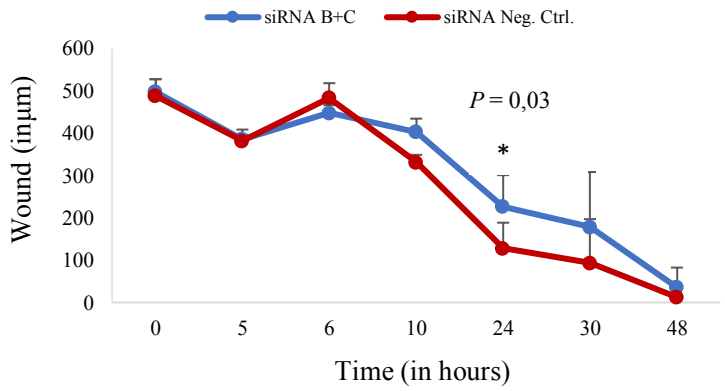

Figure 33: **The effect of FV knockdown on cell migration in Huh7 cells.** Cells were reverse transfected in 2-well inserts. The inserts were removed 24 hours after, and the migration was studied for 48 hours. Mean values in µm, (n=9) and +SD for three independent experiments are shown. Significant differences ($P \leq 0.05$) are marked with *.

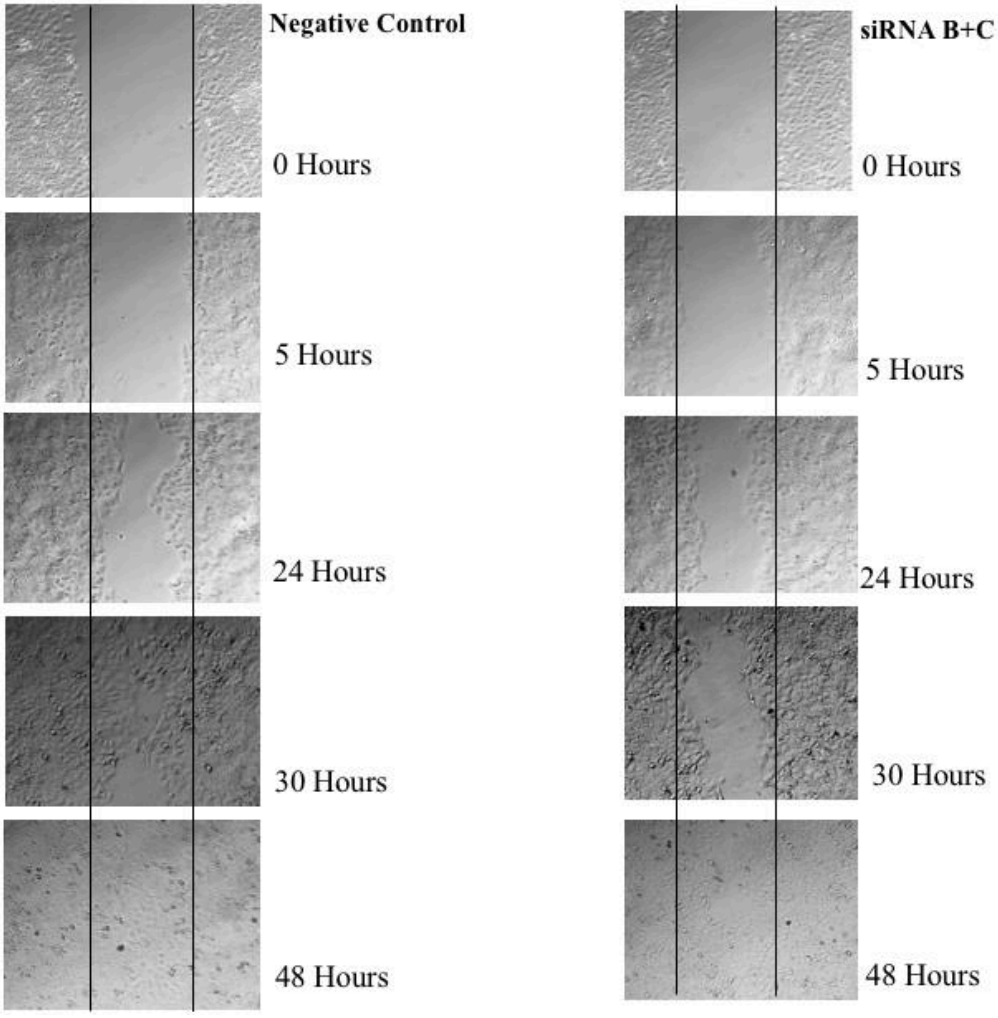

Figure 34: **Images showing the effect of FV knockdown on wound closing (healing) by migration in Huh7 cells.** Cells were reverse transfected in 2-well inserts with siRNA negative control and siRNA B and C in combination. Inserts were removed 24 hours after (marked as 0 hours), and images were taken at the 5 time-points indicated.

4.2.4 Effect of FV Knockdown on Cancer Pathway Signalling

In order to investigate the molecular mechanisms behind the functional effects of FV knockdown in the liver cancer cell lines, we performed a screening of the transcriptional activity of 10 different cancer-related pathways by the Cancer 10-Pathway Reporter Array in both HepG2 and Huh7 cell lines. Effects of FV knockdown on the signalling pathways were calculated as fold changes in transcriptional activity of cells transfected with siRNA B and C compared to the control cells (Figure 35).

The signalling pathways identified as most affected in Huh7, were the Wnt and JNK pathways, with a 60% and 55% downregulation (Figure 35, blue bars). The transcriptional activities of the pathways in the HepG2 cells seemed to be non-affected by the FV knockdown (Figure 35, orange bars).

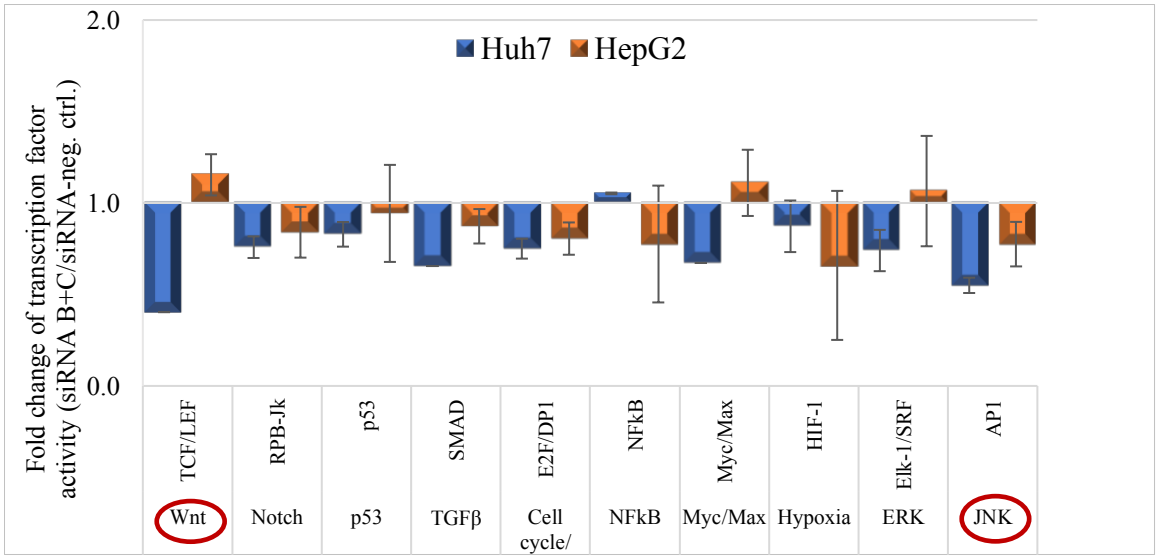

Figure 35: **Fold change of transcription factor activity in 10 cancer related pathways under FV knockdown by transfection of *F5* siRNA B and C, and siRNA negative control, in Huh7 and HepG2 cell lines.** Cells were harvested 48 hours after transfection, and transcriptional activity was measured by Luciferase array. Most affected pathways for Huh7 cells are marked in red circles for indication. Mean values (n=5) and +/- SD for two experiments are shown.

4.2.5 Effect of FV knockdown on the JNK-pathway by single reporter array in Huh7 cell lines

To confirm the observed effect of the JNK pathway after FV knockdown in Huh7 cells (shown in figure 35), a single reporter array was conducted for this pathway (Figure 36).

Cells transfected with the *F5* siRNA B and C combination resulted in a 54% reduced JNK transcriptional activity when compared to both negative controls. A JNK inhibitor was also included and confirmed the specificity of the assay.

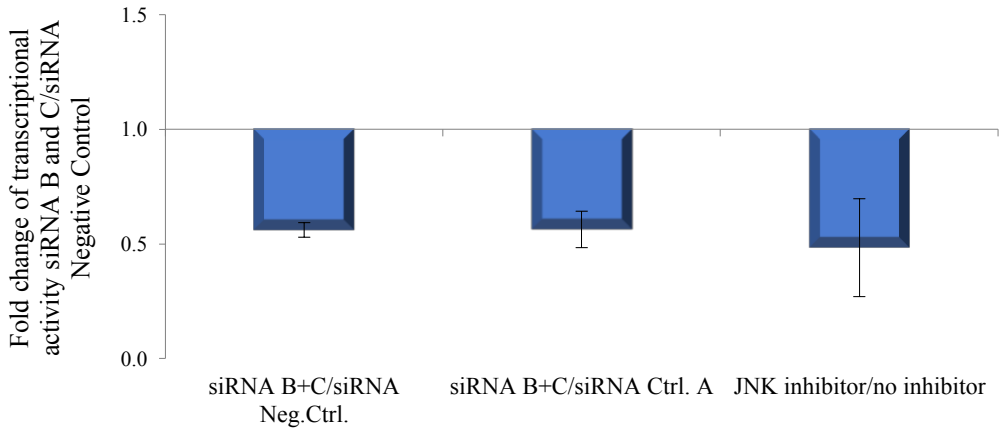

Figure 36: **The effect of FV knockdown on transcription factor activity of the JNK pathway in Huh7 cell lines.** Cells were harvested 48 hours after transfection, and the change in transcriptional activity was measured using Luciferase array. An AP-1 (JNK) inhibitor was also included. Mean values (n=9) and +/- SD are shown for three independent experiments.

4.2.6 Effect of the JNK activator, Anisomycin, on apoptosis under FV knockdown in Huh7 cell lines

As established from the 10-pathway and single reporter assays, the JNK pathway proved to be affected by FV, and we thus wanted to investigate if this pathway could also be involved in the effect of FV on apoptosis.

4.2.6.1 Verification of Anisomycin activator by western blot analysis

In order to study the effect of JNK activation further, the optimal dosage and time of JNK activation by Anisomycin had to be determined.

Anisomycin was seen to be efficient with all doses tested with 2 hours of treatment, 24 hours of treatment however, showed weak or no bands (Figure 34). All doses in cells treated for 30 minutes presented strong bands, and the Anisomycin treatment seemed to be non-affected by serum-deprived medium (results not shown). A dose of 1 µM Anisomycin for 24 and 48 hours was chosen to be able to study the down-stream effects in the cells through apoptosis. Loading control GAPDH was comparable for all samples in both blots (Figure 37).

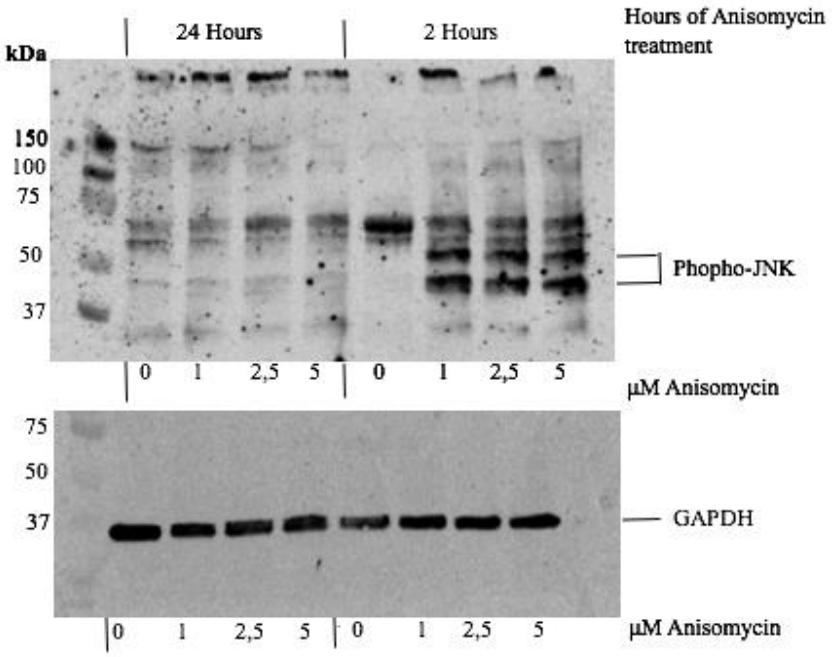

Figure 37: **Western Blot illustrating the presence of phospho-JNK by Anisomycin activation in Huh7 cell lines.** The western blot is analysed using Huh7 protein lysates treated with 24 and 2 hours of different concentrations of anisomycin. Band specific for phospho-JNK (approx. 46 and 54 kDa) and loading control GAPDH (approx. 37 kDa) are indicated by black lines.

4.2.6.1 The effect of Anisomycin on apoptosis in Huh7 cells under FV knockdown

After verifying the activation of JNK by Anisomycin treatment, the chosen dose and times were studied to investigate the effect of activated JNK on apoptosis in the Huh7 cell line under FV knockdown.

As figure 38 presents, there were no significant differences between the measured apoptosis under FV knockdown in Huh7 cells treated with Anisomycin, when compared to the untreated cells.

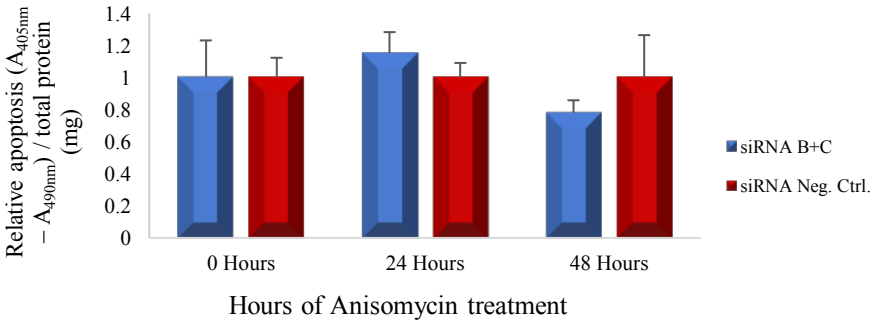

Figure 38: **The effect of Anisomycin treatment under FV knockdown on apoptosis measured by DNA fragmentation in the Huh7 cell line.** Cells were transfected with indicated siRNAs and harvested after 72 hours. Values are presented as apoptosis measured by absorbance related to mg total protein in each sample, relative to untreated transfected cells. Mean values n=6 and +SD for two independent experiments are shown.

4.3 The effect of cytostatic treatment in liver cancer cell lines

4.3.1 The effect of doxorubicin treatment on liver cancer cell proliferation

To study the sensitivity of Huh7 and HepG2 cells to doxorubicin, the effect on cell proliferation was studied in a dose- and time dependent manner (Figure 39 and 40).

All doxorubicin-treated Huh7 cells showed a reduction in cell proliferation already from 24 hours and the sensitivity increased with time of treatment, thus indicating that Huh7 cells are sensitive to doxorubicin (Figure 39). The effect of doxorubicin on the cells also seemed to increase in a dose-dependent matter.

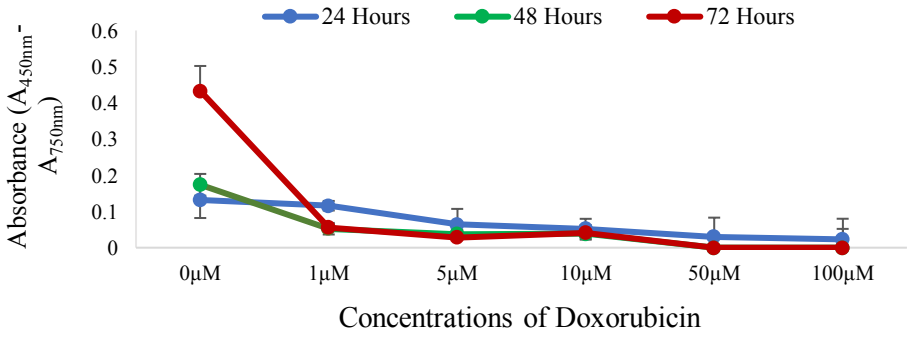

Figure 39: **Time- and dose dependent effect of doxorubicin on cell proliferation in Huh7 cells.** The cell proliferation was measured by absorbance using Wst-1 after treatment with doxorubicin at the indicated doses and time points. Mean values (n=24) and +SD for three independent experiments are shown.

No difference in cell proliferation for the different dosages after 24 hours of doxorubicin treatment was observed in the HepG2 cell line (Figure 40). However, from 48 hours to 72 hours of treatment, all doxorubicin-treated cells seemed to have a reduction in cell proliferation when compared to non-treated cells (0 µM).

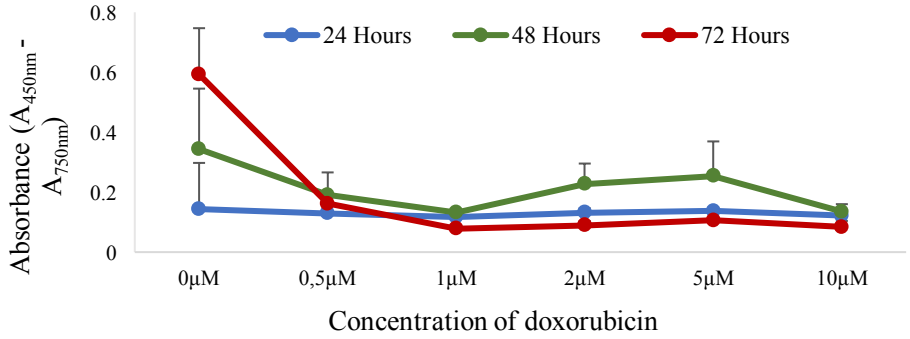

Figure 40: **Time- and dose dependent effect of doxorubicin on cell proliferation in HepG2 cells.** The cell proliferation was measured by absorbance using Wst-1 after treatment with doxorubicin at the indicated doses and time points. Mean values (n=16) and +SD for two independent experiments are shown.

4.3.2 The effect of doxorubicin on *F5* expression in liver cancer

After establishing that both the Huh7 and HepG2 cells were sensitive to doxorubicin treatment, it was interesting to study whether or not doxorubicin could affect *F5* expression in the liver cancer cells by treating them with different doses and measuring the *F5* mRNA expression.

4.3.2.1 Doxorubicin's effect on *F5* mRNA expression in Huh7

The Huh7 cells were treated with 0, 1, 10 and 50 µM of doxorubicin and harvested 24 and 48 hours after treatment before measuring *F5* mRNA expression using qRT-PCR. When compared to untreated cells, cells treated with 1 µM doxorubicin showed a reduction in *F5* mRNA expression after 24 and 48 hours by 50 and 20% respectively (Figure 41). No change in *F5* expression was observed in cells treated with 10 µM after 24 hours and expression was non-detectable after 48 because of the toxicity of doxorubicin on the cells. This was also the case for cells treated with 50 µM at both 24 and 48 hours of treatment.

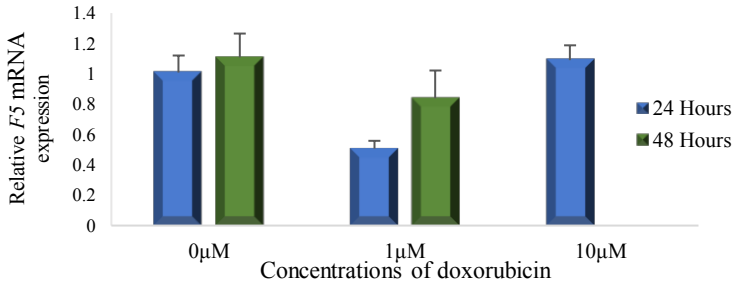

Figure 41: **Relative *F5* mRNA expression under treatment of 0, 1 and 10 µM doxorubicin in Huh7 cells.** Cells were harvested 24 and 48 hours after transfection and were measured using qRT-PCR and normalised against GAPDH as endogenous control. Results are expressed as RQ values compared to the non-treated cells at each time-point. Mean values (n=9) and +SD for three independent experiments are shown.

4.3.2.2 Doxorubicin's effect on F5 mRNA expression in HepG2

The HepG2 cells were treated with 0, 0.5, 1 and 5 µM of doxorubicin and harvested 24 and 48 hours after treatment before measuring the *F5* mRNA expression using qRT-PCR.

Cells treated with 0.5 and 1 µM doxorubicin showed a significantly increased *F5* mRNA expression (P-values of 0.0001 and >0.00001) of 150-184% after 48 hours of treatment, respectively, when compared to the untreated cells (Figure 42). The *F5* expression was reduced with 71% in cells treated with 5 µM doxorubicin due to toxicity in the cells from doxorubicin.

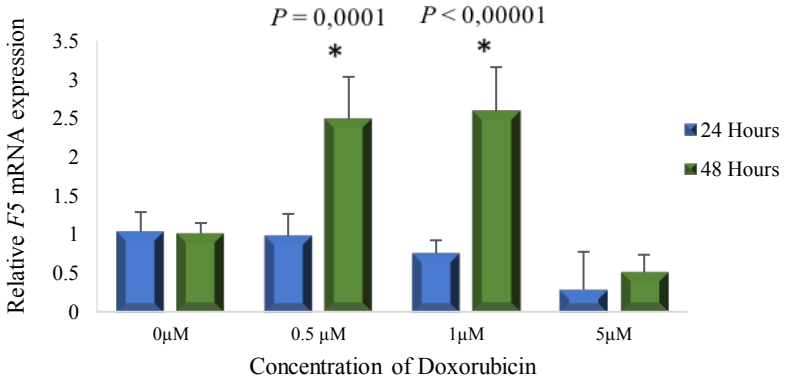

Figure 42: **Relative *F5* mRNA expression under treatment of 0, 0.5, 1 and 5 µM doxorubicin in HepG2 cells.** Cells were harvested 24, and 48 hours after transfection and *F5* mRNA expression was measured using qRT-PCR and normalised against GAPDH as endogenous control. Results are expressed as RQ values compared to the non-treated cells at each time-point. Significant differences ($P \leq 0.05$) are marked with "*". Mean values (n=9) and +SD for three independent experiments are shown.

To investigate if the induced *F5* expression seen in HepG2 with doxorubicin treatment was through p53, cells were treated with pifithrin and 1 µM doxorubicin. Pifithrin is a p53 inhibitor, which prevents transactivation of p53 responsive genes and suppresses p53 dependent apoptosis (Sohn *et al.* 2009).

Cells were treated with µM pifithrin after 24 hours doxorubicin treatment and harvested 24 hours later. The *F5* mRNA expression was then measured by qRT-PCR. The *F5* mRNA expression was increased by 40% in cells treated with 1 µM doxorubicin and DMSO when compared to untreated cells (Figure 43). In addition, *F5* expression further increased in cells treated with Pifithrin and 1 µM doxorubicin with a 94% higher expression compared to cells treated with doxorubicin only.

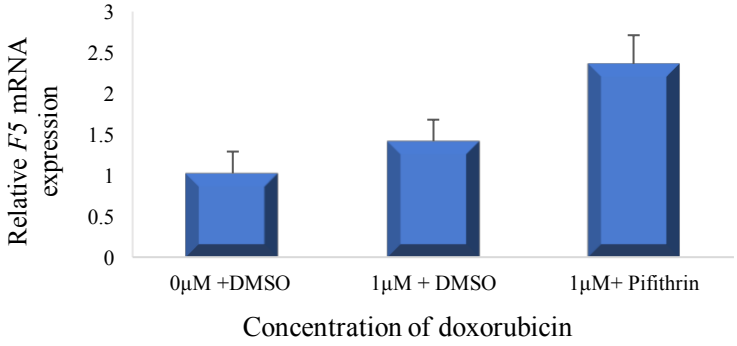

Figure 43: **Relative mRNA expression of *F5* under treatment of doxorubicin and pifithrin in HepG2 cells.** Cells were treated with 0 and 1µM doxorubicin, in addition to pifithrin and DMSO, and harvested after 48 hours of doxorubicin treatment. *F5* mRNA expression was measured using qRT-PCR and normalised against GAPDH/HPRT1 as endogenous controls. Results are expressed as RQ values compared to the non-treated cells. Mean values (n=6) and +SD for two independent experiments is shown.

5. DISCUSSION

The close relationship between cancer and coagulation has been long known, and a study has shown that patients with venous thromboembolic disease have been observed to have a 3-fold increased risk of diagnosing ovarian cancer within the next 6-12 months when compared to the general population (Sørensen *et al.* 1998). Multiple studies conducted on coagulation factors revealed that they display a role in tumor progression. Tumor cells themselves can, in fact, directly activate the hemostatic system by producing procoagulants and microparticles (Sampson *et al.* 2002; Falanga *et al.* 2009). Through studying these molecular mechanisms by which coagulation factors promote tumor cell growth, invasion and metastasis, one can achieve a better understanding of the associations for further potential clinical purposes of individualized cancer treatment.

In this thesis, the role of coagulation factor V (FV) in liver cancer was studied. And a few have suggested a link between FV and cancer where FV has been found to be expressed in different cancer tissues such as colon cancer and prostate cancer. Tinholt *et al.* (2014) also revealed the association of *F5* SNPs with breast cancer. The specific roles of FV in cancer and cancer progression however, has not been investigated so far, and the findings of FV in the different cancer tissues may seem to be more sporadic rather than suggesting a functional role. Yet, a recent study conducted by Tinholt *et al.* (2018) showed that higher expression of *F5* (encoding FV) was associated with more aggressive breast cancer tumors but also better survival among breast cancer patients, which might suggest a tumor suppressing role of FV in cancer progression. In another study, carriers of the Factor V Leiden mutation was observed with an increased risk of colorectal cancer, which linked FV mutations to cancer as a possible biological marker (Vossen *et al*. 2011).

Based on these findings, it was interesting to further investigate possible roles of FV in cancer. And, while the overexpression of FV in breast cancer was studied by the N. Iversen research group at this time, we also wanted to look at the role of FV in liver cancer. Liver is the main synthesiser of FV, and cancer data derived from TCGA revealed (see introduction section 1.4.5.1) that liver cancer presented abundant levels of FV when compared to other cancers. In this thesis, we therefore studied the knockdown effect of FV in liver cancer cell lines HepG2 and Huh7 to gain an understanding of the functional role of FV in liver cancer, and also the effect of cytostatic treatment on FV *in vitro*.

5.1 Liver cancer cell lines

Two different liver cancer cell lines; HepG2 and Huh7 were used for experiments in this thesis, and as *in vitro* study models, cell lines have several advantages. First, they are easily accessed and cost-effective, and second, the cells can easily be frozen and thawed on demand. Due to potential infinite cell division, cell lines also have a longer lifetime, which allows for culturing cells over long periods of time. With infinite cell division, mutations may occur resulting in slightly different cells than what initially was started with. In addition, culturing for longer time periods opens for a risk of cross-contamination, and so to avoid this, sterile conditions were strictly enforced in all cell experiments. Cells also require specific culture conditions, and are sensitive to changes in these conditions. Because of this, recommended culturing medium and serum was utilised and cells were incubated at 37°C and 5% CO_2.

In vitro studies involve performing studies outside a living organism, enabling experiments in fully controlled environments, like an isolated system inside a cell. However, because these experiments are so isolated, they fail to replicate the precise cellular conditions of an organism, and studies done *in vitro* should also be tested in animal models before the effects can be transferred to *in vivo* systems where overall effects of the experiment on the living subject can be observed. Huh7 and HepG2 cells were used as *in vitro* cell models for this thesis. They are both human hepatocellular carcinoma derived liver hepatocyte epithelial cells that are monolayered, adherent and easily cultured under the same conditions and using the same media and serum. The differences in the cell characteristics are observed in p53 status of these cells, where Huh7 cells have mutated p53, and HepG2 cells are p53 wild type.

5.2 Creating a FV knockdown cell model

Gene knockdown is a useful method to study the function and role of the gene and the protein it expresses. Gene knockdown by RNA interference (RNAi) does not completely shut off or eliminate the gene expression, but rather results in expression to a less extent where the end result is post-translational, down-regulation of gene expression without changing the genetic code (Mittal, 2004). By contrast, a gene knockout is a complete elimination of gene function that creates a double-strand break in the chromosome (Bogdanove & Voytas, 2011).

Deciding whether a knockdown or a knockout model is more preferable depends on the experimental goals for the study. RNAi-mediated knockdown would be a better choice in genome editing where it is not desirable to change the genetic code. For example, if one only wants to reduce the gene function temporarily by transiently transfecting siRNAs into cells, which will be lost after a few generations of cells and restoring normal gene function again.
A knockout model, on the other hand, is a better choice when it is of interest to study complete gene deletion. This could be done by, for example, making a knockout mouse to study a gene of unknown or incompletely known function by replacing the normal functioning gene with a non-functional one.

However, there are limitations and strengths to both methods which are worth considering before deciding which to go forward with. The primary issue for gene knockout, especially in knockout mouse models are regions of ES-derived genetic material surrounding the deleted gene that may contain hundreds of genes, possibly resulting in a high degree of genetic linkage between them. This can produce an observable phenotype, making it difficult to determine the exact impacts of the gene knockout itself (Eisener-Doman *et al*. 2010). Another limitation is that complete gene knockout may be compensated for in multiple ways, where alternative routes or pathways can be used in order to achieve the performance of the same function as the knocked out gene (Tymms & Kola, 2001). On the other hand, gene knockout is an effective and specific method, and in mouse models, the knockout can be seen in a biological context in which drugs and other therapies can be developed and tested directly (NIH, 2015). siRNA mediated gene knockdown is easier to perform, because it can be used directly in cell lines. This method, however, does have somewhat limited specificity because of relatively short nucleotide constraints for effectiveness, but this actually allows RNA molecules to silence entire pathways of genes. Because siRNAs only accomplish a reduced gene expression through knockdown, as opposed to the complete gene silencing in knockout, they are better facilitated for discovering therapeutic gene targets, and are more physiologically relevant for this purpose.

Because there are no known specific studies of FV in liver cancer, we wanted to begin with a transient knockdown model, where liver cancer cell lines could be used and the knockdown effect itself was easily determined and confirmed. We therefore chose to create and optimize a FV knockdown cell model using RNAi to silence *F5* expression in the liver cancer cell lines HepG2 and Huh7 to conduct functional *in vitro* studies of FV in the cell lines.

F5 siRNAs of two lengths were tested using transient transfection. The optimization revealed a more efficient transfection with the 27mer siRNAs than with the siRNAs of 21mer. This finding is in accordance with the manufacturer's claims that they were designed for optimal processing by Dicer which produces a 10-fold higher potency and specificity when compared to 21mer siRNAs. This was also confirmed in a study where Kim *et al*. (2005) tested the efficiency of siRNAs of different lengths. The higher efficiency of siRNAs with longer nucleotide sequences might be explained by the high sequence-specificity in the gene silencing. siRNAs differing only by one nucleotide may therefore show different knockdown efficiencies in the same cell line, as we observed with 21 and 27mer siRNAs. Furthermore, the same siRNA may also provide different knockdown effects in different cell lines due to more resistance to transfection in some cell lines than other (Cullen, 2006).

In the time-dependent transfection experiments, the FV knockdown was observed to be effective both at 48 and 72 hours of transfection in Huh7 and HepG2 cell lines at the mRNA and at the protein level. However, it seemed that the FV knockdown on mRNA level was slightly more effective after 48 hours than the rest. These observations were in line with findings in the report by Yong-Jiang *et al.* (2014) where they studied knockdown of TF in gastric cancer cell lines, and observed a transfection rate where knockdown was significantly higher at 48 hours, than the one of 24, and that the rate decreased after 72 hours. Our knockdown model also revealed that the knockdown effect on the protein level was best after 72 hours, compared to 48 hours in measured mRNA expression. These results were confirmed by a study previously conducted by the N. Iversen research group on the knockdown effect of TFPIα and TFPIβ in breast cancer cells (Kirkevold, 2014). The reason for an earlier mRNA expression detection is because RNA is produced by transcription of DNA by RNA polymerase, which also carries mRNA-processing proteins, and the RNA then undergoes translation into proteins. Thus, it is important to investigate the protein levels of expression as well as that of mRNA, and which time points give the most effective knockdown for the further functional protein effects of FV studied.

The reduced *F5* expression confirmed that an effective knockdown model was achieved in both cell lines, and it could be used with confidence in further functional analyses. Of note, the *F5* siRNA A showed no knockdown effect in optimizing experiments. The sequence was checked, and confirmed by the manufacturer to have no similarity with any other sequence, and was therefore included in some experiments as a second negative control.

Interestingly, the FV knockdown could not be detected in the protein cell lysates measured by both ELISA assay and Western blot analysis. These observations were in accordance to a study done by Wilson *et al.* (1984) where they found that Factor V activity in HepG2 cell medium increased nearly linearly over a 20-hour time course. This indicated FV as a secreted protein, and that the secretion itself seemed to happen so quickly that no effect was detectable in the cell lysate itself.

Transient transfection models are suitable for studying short-term effects of gene expression in for example knockdown with siRNAs on a small scale as done in this thesis. However, if long-term effects of gene expression or gene knockdown are desired, a stable transfection which sustain transgene expression even after replication of the host cell, is required (Glover *et al.* 2005), although, the knockdown effect itself is usually better in transient transfections than what is observed in stable cell lines. To be able to further study long-term effects of the FV knockdown in Huh7 and HepG2 cells, the *F5* siRNAs were cloned as shRNAs in the pSiRPG vector. The shRNAs were then transfected into Huh7 and HepG2 cells to make stable cell lines with constant FV knockdown. After 2 weeks of puromycin selection, a significant number of both Huh7 and HepG2 cells transfected with the *F5* shRNAs were dead. Yet, the control cells had sufficient number of cells. Størvold *et al.* (2007) presented a successful stable *NDRG1* gene knockdown by siRNAs in the pSiRPG vector after puromycin selection in breast cancer cell lines. Stable knockdown was also achieved siRNAs by Li *et al.* (2006) in breast and cervical cancer cell lines, and thus the method itself and the vector used should produce viable cells with continuous FV knockdown. However, because the control cells only seemed to survive the stable transfection, it might indicate that the liver cancer cells could not tolerate a stable FV knockdown to that extent.

5.3 Functional effects of FV knockdown in liver cancer cells

After establishing a successful knockdown model in the Huh7 and HepG2 cell line, studies were done to investigate the functional effects and the molecular mechanisms of FV in liver cancer cells.

Cell growth:

The role of FV on growth of liver cancer cells was studied by conducting cell proliferation experiments with FV knockdown in the Huh7 and HepG2 cell lines. The proliferation was examined using the Wst-1 cell proliferation reagent and measuring absorbance in the transfected cells at 1 to 72 hours after transfection. In Huh7 and HepG2 under FV knockdown, very little growth was observed by this assay. The increased growth under FV knockdown was also seen to be non-significant in the Huh7 cell line and only significant at 72 hours after transfection for HepG2.

Although there are no other known studies of FV on cancer cell growth, the effects of other coagulation factors have been investigated in other cancer cell lines. Studies have revealed that thrombin has a significant stimulatory effect on angiogenesis by inducing vascular growth factors, and thereby indirectly promoting growth in cancer (Huang *et al*. 2000). In addition, Yong-Jiang *et al.* (2014) found that downregulated TF significantly decreased gastric cancer cell proliferation, similarly, Pollen (2014) found that a downregulation of TFPIα and TFPIβ reduced breast cancer cell growth.

Another method for investigating growth of the cells under FV knockdown is the measure of total protein in the cell lysates. The total protein quantification is a colorimetric method that measures the total protein amount compared to a standard curve and may thus be used as an indirect growth measure. All transfected cells were observed to have very little growth in the measured time points, which reflects on the impact the transfection itself has on the cells. No significant differences were seen for any transfected cells in either of the cell lines in this total protein assay, meaning that the effect on proliferation determined in HepG2 with Wst-1 assay, was not seen in the total protein assay.

Based on these results, it seems that transiently transfected the cells right before measuring growth may not be optimal for this type of experiment because the transfection itself inhibits growth of the cells. Thus, a study in stable transfected cells should be considered for future growth experiments. On the other hand, all cells in this assay were observed to have poorer overall proliferation in 96-well plates compared to wells of bigger volume. This may be the result of an evaporation problem, even though we tried to avoid this, where content in perimeter wells on plates incubated for longer time periods (over 24 hours) evaporates and changes the concentration in the well, affecting the proliferation. Another reason for the poor growth may

be the small volume of the wells, making it difficult to seed out cells evenly and consequently, hard for the cells to grow optimally as well.

The Wst-1 proliferation assay used in this thesis measures the proliferation by quantification of formazan. This method is simple, and a more sensitive method for specifically measuring cell proliferation, as opposed to the measure of total protein. It was used as a starting method to identify what effects on cell growth to potentially further investigate, and is a good assay for this, as it is suitable for adherent cells. Nevertheless, there are multiple potentially more specific alternative methods to consider for further studying cell proliferation also. CyQUANT Cell Proliferation Assay, for example, is based on the measuring the DNA content in the wells, and is a simple yet accurate way to measure cell number, and more sensitive than colorimetric-based assays making it a good alternative. BrdU Cell Proliferation Assay is another option which measures DNA synthesis by incorporating a BrdU antibody which does not cross-react with endogenous DNA making it very sensitive. However it does require a lot of preparations and is somewhat less simple to conduct, and may be an alternative when looking into very specific effects on cell proliferation. At last, the ATP determination Kit may be another preferable method that measures quantitative ATP with recombinant firefly luciferase and its substrate D-luciferin.

Apoptosis:

Tumor cells are known to avoid apoptosis (or programmed cell death), leading to increased proliferation. Thus, studying the effect of FV on apoptosis in liver cancer cells by DNA fragmentation, and comparing the results with what was seen for cell proliferation, could give a good insight to the role of FV in liver cancer progression

In Huh7 and HepG2, apoptosis was significantly increased in all transfected cells when compared to untreated cells, thus confirming the stressful impact of the transfection itself on the cells. A FV knockdown resulted in increased apoptosis in both cell lines when compared to the control cells at 48 or 72 hours of transfection. Similarly, in the study conducted by Yong-Jiang *et al.* (2014), knockdown of TF also significantly increased apoptosis when compared to the control gastric cancer cells. Schiller *et al.* (2002) studied the effect of thrombin in leukemia and lymphoma, and presented that thrombin decreased apoptosis significantly *in vivo* and *in vitro*. Downregulated TFPIα and TFPIβ significantly also reduced the apoptosis in breast cancer cells (Kirkevold, 2014).

Higher apoptosis could mean reduced growth of cancer cells, and these findings indicate that TFPI and FV have tumor suppressing characteristics in breast cancer by increasing apoptosis, as opposed to TF in gastric cancer, FV in liver cancer and thrombin which seem to have oncogenic roles by reducing the apoptotic effects. Although FV in liver cancer was observed to reduce apoptosis in the results from this thesis, studies from TCGA provisional data on liver cancer survival presented no significant effect of *F5* expression on overall survival ($P = 0{,}168$), and a borderline difference in overall survival of liver cancer patients with large tumors ($P = 0{,}064$), where high *F5* expression seemed to give the more favourable outcome as was seen in previous FV studies in breast cancer (Tinholt *et al*. 2018).

The higher levels of apoptosis under FV knockdown contradict the results in HepG2 from the proliferation experiments, where FV knockdown had a more effective proliferation after 72 hours than control cells. However, none of the other growth results were significant, and thereby the apoptosis results are more reliable in this thesis. It should also be noted that when the results from the measured apoptosis by DNA fragmentation in Huh7 was related to the measured total protein in the lysates, the significant difference between *F5* knockdown and control was no longer a fact. Furthermore, the significant effects of apoptosis in HepG2 was somewhat reduced by relating them to the total protein measurements. Hence, relating the apoptosis measurements to the ones of total protein might not necessarily be a correct presentation of the results. Theoretically, if the level of apoptosis observed is dependent only on the FV protein level, then the differences should be compensated for when related to the total protein and any difference in level of apoptosis after adjustment can indicate differences in biological function. So it might be more explanatory to look at the apoptotic measurements under FV knockdown alone, and from the results in this thesis, and we can confirm that FV knockdown decreases apoptosis significantly in both liver cancer cells studied.

Migration:

To further investigate the functional role of FV in liver cancer, a migration assay was done in Huh7 under FV knockdown. Cell migration and invasion of cancer cells into surrounding tissue and the vasculature, is an important step in the metastatic process and tumor progression (Wurtz *et al* 2011). In addition, tumor cells often have an increased ability to migrate so they can spread to other parts of the body. (Hanahan & Weinberg, 2000). The assay was done using the Culture-Insert 2-Well μ-Dishes studying migrating cells with and without FV knockdown.

Overall, all transfected cells had closed the wound after 48 hours, however this was somewhat expected because the well volume makes it unavoidable for the wound to close completely at some point in time. Nonetheless, a trend suggesting a decrease in migration for cells transfected with FV knockdown when compared to the control cells was observed for most time points measured. Even these slight differences in migration may be interesting in order to understand the role of FV in cancer progression. In addition, the difference between cells with FV knockdown and control cells observed after 24 hours of migration was seen to be significant. No previous migration studies of FV are known, but a reduced cell migration was also seen under knockdown of TF in gastric cancer cells when compared to the control cells (Yong-Jiang *et al.* 2014), and FVII expression in an ovarian cancer cell line enhanced migration (Koizume *et al*. 2006). However, an upregulation of TFPI resulted in reduced migration in breast cancer (Pollen, 2014).

A lower migration rate of liver cancer cells with FV knockdown confirms the observed higher apoptotic effect and also substantiates the possibility of a role for FV in liver cancer as an oncogene of tumor progression. However, this experiment was only not conducted for HepG2 cells due to their growth characteristics making them unsuitable for this type of migration assay. Thus these results should be considered to be confirmed in other ways; by for example measuring the migration rates of HepG2 to investigate the effects of FV on migration in these cells for comparison with results seen in Huh7 by the Boyden Chamber Technique, but also for Huh7 cells for confirmation and to compare with the results already obtained from the insert dishes. The Boyden Chamber Technique is an alternative to the Insert 2-Well μ-Dishes, where cells migrate through a membrane and are stained and counted. At last, as mentioned in the cell growth assays, experiments with stably transfected cells should also be considered for future migration assays with FV knockdown.

In summary, studying the potential functional roles of FV in liver cancer revealed no significant differences of FV on the cell growth. Nonetheless, our knockdown studies revealed induced apoptosis and reduced migration under FV knockdown, suggesting an oncogenic role of FV in liver cancer. This is contradicting previously FV studies done in breast cancer by the N. Iversen research group where the results presented FV as a potential tumor suppressor gene. However, before concluding further, we also wanted to look into possible molecular mechanisms connecting FV and cancer to look into possible molecular mechanisms connecting FV and cancer.

5.3.1 Possible molecular mechanisms of FV in liver cancer cells

On the basis of the obtained results from the possible functional roles of FV in cell growth, cell migration and apoptosis, it was of interest to study the potential molecular mechanisms behind the effects of FV seen in the liver cancer cells. An experiment was therefore conducted using the Cancer 10-Pathway Reporter Array, to determine which of the 10 cancer pathways included in the array (See Sections 3.5.4.1 & 4.2.4), if any, would be most affected by the FV knockdown in both Huh7 and HepG2 cells.

The expression of protein-coding genes involves multiple transcriptional and post-transcriptional processes. Transcriptional activity refers to the binding and processive activity of RNA polymerase and the amount of actual transcripts are measured relative to the control array (Maniatis & Reed, 2002). The transcriptional activity in the 10 cancer-related pathways included in the array was measured in Huh7 and HepG2 cell lines by a fold-change between the transcriptional activity in cells with FV knockdown and in the control cells. From the results, we observed the JNK and Wnt pathways to be most down-regulated under FV knockdown in the Huh7 cells, and none of the pathways seemed to be affected in HepG2 cells. The result of down-regulation in the JNK pathway under FV knockdown in Huh7 was also confirmed by an AP-1 single reporter array because it was available, although it would be of interest to further confirm the Wnt downregulation as well. This should be considered for future studies of FV in liver cancer.

The JNK pathway is central in cancer progression, and JNKs belong to MAP-kinases involved in regulation of cell proliferation, differentiation and apoptosis. It has been shown that JNKs are crucial for both cell proliferation and apoptosis, and whether the activation of JNK leads to cell proliferation or apoptosis is dependent on the stimuli and the cell-type involved in the activation (Lin & Dibling, 2002)(Liu & Lin, 2005).

As the down-regulation of the JNK pathway was confirmed, it was appealing to investigate whether this pathway could be responsible for the effect seen in apoptosis in Huh7 cells. This was done by measuring apoptosis in cells with FV knockdown with or without the JNK activator Anisomycin. No significant differences were observed in FV knockdown cells treated with JNK activator when compared to the untreated cells. Yet, cells treated with the JNK activator for 48 hours showed a slight reduction in apoptosis under FV knockdown, and cells

treated for 24 hours showed a slight increase in apoptosis under FV knockdown. As mentioned, JNK may have both pro- or antiapoptotic functions, depending on cell type, nature of the death stimulus, duration of its activation and the activity of other signalling pathways (Liu & Lin, 2005) and so no conclusion should be made from this one experiment. The non-significance indicated other potential molecular mechanisms underlying the apoptotic effect, and that are also affected by the transcriptional regulation of the JNK pathway which could be interacting with FV and its functional roles.

Although we cannot yet establish the cancer-function of FV, multiple other coagulation factors have been studied for this matter, and may be comparable in order to suggest the possible roles FV might have in cancer based on our results. Overexpression studies of TFPIα and TFPIβ done by the N. Iversen group previously showed decreased adhesion and migration and indicated an anti-tumor effect of both isoforms (Pollen, 2014), contradicting the results of FV in this thesis. Stavik *et al.* (2011) also reported an association between TFPI and a decrease breast cancer cell growth, migration and invasion. Santamaria *et al.* (2017) conducted a study where FV was observed to enhance TFPI in the presence of protein S. FV also directly interacts with TFPI in the inhibition of prothrombinase assembly, thus the opposite characteristics between TFPI in breast cancer and FV seen in this thesis may suggest that the role of FV in liver cancer is not coagulation-dependent.

As described in the introduction, tissue factor (TF) is the physiological initiator of coagulation and has come to be seen as a key determinant of the coagulation/cancer interaction. TF expression has been confirmed in malignant cells, especially in cells with enhanced metastatic potential, and is seldom expressed in normal epithelial cells. Yong-Jiang *et al.* (2014) found that TF inhibited apoptosis and lead to increased migration, which is in accordance with what we observed for FV in our liver cancer studies. Another study done by Jiang *et al.* (2006) demonstrated that the TF/FVII/FX complex inhibited apoptosis in breast cancer cells via the p44/42 MAPK and PKB/Akt signalling pathways. Even though no direct effects were observed in the TF-affected pathways in our 10-pathway array, they may indirectly interfere with the effects observed of FV in liver cancer, but originate from the effects of TF. Overexpression of TF has also been found in both plasma and liver tissue of liver cancer patients, and the expression was upregulated in poorly differentiated liver cancer, which suggests that the expression of TF is related to higher grade tumors and to poorer prognosis, which is in accordance with the results of TF in gastric cancer. TF/FVII cleaves FX to FXa which activates

and complexes with FV, and so the oncogenic characteristics seen of TF in liver cancer might be affecting FV in a cancer progressive matter like we observed, rather than FV being the initiator.

Activated protein C (APC) has both anticoagulant activity and direct cell-signalling properties. A study done by Van Sluis *et al*. (2009) reported that APC promoted cancer cell migration and invasion and inhibited apoptosis. This was also confirmed by Althawadi *et al*. (2015) who found that APC induced cell migration in ovarian cancer. APC induces direct cellular effects that regulate the inflammatory response via its direct cell signalling properties (Van Sluis *et al*. 2009). This kind of APC-induced signal transduction promotes cancer cell migration, invasion and angiogenesis and inhibits cancer cell apoptosis. The APC signalling also enhances the vascular endothelial barrier function through activation of endothelial protein C receptor: protease activated receptor 1 (PAR1). This barrier has protective effect of APC seems to be pivotal for limiting inflammatory disease and sepsis-induced mortality (Van Sluis *et al*. 2009). FV plays an important role in the APC pathway as an essential cofactor to APC in the inactivation of FVa and FVIIIa (Cramer *et al.* 2010). And so the inducing effects of APC documented in cancer is in agreement with the effects we observed of FV in liver cancer in this thesis, and could mean that FV's effect is somewhat affected by APC, and is acting in a coagulation-independent manner.

Before concluding this, one should consider to further analyse the interaction between FV and other factors of the coagulation system to see whether or not these will confirm what has been documented in this thesis. The anticoagulant form of FV has been found to express an anti-inflammatory effect through its cofactor properties with APC, which abolishes the EPCR dependent inflammatory PAR2 signalling by destabilizing TF/FVIIa/FXa complex (Liang *et al.* 2015; Sun 2015). Moreover, inhibition of the TF/FVIIa/PAR2 pathway have proven to attenuate cell growth and angiogenesis (Ruf *et al.* 2011). Lin *et al*. (2016) also suggested a crucial impact of the TF/FVII/PAR2 coagulation pathway on tumor malignancy under certain circumstances in liver cancer, and thus the interactions between APC, PAR2 and FV should be investigated in liver cancer to determine if FV does have a coagulation-independent role in cancer or if it is a result of the progression of the cancer itself.

In summary, the results from this thesis have suggested an oncogenic role of FV in liver cancer, which has been seen to be in accordance with reports of TF and APC in cancer. Because both TF and APC have direct and indirect interactions with FV in the coagulation pathway, it seems

that the effects of FV in liver cancer may be affected by these factors. On the other hand, TFPI has previously been shown to have tumor suppressing activities in breast cancer, and because of the direct interactions between FV and TFPI in coagulation, the effect of TFPI may be compensational. Furthermore, Chen *et al.* (2016) found that patients with high levels of FVII in liver cancer tissue showed poorer survival rates than those without, and so some parts of the coagulation system does have significance for liver cancer progression and survival, but it may not be FV.

5.4 The effect of doxorubicin on liver cancer cells

Chemotherapeutic agents are related to risks of thrombotic complications and in addition to this, anticoagulant therapy in cancer patients is challenging because these patients also have an increased risk of major bleeding. However, little is known about the molecular mechanisms underlying the pro-thrombotic doxorubicin-induced trigger in cancer patients.

In liver cancer cells, systemic chemotherapeutic treatment is a challenge, and chemotherapy is documented to be ineffective and limited by acquired resistance of the tumors after exposure (Beaugrand M., *et al.,* 2005) (Llovet, M., 2005). Thus, it was interesting to study the cell viability and sensitivity to doxorubicin in both Huh7 and HepG2 cell lines treated with increased concentrations and treatment times of doxorubicin.

The results showed sensitivity to doxorubicin in a time- and dose-dependent matter. Thus, at higher concentrations and with longer treatment, the cells' response was observed to be increasingly sensitive. However, both Huh7 and the HepG2 cells seemed to be already responding sensitively to the lowest concentrations of doxorubicin (1 & 0,5 μM, respectively) after 48 hours of treatment. This indicated a strong sensitivity which contradicts a study done by Llovet (2005) who investigated treatment options of liver cancer, and found that systemic doxorubicin only provided partial responses in 10% of cases, and with no proven survival advantages indicating a doxorubicin resistance of liver cancer. A previous study done by Lai C-L *et al*. in 1988 documented similar results, where an overall survival rate of liver cancer patients treated with doxorubicin was 3 weeks longer than for untreated patients. However, only 3% of treated patients showed a doxorubicin-induced tumor regression of over 50%, and as a result of the experienced fatal complications (septicaemia and cardiotoxicity) in 25% of the

patients, concluding that doxorubicin may not be the ideal drug for treatment of inoperable HCC.

Despite the fact that our results presented sensitivity, and other documented studies did not, one should keep in mind how resistance to chemotherapy may be developed. Cancer tissues consist of a various population of malignant cells, and some of these may be sensitive to cancer drugs, while others are resistant (Eramo *et al*. 2010). One chemo-resistance mechanism is environmental-mediated drug resistance, which is based on communication between the tumor cells and their microenvironment. Signalling in this environment allow these cells to escape chemotherapy-induced apoptosis, leading to surviving foci of residual cells (Meads *et al*. 2009). Thus, the resistance may not be visible over the short time periods we measured. In the HepG2 cell line, however, a slight increase in cell proliferation was seen for 2 and 5 μM after 72 hours of treatment, which may indicate cells exhibiting a slight resistance. However, this was not visible when observing the cells in the microscope, and may just be inconsistencies in measurements by Wst-1.

Based on the knowledge obtained from the cell survival experiment under dose- and time-dependent doxorubicin treatment, knowing both cell lines were sensitive to doxorubicin at certain concentrations and time points, it was also of interest to investigate if FV may be involved in the treatment response somehow. No change in *F5* mRNA expression was observed in Huh7 cells for any concentrations of doxorubicin when compared to untreated cells. In the HepG2 cells, however, the *F5* expression was seen to be significantly increased under treatment of 0,5 and 1 μM at 48 hours. Nevertheless, a doxorubicin concentration of 5 μM in these cells showed no further increase in the *F5* mRNA expression, actually it was significantly reduced. This was most likely due to the toxicity of doxorubicin at this dose, as was also observed in the cell viability experiments for the same cells.

The doxorubicin-induced *F5* mRNA expression has been reported in breast cancer cells by our research group previously, but has not been reporter otherwise. However, previous studies have shown multiple interactions of doxorubicin and the coagulation pathway. A study conducted by Woodley-Cook *et al.* (2006) reported that doxorubicin affected the haemostatic balance via downregulating the APC anticoagulant pathway in vascular ECs. The endothelial protein C receptor (EPCR) and thrombomodulin are two endothelial cell surface receptors required for the conversion of protein C to APC. Under doxorubicin treatment, they observed a decrease in EPCR mRNA levels, and an increase of thrombomodulin mRNA levels. These effects resulted

in decreased conversion of protein C to APC. Because FV is an important cofactor to APC in the inactivation of FVa, reduced APC as a result of doxorubicin could result in decreased inactivation of FVa and increased coagulation in patients which may the result of the increased *F5* mRNA levels seen in this thesis.

In addition, Tang *et al.* (2007) have shown that doxorubicin-induced apoptosis was inhibited by TF overexpression through the interaction of FVII and TF activating the downstream PI3K/Akt pathway in glioblastomas. Thus, suggesting a role of TF in chemotherapy resistance (Tang *et al.* 2007). Doxorubicin has also been seen to increase TF activity, while the *TF* mRNA expression (unlike the *F5* mRNA expression in our studies) was slightly downregulated (Swystun *et al.* 2009).

The Huh7 and HepG2 cells differ in their p53 activity, where Huh7 is documented to be p53 mutant, and HepG2 p53 wild type. A distinct increase of *F5* expression was only shown in HepG2, and none in Huh7, which also have been observed in previous experiments done by our research group in breast cancer cell lines as well. Doxorubicin has been shown to induce cell death through the p53 pathway (Sun *et al.* 2016), and thus it was interesting that no *F5* is induced by doxorubicin in the p53 mutant Huh7 cell line. These results may indicate that the action of p53 is involved in doxorubicin induced *F5* mRNA expression.

Based on the possible relationship between the p53 status and induced *F5* expression under doxorubicin treatment, it was also interesting to directly test if p53 was involved in this mechanism in HepG2 cells. This was done by inhibiting p53 by pifithrin in cells treated with doxorubicin. The results from the experiments revealed stimulated *F5* expression even after inhibition of p53 which suggests that the induced *F5* expression observed under doxorubicin treatment is not through the actions of p53, and because doxorubicin functions by inducing activation of p53 to induce the cell apoptosis (Wang *et al.* 2004), there is no reason to believe a connection between FV activity and doxorubicin in relation to apoptotic action. In addition, FV knockdown in cells treated with doxorubicin showed no differences in cell proliferation (results not shown), which may point to the fact that doxorubicin does not interact with the cells via FV. However, before concluding this, further studies should be done. For example, one could study the effect of doxorubicin directly on apoptosis in the cells under FV knockdown to establish if doxorubicin actually interacts with FV in liver cancer or not.

Although no real effect was seen to be due to p53, cells treated with dimethyl sulfoxide (DMSO) and doxorubicin showed a reduced *F5* expression compared to the p53 inhibited cells and cells only treated with doxorubicin. These results were surprising because it was expected that they would exhibit the same expression as observed in cells treated with doxorubicin only. DMSO is usually used to solubilize poorly soluble drugs, like pifithrin (Da Violante *et al.* 2002). However, treatment of cells by DMSO has been reported to substantially alter the morphology of cells, and also significantly reduce the cell viability in a dose-dependent matter (Pal *et al.* 2012). In addition, Pal *et al.* (2012) showed that DMSO exposure not only affected the phenotypic characteristics of the cells, but also induced significant alterations in gene expression, protein content and functionality of the cells studied. And so, the results seen of *F5* expression in the DMSO treated cells could be a result of toxicity from the DMSO itself, due to a higher concentration than what was tolerated of the cells, which may have interfered with our results.

Together, our results from this thesis showed a liver cancer time- and dosage-dependent sensitivity to doxorubicin. *F5* mRNA expression seemed to be induced in the p53 wild type cell line HepG2, which could be an effect of documented APC decrease and thrombin increase as a result of the treatment and indicating a role of FV as a coagulation-activation in doxorubicin patients. However, further studies revealed that the FV induced expression had no interaction with p53, and the cell proliferation under FV knockdown showed no difference when compared to control cells, we then have no evidence for a clear interaction between doxorubicin effects and FV expression in liver cancer.

6. CONCLUSION

In this thesis, our aim was to better understand the functional role of FV in liver cancer by investigating functional effects under FV knockdown, and possible molecular mechanisms *in vitro*. An optimized *in vitro* FV knockdown cell model was obtained after transfection using *F5* 27mer siRNAs in the Huh7 and HepG2 cell lines, and showed a highly effective FV knockdown at both the mRNA and the protein level to use in the functional assays of the thesis. A stable FV knockdown model was also created, but unfortunately cells with FV knockdown died during selection. Although no significant effects were observed for FV in liver cancer cell growth in the transient FV knockdown model, experiments on apoptosis and migration revealed oncogenic characteristics of FV in both liver cancer cell lines. However, these results contradict the ones documented of FV in breast cancer by our research group previously, suggesting a tumor supressing role.

To establish what possible molecular mechanisms could be the cause of the observed FV effects, cancer-related signalling pathways were investigated. The JNK and Wnt signalling pathways were determined as most affected by FV in Huh7 cells. Yet, an assay of the effect of JNK on apoptosis did not reveal any significant differences, making us believe there might be other possible ways FV affects liver cancer apoptosis and migration. Studies done on the effects of APC and TF on different cancers was in accordance to the effects we observed of FV in liver cancer, and because of the interactions they have with FV in the coagulation pathway, it seems that FV may be exhibiting the same tumor-inducing effects either via a specific pathway or by adhesion of a specific molecule. TFPI is also highly interactive with FV, and TFPI in breast cancer revealed a tumor suppressing activity that may be compensational for FV's effects. Nevertheless, studies have shown central roles of the coagulation system, specifically TF, in liver cancer progression and survival. Thus, in order to confirm the coagulation-independent role of FV, further possible mechanisms of FV's effects in connection with some of these factors and proteins should be studied to establish this relationship.

Our aim for this thesis was also to study the sensitivity of doxorubicin treatment on the cell lines and the possible effect doxorubicin could have on FV. Both cell lines were established to be doxorubicin-sensitive in a dose- and time-dependent matter. In HepG2 cells, the doxorubicin treatment also revealed an induced *F5* mRNA expression, but showed no interaction with the p53-induced apoptosis in doxorubicin, and FV had no effect on cell proliferation under

doxorubicin treatment. Thus, evidence point to no clear interaction between doxorubicin and FV expression in liver cancer.

7. REFERENCES

©CancerResearchUK. (2014). *Worldwide cancer mortality statistics:* ©CancerResearchUK. Online. Available at: http://www.cancerresearchuk.org/health-professional/cancer-statistics/worldwide-cancer/mortality#heading-One (accessed on 10.10.2017)

©CancerResearchUK. (2017) *How chemotherapy works.* ©CancerResearchUK. Online. Available at: http://www.cancerresearchuk.org/about-cancer/cancer-in-general/treatment/chemotherapy/how-chemotherapy-works (accessed on 25.03.2018)

Allen, D.H. & Tracy, P.B. (1995). Human coagulation factor V is activated to the functional cofactor by elastase and cathepsin G expressed at the monocyte surface. *The journal of biological chemistry,* 270(3): 1408-1415.

Althawadi, H., Alfarsi, H., Besbes, S., Mirshahi, S., Ducros, E., Rafii, A., Pocard, M., Therwath, A., Soria, J. & Mirshahi, M. (2015). Activated protein C upregulates ovarian cancer cell migration and promotes unclottability of the cancer cell microenvironment. *Oncology Reports,* 34(2): 603-609.

American cancer society. *What is Liver Cancer?*. Online. Available at: https://www.cancer.org/cancer/liver-cancer/about/what-is-liver-cancer.html (accessed 26.09.2017)

Ananthakrishnan, A., Gogineni, V., & Saeian, K. (2006). Epidemiology of Primary and Secondary Liver Cancers. *Seminars in Interventional Radiology*, 23(1), 47–63.

Arias, A.M. (2001). Epithelial Mesenchymal Interactions in Cancer and Development. *Cell,* 105(4): 425-531.

Asselta, R., Tenchini, M. & Duga, S. (2006). Inherited defects of coagulation factor V: the hemorrhagic side. *Journal of Thrombosis and Haemostasis,* 4(1): 26-34.

Bach, R.R. (1988). Initiation of coagulation by tissue factor. *CRC Critical Reviews in Biochemistry*, 23(4): 339-368.

Bernat, A., & Herbert, J.M. (1994). Effect of various drugs on Adriamycin-enhanced vneous thrombosis in the rat: importance of PAF. *Thromb.Res.,* 75: 91-97.

Bernuau, J., Rueff, B. & Benhamou, J.P. (1986). Fulminant and subfulminant liver failure: definitions and causes. *Seminars in liver diseases,* 6(2): 97-106.

Beaugrand, M., N'kontchou, G., Seror, O., Ganne, N. & Trinchet, J.C. (2005). Local/regional and systemic treatments of hepatocellular carcinoma. *Seminars in Liver Disease,* 25(2): 201-211.

Blom, J.W., Doggen, C.J., Osanto, S. & Rosendaal, F.R. (2005). Malignancies, prothrombotic mutations, and the risk of venous thrombosis. *JAMA,* 293(6): 715-722.

Bodley, A., Liu, L.F, Israel, M., Seshadri, R., Koseki, Y., Giuliani, F.C., Kirschenbaum, S., Silber, R. & Potmesil, M. (1989). DNA topoisomerase II-mediated interaction of doxorubicin and daunorubicin congeners with DNA. *Cancer Research,* 49(21): 5969-5978.

Bréchot, C. (2004). Pathogenesis of hepatitis B virus – related hepatocellular carcinoma: Old and new paradigms. *Gastroenterology,* 127(5): 56-61.

Broze, G.J. (1995). Tissue factor pathway inhibitor. *Thrombosis and Haemostasis,* 74: 90-93.

Brunt, E.M. (2012). Histopathologic features of hepatocellular carcinoma. *Clinical Liver Disease, A Multimedia Review Journal,* 1(6): 194-199.

Chen, K-D, Huang, K-T, Tsai, M-C, Wu, C-H, Kuo, I-Y, Chen, L-Y, Hu, T-H, Chen, C-L & Lin, C-C. (2016). Coagulation Factor VII and malignant progression of hepatocellular carcinoma. *Cell Death & Disease,* 7(2).

Clevers, H. (2006). Wnt/beta-catenin signaling in development and disease. *Cell,* 127(3): 469-480.

Copper, G.M. (2000). A Molecular Approach. *The cell, 2nd edition*.

Cosemans, J.M., Schols, S.E., Stefanini, L., de Witt, S., Feijge, M.A., Hamulyák, K., Deckmyn, H., Bergmeier, W. & Heemskerk, J.W. (2011). Key role of glycoprotein Ib/V/IX and von Willebrand factor in platelet activation-dependent fibrin formation at low shear flow. *Blood,* 117(2): 651-660.

Cramer, T.J., Griffin, J.H. & Gale, A.J. (2010). Factor V is an anticoagulant cofactor for activated protein C during inactivation of factor Va. *Pathophysiology of haemostasis and thrombosis,* 37(1): 17-23.

Cullen, B.R. (2006). Enhancing and confirming the specificity of RNAi experiments. *Nature Methods,* 3(9): 677-681.

Curnow, J., Pasalic, L., Favaloro, E.J. (2016). Why Do Patients Bleed? *The Surgery Journal*, 2(1):29-43.

Dahlbäck, B. (2008) Advances in understanding pathogenic mechanisms of thrombophilic disorders. *Blood,* 112(1): 19-27.

Da Voliante, G., Zerrouk, N., Richard, I., Provot, G., Chaumeil, J.C. & Arnaude, P. (2002). Evaluation of the Cytotoxicity Effect of Dimethyl Sulfoxide (DMSO) on Caco2/TC7 Colon Tumor Cell Cultures. *Biological and pharmaceutical bulletin,* 25(12): 1600-1603.

Dashty, M., Akbarkhanzadeh, V., Zeebregts, C.J., Spek, C.A., Sijbrand, E.J., Peppelenbosch, M.P. & Rezaee, F. (2012). Characterization of coagulation factor synthesis in nine human primary cell types. *Scientific reports,* 2(787).

Loof, T., Deicke, C. & Medina, E. (2014). The role of coagulation/fibrinolysis during Streptococcus pyogenes infection. *Frontiers in cellular and infection microbiology,* 4:128.

Dominiska, M. & Dykxhoorn, D.M. (2010). Breaking down the barriers: siRNA delivery and endosome escape. *Journal of Cell Science,* 123: 1183-1189.

Doroshow, J.H. (1986). Role of hydrogen peroxide and hydroxyl radical formation in the killing of Ehrlich tumor cells by anticancer quinones. *Proceedings of the National Academy of Sciences of the United States of America,* 83(12): 4514-4518

Dragani, T.A. (2010). Risk of HCC: Genetic heterogeneity and complex genetics. *Journal of Hepatology vol, 52:* 252-257.

Drake, T.A., Morrissey, J.H. & Edgington, T.S. (1989). Selective cellular expression of tissue factor in human tissues. Implications for disorders of hemostasis and thrombosis. *American Journal of Pathology,* 134(5): 1087-1097.

El-Serag, H.B., Mason, A.C. (2000). Risk Factors for the Rising Rates of Primary Liver Cancer in the United States. *Arch Intern Med,* 160(21): 3227–3230.

Elbashir, S.M., Harborth, J., Lendeckel, W., Yalcin, A., Weber, K. & Tuschi, T. (2001). Duplexes of 21-nucleotide RNAs mediate RNA interference in cultured mammalian cells. *Nature,* 411(6836): 494-498.

Engel, L.W., Young, N.A., Tralka, T.S., Lippman, M.E., O'Brien, S.J., Joyce, M.J. (1978). Establishment and characterization of three new continuous cell lines derived from human breast carcinomas. *Cancer research,* 38(10): 3352-3364.

Eramo, A., Haas, T.L. & De Maria, R. (2010). Lung cancer stem cells: tools and targets to fight lung cancer. *Oncogene,* 29(33): 4625-4635.

Esmon, C.T. (2006). Inflammation and the activated protein C anticoagulant pathway. *Semin Thromb Hemost*, 32:49-60

Esmon, C.T. (2000) Regulation of blood coagulation. *Biochim Biophys Acta,* 1477(1-2): 349 60.

Esmon, C.T. (1989). The Roles of Protein C and Thrombomodulin in the Regulation of Blood Coagulation. *The Journal of Biological Chemistry,* 264(9): 4743-4746.

Falanga, A., Marchetti, M. & Vignoli, A. (2013). Coagulation and cancer: biological and

clinical aspects. *Journal of Thrombosis and Haemostasis,* 11: 223-233.
Falanga, A., Panova-Noeva, M. & Russo, L. (2009). Procoagulant mechanisms in tumor cells. *Best practice & research. Clinical Haematology,* 22(1): 49-60.
Feitelson, M.A. (1999). Hepatitis B virus in hepatocarcinogenesis. *Journal of Cellular Physiology,* 181(2): 188-202.
Feitelson, M.A. & Lee, J. (2007). Hepatitis B virus integration, fragile sites, and hepatocarcinogenesis. *Cancer letters,* 252(2): 157-170.
Fire, A., Xu, S., Montgomery, M.K., Kostas, S.A., Driver, S.E., & Mello, C.C. (1998). Potent and specific genetic interference by double-stranded RNA in Caenorhabditis elegans. *Nature,* 391: 806-811.
Fujikawa, K., Coan, M.H., Legaz, M.E. & Davie, E.W. (1974). The mechanism of activation of bovine factor X (Stuart factor) by intrinsic and extrinsic pathways. *Biochemistry,* 13(26): 5290-5299.
Gale, A.J. (2011). Current Understanding of Hemostasis. *Toxicologic pathology,* 39(1):273 280.
Gawaz, M. (2004). Role of platelets in coronary thrombosis and reperfusion of ischemic mycocardium. *Cardiovasc. Res,* 61: 498-511.
Genetics Home Research. (2018). *Factor V Leiden thrombophilia:* Online. Available at: https://ghr.nlm.nih.gov/condition/factor-v-leiden-thrombophilia. (Accessed on 24.03.2018)
GLOBOCAN (IARC). (2012) *Liver Cancer Estimated Incidence, Mortality and Prevalence Worldwide in 2012.* Online. Available at: http://globocan.iarc.fr/old/FactSheets/cancers/liver-new.asp (Accessed on 23.04.2018).
Goodnough, L.Y., Saito, H., Manni, A., Jones, P.K. & Pearson, O.H. (1984). Increased incidence of thromboembolism in stage IV breast cancer patients treated with a five-drug chemotherapy regimen. A study of 159 patients. *Cancer,* 54: 1264-1268.
Goosens, N., Sun, X. & Hoshida, Y. (2015). Molecular classification of hepatocellular carcinoma: potential therapeutic implications. *Hepat Oncol.,* 2 (4): 371-379.
Guinto, E.R. & Esmon, C.T. (1984). Loss of prothrombin and factor Xa-factor Va interactions upon inactivation of factor Va by activated protein C. *The journal of biological chemistry,* 259(22): 13986-13992.
Hanahan, D. & Weinberg, R.A. (2011). Hallmarks of Cancer: The Next Generation. *Cell, 144*: 646-674.
Heemskerk, J.W., Mattheij, N.J. & Cosemans, J.M. (2013). Platelet-based coagulation: different populations, different functions. *Journal of thrombosis and haemostasis (JTH),* 11(1): 2-16.
Hockin, M.F., Jones, K.C., Everse, S.J., Mann, K.G. (2002) A model for the stoichiometric regulation of blood coagulation. *J Biol Chem,* 277:18322-18333
Hockin, M.F., Kalafatis, M., Shatos, M.A., Mann, K.G. (1997). Protein C activation and factor Va inactivation on human umbilical vein endothelial cells. *Arterioscler Thromb Vasc Biol,* 17: 2765-2775
Hoffman, M. & Monroe, D.M. 3rd. (2001). A Cell-Based Model of Hemostasis. *Thrombosis and Haemostasis,* 85(6): 958-65.
Hoshida, Y., Nijman, S.M., Kobayashi, M., Chan, J.A., Brunet, J.P., Chiang, D.Y., Villanueva, A., Newell, P., Ikeda, K., Hashimoto, M., Watanabe, G., Gabriel, S., Friedman, S.L., Kumada, H., Llovet, J.M. & Golub, T.R. (2009). Integrative transcriptome analysis reveals common molecular subclasses of human hepatocellular carcinoma. *Cancer Research,* 69(18): 7385-7392.
Huang, Y.Q., Li, J-J., Hu, L. & Karpatkin, S. (2000). Thrombin induces the synthesis of VEGF and Angiopoletin-2 (Ang-2). *Blood,* (99)5: 1646-1650.

Hussain, S.P., Schwank, J., Staib, F., Wang, X.W. & Harris, C.C. (2007). TP53 Mutations and hepatocellular carcinoma: insights into the etiology and pathogenesis of liver cancer. *Oncogene*, 26: 2166-2176.

Iakhiaev, A., Pendruthi, U.R., Voigt, J., Ezban, M. & Rao, L.V.M. (1999). Catabolism of Factor VIIa Bound to Tissue Factor in Fibroblasts in the Presence and Absence of Tissue Factor Pathway Inhibitor. *Journal of Biological Chemistry,* 274(52): 36995-37003.

International Agency for Research on Cancer. *TP53 Database*. Online. Available at: http://p53.iarc.fr/CellLines.aspx (accessed on 18.12.2017).

Izumi, S., Langley, P.G., Wendon, J., Ellis, A.J., Pemambuco, R.B., Hughes, R.D. & Williams, R. (1996). Coagulation factor V levels as prognostic indicator in fulminant hepatic failure. *Hepatology,* 23(6): 1507-1511.

Kane, W.H., & Davie, E.W. (1988). Blood coagulation factors V and VIII: structural and functional similarities and their relationship to hemorrhagic and thrombotic disorders. *Blood*, 71(3): 539-555.

Kim, D-H., Behlke, M.A., Rose, S.D., Chang, M-S., Choi, S. & Rossi, J.J. (2005). Synthetic dsRNA Dicer substrates enhance RNAi potency and efficacy. *Nature Biotechnology,* 23: 222-226.

Kirkevold, M. (2014). Characterization of TFPIalpha and TFPIbeta on Apoptosis and Growth in Breast Cancer Cells. (Master Thesis). *Norwegian University of Life Sciences, Faculty of Veterinary Medicine and Biosciences, Department of Chemistry, Biotechnology and Food Science.*

Koizume, S., Jin, M-S., Miyagi, E., Hirahara, F., Nakamura, Y., Piao, J-H., Asai, A., Yoshida, A., Tsuchiya, E., Ruf, W. & Miyagi. Y. (2006). Activation of Cancer Cell Migration and Invasion by Ectopic Synthesis of Coagulation Factor VII. *Cancer Research,* 66(19): 9453-9460.

Kreidy, R. (2012) Factor V-Leiden Mutation: A Common Risk Factor for Venous Thrombosis among Lebanese Patients. *Thrombosis,* 2012: 380681.

Jeffrey, L. & Weitz, M.D. (2010). Coagulation Simplified. *Medscape Education Cardiology.*

Jenny, R.J., Pittman, D.D., Toole, J.J., Kriz, R.W., Aldape, R.A., Hewick, R.M., Kaufman, R.J. & Mann, K.G. (1987). Complete cDNA and derived amino acid sequence of human factor V. *Proceedings of the National Academy of Sciences of the United States of America,* 84:4846-4850

Kalafatis, M., Mann, K.G. (2001). The role of the membrane in the inactivation of factor Va by plasmin: amino acid region 307-348 of factor V plays a critical role for factor Va cofactor function. *J Biol Chem,* 276:18614-18623

Kanda, M., Sugimoto, H. & Kodera, Y. (2015). Genetic and epigenetic aspects of initiation and progression of hepatocellular carcinoma. *World J Gastroenterol,* 21 (37): 10584-10597.

Keller, F.G., Ortel, T.L., Quinn-Allen, M-A. & Kane, W.H. (1995). Thrombin-Catalyzed Activation of Recombinant Human Factor V. *Biochemistry,* 34(12): 4118-4124.

Khorana, A.A. (2012). Cancer and coagulation. *American Journal of Hematology,* 87(1): 582-587.

Kim, S-H., Lim, K-M., Noh, J-Y., Kim, K., Kang, S., Chang, Y.K., Shin, S. & Chung, J-H. (2011). Doxorubicin-Induced Platelet Procoagulant Activities: An Important Clue Chemotherapy-Associated Thrombosis. *Toxicological Sciences,* 124(1): 215-224.

Knöbl, P. & Lechner. K. (1998). Acquired factor V inhibitors. *Bailliere's clinical haematology,* 11(2): 305-308.

Krishnaswamy, S., Russel, G.D. & Mann, K.G. (1989). The reassociation of factor Va from its isolated subunits. *J Clin Invest,* 264: 3160-3168

Kujovich, J.L. (1999). Factor V Leiden Thrombophilia. *GeneReviews®.*
Kumar, M., Zhao, X. & Wang, X.W. (2011). Molecular carcinogenesis of hepatocellular carcinoma and intrahepatic cholangiocarcinoma: one step closer to personalized medicine? *Cell & Bioscience,* 1(1): 5.
Kumar, V., Abbas, A., Fausto, N., Aster, J. & Mitchell, R.N. (2010). Hemodynamic disorders, thromboembolic disease, and shock. *Robbins and Cotran Pathologic Basis of Disease, Professional Edition,* 8th ed.
LaBonte, M.L. (2013). Anticoagulant factor V: Factors affecting the integration of novel scientific discoveries into the broader framework. *Department of Biological Sciences.*
Lai, C-L., Lok, A.S-F., Wu, P-C., Chan, G.C-B. & Lin, H-J.L. (1988). Doxorubicin versus no antitumor therapy in operable hepatocellular carcinoma. A prospective randomized trial. *Cancer,* 62(3).
Lee, J.Y., Lee, M.Y., Chung, S.M. & Chung, J.H. (1998). Chemically induced platelet lysis causes vasoconstriction by release of serotonin. *Toxicol. Appl. Pharmacol.,* 149: 235-242.
Lentz, B.R. (2003). Exposure of platelet membrane phosphatidylserine regulates blood coagulation. *Prog. Lipid. Res,* 42: 423-438.
Letal, A. & Kuter, D.J. (1999). Cancer, Coagulation and Anticoagulation. *The Oncologist.* 4(6): 443-449.
Li, Q-X., Zhao, J., Liu, J-Y., Jia, L-T., Huang, H-Y., Xu, Y-M., Zhang, Y., Zhang, R., Wang, C-J., Yao, L-B., Chen, S-Y. & Yang, A-G. (2006). Survivin stable knockdown by siRNA inhibits tumor cell growth and angiogenesis in breast and cervical cancers. *Cancer Biology & Therapy,* 5(7): 860-866.
Liang, H.P., Kerschen, E.J., Basu, S., Hernandex, I., Zogg, M.m Jia, S., Hessner, M.J., Toso, R., Rezaie, A.R., Fernández, J.A., Camire, R.M., Ruf, W., Griffin, J.H. & Weiler, H. (2015). Coagulation factor V mediates inhibition of tissue factor signaling by activated protein C in mice. *Blood,* 126(21): 2415-2423.
Libourel, E.J., Sonneveld, P., van der Holt, B., de Maat, M.P. & Leebeek, F.W. (2010). High incidence of arterial thrombosis in young patients treated for multiple myeloma: results of a prospective cohort study. *Blood,* 116: 22-26.
Lima, L.G. & Monteiro, R.Q. (2013). Activation of blood coagulation in cancer: implications for tumor progression. *Bioscience Reports.,* 33 (5): e00064.
Lin, A. & Dibling, B. (2002). The true face of JNK activation in apoptosis. *Aging cell*. 1(2): 112-116.
Lin, C-C., Lin, C-W., Tsai, M-C., Huang, K-T., Chen, C-L. & Chen, K-D. (2016). Autophagy and Coagulation in Liver Cancer and Disorders. *Autophagy in Current Trends in Cellular Physiology and Pathology*.
Liu, C-Y. (2015). Treatment of Liver cancer. *Cold Spring Harbor Perspectives in Medicine*, 1-16.
Liu, J. & Lin, A. (2005). Role of JNK activation in apoptosis: a double edged sword. *Cell Research.,* 15(1): 36-42.
Llovet, J.M. (2005). Updated treatment approach to hepatocellular carcinoma. *Journal of gastroenterology.* 40(3): 225-235.
Llovet, J.M., Brú, C. & Bruix, J. (1999). Prognosis of Hepatocellular Carcinoma: The BCLC Staging Classification. *Seminars in Liver Disease* 19(3): 329-338.
Llovet, J.M., Ricci, M.D., Massaferri, V. M.D., Hilgard, P., Gane, E., Blanc, J-F., Oliveira, A.C., Santoro, A., Raoul, J-L., Forner, A., Schwartz, M., Porta, C., Zeuzem, S., Bolondi, L., Greten, T.F., Galle, P.R., Seitz, J-F., Borbath, I., Häussinger, D., Giannaris, T., Shan, M., Moscovici, M., Voliotis, D. & Bruix, J. (2008). Sorafenib in

Advanced Hepatocellular Carcinoma. *The New England Journal of Medicine,* 359: 378-390.
Logan, C.Y. & Nusse, R. (2004). The Wnt signaling pathway in development and disease. *Annual review of cell and developmental biology,* 20: 781-810.
Loreto, M.F., De Martinis, M., Corsi, M.P., Modesti, M. & Ginaldi, L. (2000). Coagulation and Cancer: Implications for Diagnosis and Management. *Pathology oncology research,* 6(4): 301-309.
Lotem, J., Peled-Kamar, M., Groner, Y. & Sachs, L. (1996). Cellular oxidative stress and the control of apoptosis by wild-type p53, cytotoxic compounds, and cytokines. *Proc. Natl. Acad. Sci. U.S.A.,* 93: 9166-9171.
Louzada, S., Adega, F., Chaves, R. (2012). Defining the sister rat mammary tumor cell lines HH 16 cl.2/1 and HH-16.cl.4 as an in vitro cell model for Erbb2. PloS one. 7(1).
Lowe, K.L., Navarro-Nunez, L. & Watson, S.P. (2012). Platelet CLEC-2 and podoplanin in cancer metastasis. *Thrombosis research,* 129(1): 30-37.
Lowe, S.W., Bodis, S., McClatchey, A., Remington, L., Ruley, H.E., Fisher, D.E., Housman, D.E. & Jacks, T. (1994). P53 status and the efficacy of cancer therapy in vivo. *Science*, 266(5186): 807-810.
Lu, D., Kalafatis, M., Mann, K.G., Long, G.L. (1996). Comparison of activated protein C/protein S mediated activation of human factor VIII and factor V. *Blood,* 87: 4708-4717.
MacDonald, B.T., Tamai, K., He, X. (2009). Wnt/β-catenin signaling: components, mechanisms, and diseases. *Developmental cell,* 17(1):9-26.
Maniatis, T., & Reed, R. (2002). An extensive network of coupling among gene expression machines. *Nature,* 416(6880): 499-506.
Mann, K.G. & Kalafatis, M. (2002). Factor V: a combination of Dr Jekyll and Mr Hyde. *Blood,* 101: 20-30.
Martinelli, I., Bottaso, B., Duca, F., Faioni, E. & Manucci, P.M. (1996). Heightened thrombin generation in individuals with resistance to activated protein C. *Thrombosis and haemostasis,* 75: 703-705.
Martin-Vilchez, S., Lara-Pezzi, E., Trapero-Marugán, M., Moreno-Otero, R. & Sanz P.C. (2011). The molecular and pathophysiological implications of hepatitis B X antigen in chronic hepatitis B virus infection. *Rev. Med. Virol.*
Mazoyer, E., Ripoll, L., Gueguen, R., Tiret, L., Collet, J.P., dit Sollier, C.B., Roussi, J., Drouet, L. & FITENAT Study Group. (2009). Prevalence of factor V Leiden and prothrombin G20210A mutation in a large French population selected for nonthrombotic history: geographical and age distribution. *Blood coagulation & fibrinolysis: an international journal in haemostasis and thrombosis,* 20(7): 503-510.
Meads, M.B., Gatenby, R.A. & Dalton, W.S. (2009). Environment-mediated drug resistance: a major contributor to minimal residual disease. *Nature Reviews. Cancer,* 9(9): 665-674.
Medscape: Cicalese, L. (2017*). Hepatocellular Carcinoma.* Online. Available at: http://emedicine.medscape.com/article/197319-overview#a4) (accessed 03.10.2017).
Mesri, A.E., Feitelson, M.A., Munger, K. (2014). Human Viral Oncogenesis: A Cancer Hallmark Analysis. *Cell Host & Microbe,* 15: 266-282.
Mohle, R., Green, D., Moore, M.A., Nachman, R.L. & Rafii, S. (1997). Constitutive production and thrombin-induced release of vascular endothelial growth factor by human megakaryocytes and platelets. *Proceedings of the National Academy of Sciences of the United States of America,* 94(2): 663-668.
Monkovic, D.D. & Tracy, P.B. (1990). Activation of human factor V by factor Xa and thrombin. *Biochemistry,* 29(5): 1118-1128.

Monroe, D.M., Hoffman, M. & Roberts, H.R. (2002). Platelets and thrombin generation. *Arteriosclerosis, Thrombosis, and vascular biology,* 22(9): 1381-1389.
National Human Genome Research Institute. *Knockout Mice Fact Sheet.* Available at: https://www.genome.gov/12514551/knockout-mice-fact-sheet/ (accessed 04.05.2018).
Nesheim, M.E., Canfield, W.M., Kisiel, W. & Mann, K.G. (1982). Studies of the capacity of factor Xa to protect factor Va from inactivation by activated protein C. *The Journal of Biological Chemistry,* 257: 1443-1447.
Okamura, K., Balla, S., Martin, R., Liu, N., & Lai, E.C. (2008). Two distinct mechanisms generate endogenous siRNAs from bidirectional transcription in Drosophila melanogaster. *Nat. Struct. Mol. Biol.,* 15: 581-590.
Pal, R., Mamidi, M.K., Das, A.K. & Bhonde, R. (2012). Diverse effects of dimethyl sulfoxide (DMSO) on the differentiation potential of human embryonic stem cells. *Archives of toxicology,* 86(4): 651-61.
Palta, S., Saroa, R., Palta, A. (2014). Overview of the coagulation system. *Indian Journal of Anaesthesia,* 58(5):515-523.
Palumbo, J.S., Talmage, K.E., Massari, J.V., La Jeunesse, C.M., Flick, M.J., Kombrinck, K.W., Jirouskova, M. & Degen, J.L. (2005). Platelets and fibrin(ogen) increase metastatic potential by impending natural killer cell-mediated elimination of tumor cells. *Blood,* 105: 178-185.
Pike, R.N., Buckle, A.M., le Bonniec, B.F., & Chruch, F.C. (2005). Control of the coagulation system by serpins. *The FEBS Journal,* 272 (19): 4842-4851.
Pollen, I. (2014). Characterization of TFPIalpha and TFPIbeta on Growth, Adhesion and Migration in Breast Cancer Cells. (Master Thesis). *Norwegian University of Life Sciences, Faculty of Veterinary Medicine and Biosciences, Department of Chemistry, Biotechnology and Food Science.*
Prelich, G. (2012). Gene Overexpression: Uses, Mechanisms, and Interpretation. *Genetics,* 190 (3): 841-854.
Reece, J.B., Urry, L.A., Cain, M.L., Wasserman, S.A., Minorsky, P.V. & Jackson, R.B. (2011). *Campbell Biology Pearson*, (9) 288-289.
Recillas-Targa, F. (2006). Multiple strategies for gene transfer, expression, knockdown and chromatin influence in mammalian cell lines and transgenic animals. *Molecular Biotechnology,* 34 (3): 337-354.
Rijken, D.C. & Lijnen, H.R. (2009). New insights into the molecular mechanisms of the fibrinolytic system. *Journal of Thrombosis and Hemostasis (JTH),* 7(1):4-13.
Rine, J., Hansen, W., Hardeman, E., Davis, R.W. (1983). Targeted selection of recombinant clones through gene dosage effects. *Proceedings of the National Academy of Sciences of the United States of America,* 80 (22): 6750-6754.
Ruf, W. (2007). Tissue factor and PAR signaling in tumor progression. *Throm Res.,*120:7-12
Ruggeri, Z.M. (2002). Platelets in atherothrombosis. *Nat.Med.,* 8: 1227-1234.
Santamaria, S., Reglinska-Matveyev, N., Gierula, M., Camire, R.M., Crawley, J.T.B., Lane, D.A. & Ahnstrøm, J. (2017). Factor V has an anticoagulant cofactor activity that targets the early phase of coagulation. *The Journal of Biological Chemistry,* 292: 9335-9344.
Schen, L., Dahlbäck, B. (1994). Factor V and protein S as synergistic cofactors to activated protein C in degradation of factor VIIa. *The Journal of biological chemistry,* 269(29): 18735-18738.
Schiller, H., Bartscht, T., Arit, A., Zahn, M.O., Seifert, A., Bruhn, T., Bruhn, H.D. & Gieseler, F. (2002). Thrombin as a survival factor for cancer cells: thrombin activation in malignant effusions in vivo and inhibition of idarubicin-induced cell death in vitro. *International Journal of Clinical Pharmacology and Therapeutics,* 40(8): 329-335.

Schlageter, M., Terracciano, L.M., D'Angelo, S. & Sorrentino, P. (2014). Histopathology og hepatocellular carcinoma. *World Journal of Gastroenterology,* 20 (43): 15955-15964.
Schroeder, V. & Kohler, H.P. (2013). Factor XII deficiency: an update. *Seminars in thrombosis and hemostasis,* 39(6): 632-641.
Scott, E.M., Ariëns, R.A. & Grant, P.J. (2004). Genetic and environmental determinants of fibrin structure and function: revelande to clinical disease. *Arteriosclerosis, thrombosis and vascular biology,* (9): 1558-1566.
Segers, K., Dahlbäck, B. & Nicolaes, G.A. (2007). Coagulation factor V and thrombophilia: background and mechanisms. *Thrombosis and haemostasis,* 98(3): 530-542.
Sia, D., Villanueva, A., Friedman, S.L. & Llovet, J.M. (2017). Liver Cancer Cell of Origin, Molecular Class, and Effects on Patient Prognosis. *Gastroenterology,* 152: 745-761.
Sigma- Aldrich. *Cell death detecetion ELISA^{PLUS}.* Online. Available at: https://www.sigmaaldrich.com/content/dam/sigma-aldrich/docs/Roche/Bulletin/1/celldethrobul.pdf (accessed on 20.12.2017)
Sigma-Aldrich. *Cell Proliferation Reagent WST-1*. Online. Available at: https://www.sigmaaldrich.com/catalog/product/roche/cellproro?lang=en&region=NO (accessed 04.12.2017)
Sohn, D., Grauper, V., Neise, D., Essmann, F., Schulze-Osthoff, K. & Jänicke, R.U. (2009). Pifithrin- α protects against DNA damage-induced apoptosis downstream of mitochondria independent of p53. *Cell Death and Differentiation,* 16: 869-878.
Spek, C.A. & Arruda, V. (2011). The Role of Activated Protein C in Cancer. *Blood,* 118(21): SCI-118.
Stavik, B., Skretting, G., Aasheim, H.C., Tinholt, M., Zemichow, L., Sletten, M., Sandset, P.M. & Iversen, N. (2011). Downregulation of TFPI in breast cancer cells induces tyrosine phopshorylation signaling and increases metastatic growth by stimulating cell motility. *BMC Cancer,* 11(357).
Størvold, G.L., Gjernes, E., Askautrud, H.A., Børresen-Dale, A-L., Perou, C.M. & Frengen, E. (2007). A Retroviral Vector for siRNA Expression in Mammalian Cells. *Molecular Biotechnology,* 35: 275-282.
Sun, Y., Peng, X., Zhang, H., Liu, B. & Shi, Y. (2016). P53 is required for Doxorubicin induced apoptosis via the TGF-beta signaling pathway in osteosarcoma-derived cells. *American Journal of Cancer Research,* 6(1): 114-125.
Solymoss, S., Tucker, M.M. & Tracy, P.B. (1988). Kinetics of inactivation of membrane bound factor Va by activated protein C: protein S modulates factor X protection. *The Journal of Bioloical Chemistry,* 263: 14884-14890.
Swystun, L.L., Shin, L.Y., Beaudin, S. & Liaw, P.C. (2009). Chemotherapeutic agents doxorubicin and epirubicin induce a procoagulant phenotype on endothelial cells and blood monocytes. *Journal of thrombosis and haemostasis,* 7(4): 619-626.
Tang, H., Fang, J., Shu, K., Zhou, M., Song, S., Ling, L. & Ting, L. (2007). Tissue factor/FVII regulates doxorubicin-induced apoptosis in glioblastoma via activating PI3K/Akt signaling. *The Chinese-German Journal of Clinical Oncology,* 6(5): 487-491.
Tewey, K.M., Rowe, T.C., Yang, L., Halligan, B.D. & Liu, L.F. (1984). Adriamycin-induced DNA damage mediated by mammalian DNA topoisomerase II. *Science,* 226(4673): 466-468.
Thermo Fisher Scientific. *Introduction to Gene Expression: Getting Started Guide.* Online. Available at: https://www.thermofisher.com/no/en/home/life-science/pcr/real-time-pcr/qpcr-education/what-can-you-do-with-qpcr/introduction-to-gene-expression.html (accessed on 03.12.2017)
Thermo Fisher Scientific. *Overview of Western Blotting.* Online. Available at:

http://www.thermofisher.com/no/en/home/life-science/protein-biology/protein-biology-learning-center/protein-biology-resource-library/pierce-protein-methods/overview-western-blotting.html (accessed on 28.04.2018)
Thermo Fisher Scientific. *Pierce™ BCA Protein Assay Kit.* Online. Available at: https://www.thermofisher.com/order/catalog/product/23225 (accessed 03.12.2017).
Thermo Fisher Scientific. *RNAi Overview.* Online. Available at: https://www.thermofisher.com/no/en/home/life-science/rnai/rna-interference-overview.html (accessed on 19.12.2017)
Thermo Fisher Scientific. *Transient Transfection.* Online. Available at: http://www.thermofisher.com/no/en/home/references/gibco-cell-culture-basics/transfection-basics/transfection-methods/transient-transfection.html (accessed 03.12.2017).
Thorelli, E. (1999). Mechanisms that regulate the anticoagulant function of coagulation facor V. *Scandinavian Journal of Clinical and Laboratory Investigation,* 229: 19-26.
Thorelli, E., Kaufman, R.J. & Dahlbäck, B. (1999). Cleavage of Factor V at Arg506 by Activated Protein C and the Expression of Anticoagulant Activity of Factor V. *Blood*, 93(8): 2552-2558.
Thorn, C.F., Oshiro, C., Marsh, S., Hernandez-Boussard, T., McLeod, H., Klein, T.E. & Altman, R.B. (2011). Doxorubicin pathways: pharmacodynamics and adverse effects. *Pharmagoenet Genomics,* 21(7): 440-446.
Tinholt, M., Garred, Ø., Borgen, E., Beraki, E., Schlichting, E., Kristensen, V., Sahlberg, K.K. & Iversen, N. (2018). Subtype-specific clinical and prognostic relevance of tumor-expressed F5 and regulatory F5 variants in breast cancer-the CoCaV study. *In press in JTH.*
Tinholt, M., Viken, M.K., Dahm, A.E., Vollan, H.K., Sahlberg, K.K., Garred, O., Borresen Dale, A.L., Jacobsen, A.F., Kristensen, V., Bukholm, I., Karesen, R., Schlichting, E., Skretting, G., Lie, B.A., Sandset, P.M. & Iversen, N. (2014). Increased coagulation activity and genetic polymorphisms in the F5, F10 and EPCR genes are associated with breast cancer: a case-control study. *BMC Cancer*, 14: 845.
Togna, G.I., Togna, A.R., Franconi, M. & Caprino, L. (2000). Cisplatin triggers platelet activation. *Thromb. Res.,* 99: 503-509.
Toso, R. & Camire, R.M. (2004). Removal of B-domain sequences from factor V rather than specific proteolysis underlies the mechanism by which cofactor function is realized. *The journal of biological chemistry,* 279(20): 21643-21650.
Tymms, M.J. & Ismail, K. (2001). Gene knockout. *Gene Knockout Protocols,* 158: 5-6.
Ueda, H., Ullrich, S.J., Gangemi, J.D., Kappel, A.C., Ngo, L., Feitelson, M.A. & Jay, G. (1995). Functional inactivation but not structural mutation of p53 causes liver cancer. *Nature Genetics,* 9: 41-47.
Uusitalo-Jarvinen, H., Kurokawa, T., Mueller, B.M., Andrade-Gordon, P., Friedlander, M. & Ruf, W. (2007). Role of protease activated receptor 1 and 2 signaling in hypoxia-induced angiogenesis. *Arterioscler Thromb Vasc Biol.,* 27:1456-1462
VanDerWater, L., Tracy, P.B., Aronson, D., Mann, K.G. & Dvorak, H.F. (1985). Tumor Cell Generation of Thrombin via Functional Prothrombinase Assembly. *Cancer Research,* 45: 5521-5525.
Van Sluis, G.L., Niers, T.M.H., Esmon, C.T., Tigchelaar, W., Richel, D.J., Buller, H.R., Van Noorden, C.J.F. & Spek, A. (2009). Endogenous activated protein C limits cancer cell extravasation through sphingosine-1-phosphate receptor 1-mediated vascular endothelial barrier enhancement. *Blood,* 114(9): 1968-1973.
Van Staveren, W.C., Solis, D.Y., Hebrant, A., Detours, V., Dumont, J.E. & Maenhaut, C.

(2009). Human cancer cell lines: Experimental models for cancer cells in situ? For cancer stem cells? *Biochimica et biophysia acta.,* 1795(2): 92-103.
Versteeg, H.H., Spek, C.A., Peppelenbosch, M.P. & Richel, D.J. (2004). Tissue Factor and Cancer Metastasis: The Role of Intracellular and Extracellular Signaling Pathways. *Molecular Medicine,* 10(1-6):6-11.
Vilchez, V., Turcois, L., Marti, F. & Gedaldy, R. (2016). Targeting Wnt/B-catenin pathway in hepatocellular carcinoma treatment. *World J Gastroenterol.,* 22 (2): 823-832.
Vossen, C.Y., Hoffmeister, M., Chang-Claude, J.C., Rosendaal, F.R. & Brenner, H. (2011). Clotting factor gene polymorphisms and colorectal cancer risk. *Journal of clinical oncology: official journal of the American Society of Clinical Oncology,* 29(13): 1722-1727.
Vu, N.B., Nguyen, T.T., Tran, L.C.D., Do, C.D., Nguyen, B.H., Phan, N.K. & Pham, P.V. (2013). Doxorubicin and 5-fluorouracil resistant hepatic cancer cells demonstrate stem-like properties. *Cytotechnology,* 65 (4): 491-503.
Walker, F.J. (1980). Regulation of activated protein C by a new protein. A possible function for bovine protein S. *Journal of biological chemistry,* 255(12): 5521-5524.
WCRF International (2012). *Liver cancer statistics.* Online. Available at: http://www.wcrf.org/int/cancer-facts-figures/data-specific-cancers/liver-cancer-statistics (accessed 03.10.2017).
Wilson, D.B., Salem, H.H., Mruk, J.S., Maruyama, I. & Majerus, P.W. (1984). Biosynthesis of Coagulation Factor V by a Human Hepatocellular Carcinoma Cell Line. *The Journal of Clinical Investigation,* 73(3): 654-658.
Wojtukiewicz, M.Z., Zacharski, L.R., Memoli, V.A., Kisiel, W., Kudryk, B.J., Rousseau, S.M. & Stump, D.C. (1989). Indirect activation of blood coagulation in colon cancer. *Thrombosis and Haemostasis,* 62(4): 1062-1066.
Woodley-Cook, J., Shin, L.Y., Swystun, L., Caruso, S., Beaudin, S. & Liaw, P.C. (2006). Effects of the chemotherapeutic agent doxorubicin on the protein C anticoagulant pathway. *Molecular Cancer Therapeutics,* 5(12): 3303-3311.
World Federation of Hemophilia. (2012). *What is factor V deficiency?* Online. Available at: https://www.wfh.org/en/page.aspx?pid=670 (accessed 24.04.2018).
Wu, X-Z. & Chen, D. (2006). Origin of hepatocellular carcinoma: Role of stem cells. *Journal of Gastroenterology and Hepatology,* 21(7): 1093-1098.
Yong-Jiang, Y., Xu-Dong, H. & Yu-Min, L. (2014). Effect of tissue factor knockdown on the growth invasion, chemoresistance and apoptosis of human gastric cancer cells. *Experimental and therapeutic medicine,* 7(5): 1376-1382.
Zamore, P.D., Tuschl, T., Sharp, P.A., & Bartel, D.P. (2000) RNAi: double-stranded RNA directs the ATP-dependent cleavage of mRNA at 21 to 23 nucleotide intervals. *Cell,* 101: 25-33.
Zangari, M., Anaissie, E., Barlogie, B., Badros, A., Desikan, R., Gopal, A.V., Morris, C., Toor, A., Siegel, E., Fink, L. & Tricot, G. (2001). Increased risk of deep-vein thrombosis in patients with multiple myeloma receiving thalidomide and chemotherapy. *Blood,* 98(5): 1614-1615.
Zhao, X., Chen, Q., Liu, W., Li, Y., Tang, H., Liu, X. & Yang, X. (2015). Codelivery of doxorubicin and curcumin with lipid nanoparticles result in improved efficacy of chemotherapy in liver cancer. *International Journal of Nanomedicine,* 10: 257-270.
Zemel, R., Issachar, A. & Tur-Kaspa, R. (2011). The role of oncogenic viruses in the pathogenesis of hepatocellular carcinoma. *Clin. Liver Dis.,* 15: 261-279.
Zöller, B., Holm, J., Svensson, P. & Dahlbäck, B. (1996). Elevated levels of prothrombin

activation fragment 1+2 in plasma from patients with heterozygous Arg506 to Gln mutation in the factor V gene (APC-resistance) and/or inherited protein S deficiency. *Thrombosis and haemostasis,* 75: 270-274.

8. APPENDIX

Appendix A

Appendix A contains tables of instruments, software, kits, reagents and disposables used in this study.

Table A1 – Instruments and suppliers

Instrument	Supplier
ABI 3730 DNA Analyser	Applied Biosystems
Applied Biosystems™ QuantStudio™ 12K Flex Real-Time System	Thermo Scientific
Forma™ 370 Steri-Cycle™ CO_2 Incubator	Thermo Scientific
NanoDrop® ND-1000	Thermo Scientific
Nikon Eclipse TE 300	Nikon
Nikon Eclipse Ts2-FL	Nikon
NucleoCounter® NC-100™	ChemoMetec A/S
Synergy H1 Microplate Reader	BioTek Instruments, Inc.
Steri-Cycle CO_2 Incubator	Thermo Electron Corporation
Veriti™ 96 well Thermal Cycler	Applied Biosystems
VersaMax™ Microplate Reader	Molecular Devices
QuantaStudio 12k Flex	Thermo Fisher

Table A2 – Software and suppliers

Software	Supplier
CleanSEQ® for BioMek® FX v.2.74	Agencourt®
Gen5 micorplate Reader and Imager Software	BioTek Instruments, Inc.
ImageQuant™ TL 1D v8.1	GE Healthcare Life Sciences
Sequence Scanner Software 2.0	Applied Biosystems
SoftMax® Pro 6.4	Molecular Devices

Table A3 – Disposables and suppliers.

Disposables	Supplier
Culture-Insert 2-Well µ-Dishes	Ibidi
Microcellulose Membranes, 0,2 µm	Bio-Rad
Microplate, 96 well, half area, µclear®, white, med. Binding	Greiner bio-one GmbH
Mini-PROTEAN® TGX™ Gels, 10%, 10-well comb, 50µl	Bio-Rad
Nunc™ Cell Culture Treated Multidishes (96, 12, and 6-well)	Thermo Scientific
NucleoCassette™	ChemoMetec A/S

Table A4 – Kits, suppliers and catalogue numbers.

Kit	Supplier	Catalogue number
BigDye®Terminator v3.1 Cycle Seqeuncing Kit	Applied Biosystems, Foster City, USA	4337455
Cancer 10-pathway Reporter Luciferase Kit	QIAGEN, Alameda, CA, USA	301005
Cell Death Detection ELISA^{PLUS} Kit	Roche Applied Science, IN, USA	11774425001
Dual-Luciferase® Reporter Assay System	Promega, Madison, Wi, USA	E1960
ECL™ Prime Western Blotting Detection Reagent	GE Healthcare, Buckinghamshire, UK	RPN2232
High Capacity cDNA Reverse Transcription Kit, 1000 reactions	Applied Biosystems®	4368813
MycoAlert™ Mycoplasma Detection Kit	Lonza, Walkersville, Inc., Verviers, Belgium	LT07
Pierce™ BCA Protein Assay Kit	Thermo Fisher Scientific, Waltham, MA, USA	23225
RNAqueous® Total RNA Isolation Kit	Thermo Fisher Scientific, Waltham, MA, USA	AM1912
ZymoPURE™ Plasmid Maxiprep Kit	Zymo Research, Irvine, CA, USA	D4202 & D4203
Zyumtest Factor V ELISA Kit	Hyphen-BioMed, Neuville-sur-Oise, France	RK009A
Zyppy™ Plasmid Miniprep Kit	Zymo Research, Irvine, CA, USA	D4036, D4019 & D4037

Table A5 – Chemicals, reagents, suppliers and catalogue numbers.

Chemicals	Supplier	Catalogue number
Amersham™ ECL Prime Western Blotting Detection Reagents	GE Healthcare, Buckinghamshire, UK	RPN2232
Ampicillin, Sodium Salt	Calbiochem®	171254
Bovine Serum Albumin	Sigma-Aldrich®	A7906-100G
Cell proliferation reagent WST-1	I Sigma-Aldrich®	11644807001
Dulbecco's phosphate-buffered Saline (DPBS)	Thermo Fisher Scientific	A7906-100G
Dulbecco's Modified Eagle Medium (DMEM)	Lonza, Verviers, Belgium	
GelRed Nucleic Acid Gel Stain	VWR, Oslo, Norway	730-2958
Generuler DNA Ladder Mix	Thermo Fisher Scientific	SM0331
Halt™ Protease & Phosphatase Inhibitor cocktail (100x)	Thermo Fisher Scientific	1861281
Lipofectamine®RNAiMAX	Invitrogenm Carslbad, CA, USA	13778150
Methanol	Gibco by Life Technologies	14190-094
OPTI-MEM®	Gibco by Life Technologies	31985-062
Precision Plus Protein™ Dual Xtra Standards	BioRad, CA, USA	161-0374
Reagent A100 Lysis buffer	Chemometec, Allerød, Denmark	910-0003
Reagent B Stabilizing buffer	Chemometec, Allerød, Denmark	910-0002
Restriction enzyme *Bgl*II	Fermentas, Vilnius, Lithuania	FD0083
Restriction enzyme *Bst*X1	Fermentas, Vilnius, Lithuania	FD1024
RIPA Buffer	Sigma-Aldrich, St. Louis, USA	R0278
Seakem® LE Agarose	Lonza, Rockland, USA	50004
S.O.C Medium	Invitrogen, Carlsbad, CA, USA	1749148
Taqman® Gene Expression Master Mix	Applied Biosystems, Foster City, USA	4369016
TBE Electrophoresis buffer (10X)	Fermentas, Vilnius, Lithuania	5B2
Trizma® base	Sigma-Aldrich®, St. Louis, USA	T1503-1KG

Trypsin-EDTA (0.05%)	Thermo Fisher Scientific	25300054
Tween® 20 viscous liquid	Sigma-Aldrich®	P1379
10X Fast Digest Buffer	Fermentas, Vilnius, Lithuania	B64
10x TBS	Bio-Rad	170-6435

Table A6 – Primary and secondary antibodies used in Western Blotting

	Name	Catalogue Number#	Supplier
Primary Antibody	GAPDH Loading Control	TA802519	OriGene
	Anti-Human Factor V	AHV-5146	Haematologic Technologies Inc.
Secondary Antibody	Phospho-SAPK/JNK (Thr183/Tyr185)	9251	Cell Signaling Technology
	Polyclonal Goat Anti-Rabbit Immunoglobin /HRP	P0448	DAKO
	Polyclonal Goat Anti-Mouse Immunoglobin /HRP	P0447	DAKO

Appendix B

Appendix B contains standard curves of albumin and FV concentrations used in this study.

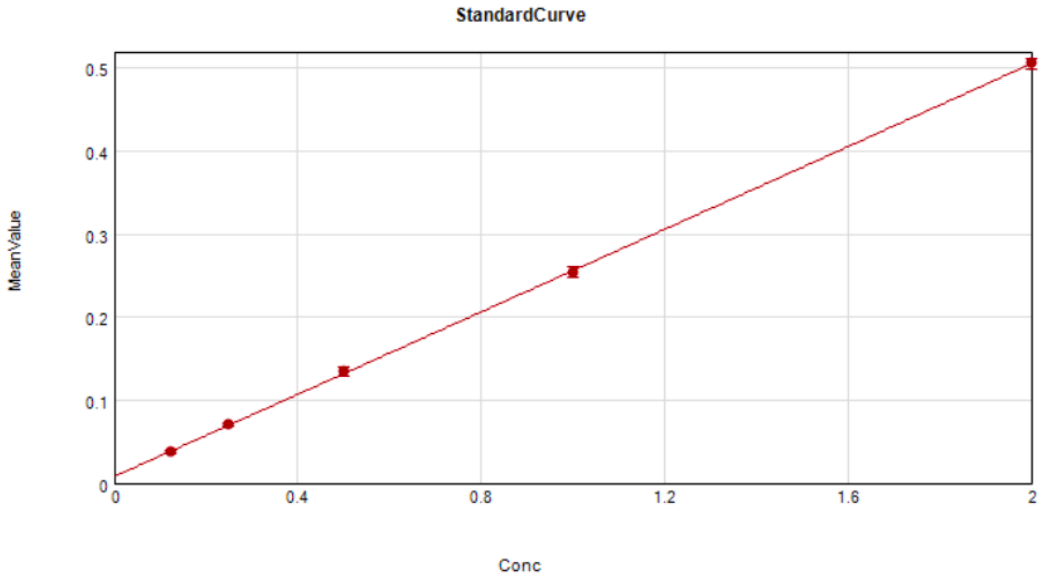

Figure 1B: **Standard curve displaying albumin concentration (mg/mL) at 570nm absorbance.** The standard curve was used for measuring total protein levels in cell lysates from Huh7 and HepG2 cells.

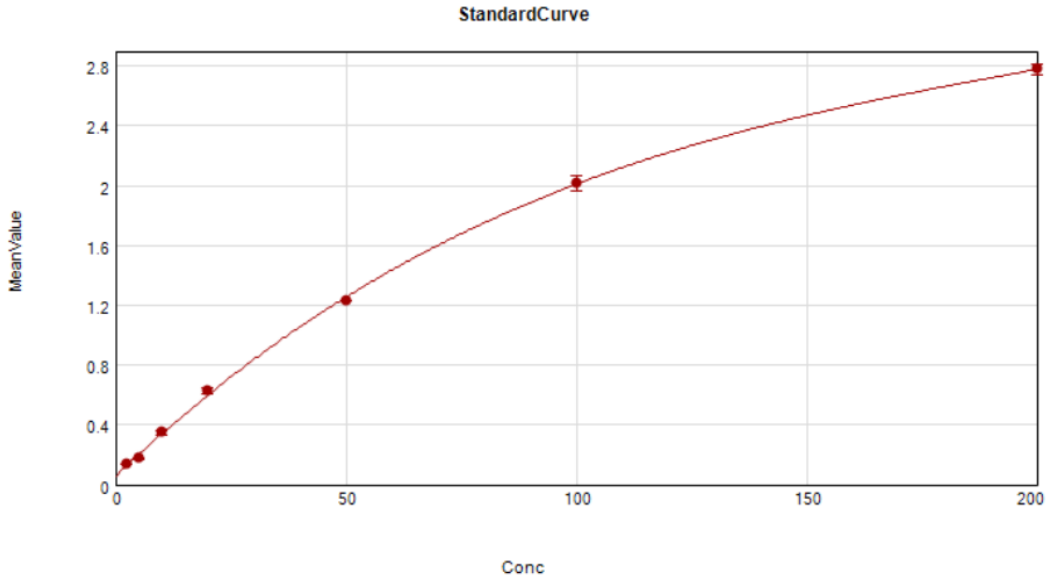

Figure 2B: **Standard curve displaying FV concentrations in % at 450nm absorbance.** The standard curve was used for measuring FV amount in unknown samples from FV ELISA in Huh7 and HepG2 cells.

Appendix C

This section of the appendix contains primers and sequences for shRNA oligos used in this thesis.

Table C1 – Taqman assays used in qRT PCR

Taqman Assay	Name	Sequence (5'→3')
PMM1	PMM1-80 Forward Primer	CCGGCTCGCCAGAAAATT
	PMM1-149 Reverse primer	CGATCTGCACTCTACTTCGTAGCT
	PMM1-99 Probe	ACCCTGAGGTGGCCGCCTTCC
GAPDH	TaqMan assay Hs99999905_m1	-
FV 250rx	TaMan Gene Expression assay Hs00914120_m1	-

Table C2 – *F5* sequencing primers used in verification of *F5* shRNA plasmid DNA sequence

Name	Direction	Sequence (5'→3')
pSiRPG vector	Forward primer	GTCTCTCCCCCTTGAACCTC
	Reverse primer	GGGGAACTTCCTGACTAGGG

Table C3 – *F5* oligo sequences used in annealing shRNA before cloning into the pSiRPG vector

Name	Direction	Sequence (5'→3')
FV-shRNA #SR301500B	Sense	CTTCCATGAATTCTAGTCCAAGAAG
	Antisense	CTTCTTGGACTAGAATTCATGGAAG
FV-shRNA #SR301500C	Sense	GGCTGTGATATTTACTAGAATTGAA
	Antisense	TTCAATTCTAGTAAATATCACAGCC
FV-shRNA scrambled #SR301500B control	Sense	GAAACTTCCTAACGTCGCTGTATAA
	Antisense	TTATACAGCGACGTTAGGAAGTTTC

Appendix D

This section of the appendix contains recipes for solutions used in the thesis

Blotting buffer (Western blotting)
3 g Trizma base
14.4 g glycine
100 mL methanol
900 mL MQ-H_2O

Lysogeny broth (LB) medium
10 g tryptone
10 g NaCl
5 g yeast extract
900 mL MQ-H_2O
pH adjusted to 7.0 with 12 M HCl
Volume adjusted to 1 L using MQ-H_2O and autoclaved

Primary antibody solution
1 mL 5% BSA
4 mL TBST
Antibody (1:1000)

Running buffer/1X TGS buffer (Western blotting)
100 mL 10x TGS (Tris/Glycine/SDS)
900mL MQ-H_2O

RIPA lysis buffer with inhibitor cocktail
1x RIPA buffer
1:100 100x Halt™ Protease & Phosphatase Inhibitor cocktail

Secondary antibody solution
4.8 mL TBST 1X
0.2 mL 5% Magermilchpulver
Antibody (1:1000)

1X TBST (Western blotting)
100 mL TBS 10X
900 mL H_2O
1 mL Tween® 20

10X TBS (Western blotting)
24.23 g Trizma® base
80.06 g NaCl
H_2O to 1L

1% Agarose Gel
0.75 g Seakem® LE Agarose

50 mL 1X TBE Electrophoresis buffer
Boil for 30 sec, then add 5 ul GelRed Nucleic Acid Gel Stain

5% Bovine serum albumin (BSA, Western Blotting)
2.5 g Bovine serum albumin
50 mL TBST

Norges miljø- og biovitenskapelige universitet
Noregs miljø- og biovitskapelege universitet
Norwegian University of Life Sciences

Postboks 5003
NO-1432 Ås
Norway